Relevance of Oxysterol 7-Alpha-Hydroxylase (CYP7B1) for Lipid Metabolism and Fatty Liver Disease

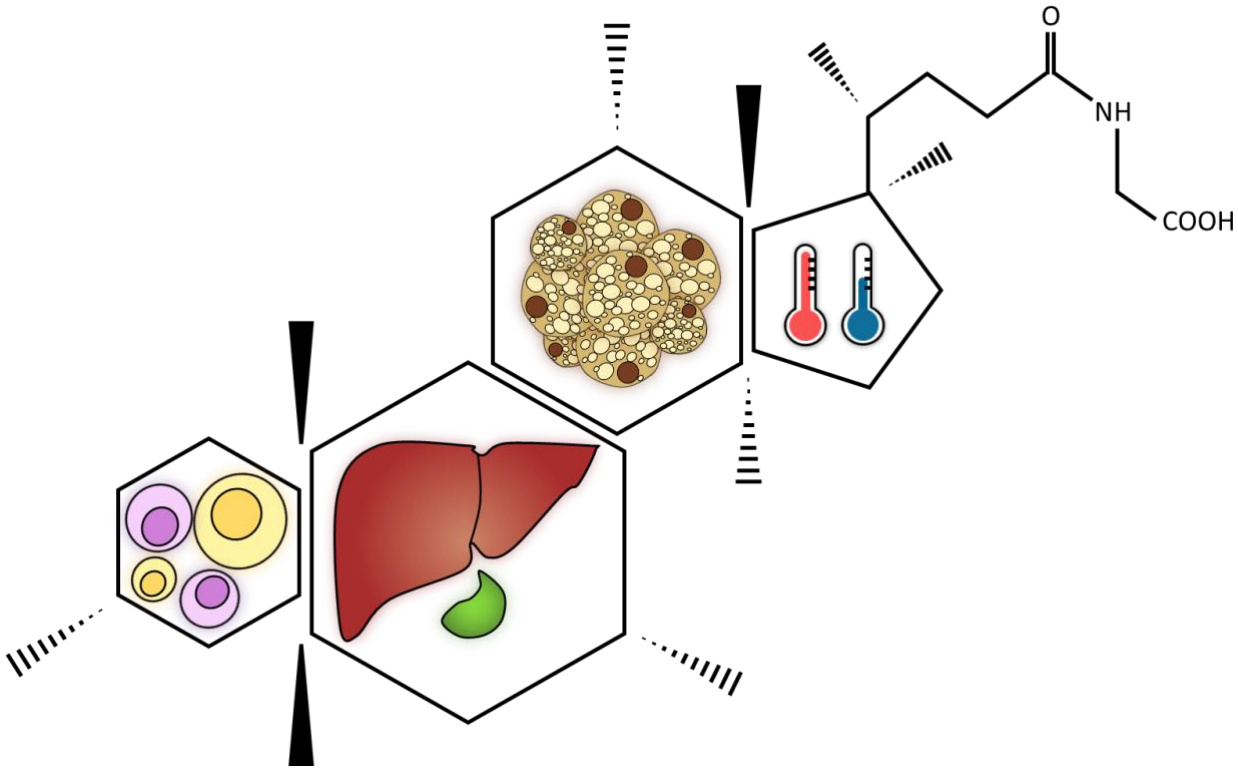

Dissertation

Dissertation with the aim of achieving a doctoral degree at the Faculty of Mathematics, Informatics and Natural Sciences

Department of Chemistry of University of Hamburg

Submitted by
Ioannis Evangelakos
from Athens

Hamburg 2022

Evaluators:

1. Evaluator: Jörg Heeren,
2. Evaluator: Markus Perbandt

Examination committee:

1. Hartmut Schlüter (chair)
2. Jörg Heeren
3. Chris Meier

The present work was carried out externally at the Institute of Biochemistry and Molecular Cell Biology of the University Medical Center Hamburg-Eppendorf under the supervision of Prof. Dr. Jörg Heeren from December 2017 to October 2021. The work was supervised by Prof. Dr. Markus Fischer at the Department of Chemistry, University of Hamburg.

Oral defense date: 20/05/2022

Approved date for publishing: 20/05/2022

Στην οικογένειά μου...

(To my family...)

1. Publications, presentations and abstracts at national and international congresses

1.1 Publications

1. Evangelakos I, Schwinge D, Worthmann A, John C, Roeder N, Pertzborn P, Behrens J, Schramm C, Scheja L, Heeren J. Oxysterol 7-α Hydroxylase (CYP7B1) Attenuates Metabolic-Associated Fatty Liver Disease in Mice at Thermoneutrality. *Cells*. 2021 Oct;10(10):2656

2. Evangelakos I, Heeren J, Verkade E, Kuipers F. Role of bile acids in inflammatory liver diseases. *Semin Immunopathol*. 2021 Aug;43(4):577-590

3. Pauly MJ, Rohde JK, John C, Evangelakos I, Koop AC, Pertzborn P, Tödter K, Scheja L, Heeren J, Worthmann A. Inulin Supplementation Disturbs Hepatic Cholesterol and Bile Acid Metabolism Independent from Housing Temperature. *Nutrients*. 2020 Oct 20;12(10):3200

4. Tian T, Heine M, Evangelakos I, Jaeckstein MY, Schaltenberg N, Stähler T, Koch-Nolte F, Kumari M, Heeren J. The P2X7 ion channel is dispensable for energy and metabolic homeostasis of white and brown adipose tissues. *Purinergic Signal*. 2020 Dec;16(4):529-542

5. Nasias D, Evangelakos I, Nidris V, Vassou D, Tarasco E, Lutz TA, Kardassis D. Significant changes in hepatic transcriptome and circulating miRNAs are associated with diet-induced metabolic syndrome in apoE3L.CETP mice. *J Cell Physiol*. 2019 Nov;234(11):20485-20500

6. Jaeger A, Zollinger L, Saely CH, Muendlein A, Evangelakos I, Nasias D, Charizopoulou N, Schofield JD, Othman A, Soran H, Kardassis D, Drexel H,

Eckardstein AV. Circulating microRNAs -192 and -194 are associated with the presence and incidence of diabetes mellitus. *Sci Rep*. 2018 Sep 24;8(1):14274

1.2 Sumbitted manuscripts

1. Evangelakos I, Kuhl A, Baguhl M, Schlein C, John C, Rohde JK, Heine M, Heeren J, Worthmann A. Cold-induced lipoprotein clearance in *Cyp7b1* deficient mice. *Front Cell Dev Biol* (in revision)

2. Rohde JK, Fuh MM, Evangelakos I, Pauly MJ, Schaltenberg N, Siracusa F, Gaglini N, Tödter K, Heeren J, Worthmann A. A gas chromatography mass spectrometry-based method for the quantification of short chain fatty acids. *Metabolites* (in revision)

3. Thiemann E, Schwaerzer G, Evangelakos I, Fuh M, Jaeckstein M, Behrens J, Nilsson SK, Kumari M, Scheja L, Pfeifer A, Heeren J, Heine M. Role of Endothelial Cell Lipoprotein Lipase for Brown Adipose Tissue Lipid and Glucose Handling *Front Physiol* (in revision)

4. Moschandrea C, Kondylis V, Herholz M, Szczepanowska K, Schwarzer R, Evangelakos I, Heine M, Jaeckstein MY, Schmidt C, Yang M, Nikitopoulou E, Bock T, Krüger M, Brodesser S, Frezza C, Heeren J, Trifunovic A, Pasparakis M. Mitochondria regulate dietary lipid processing in enterocytes. *Nature* (in revision)

1.3 Presentations at national and international congresses

- *Role of the alternative pathway-derived bile acids in lipid metabolism*
  Ioannis Evangelakos, Anna Worthmann, Clara John, Ludger Scheja, Joerg Heeren **2018**, 41st European Lipoprotein Club (ELC), Tutzing, Germany

- *The role of the alternative pathway-derived bile acids in NAFLD progression*

Ioannis Evangelakos, Anna Worthmann, Clara John, Ludger Scheja, Joerg Heeren **2019**, 42nd European Lipoprotein Club (ELC), Tutzing, Germany

- *The role of the Cyp7b1-derived cholesterol metabolites in NASH development*
  Ioannis Evangelakos, Anna Worthmann, Clara John, Ludger Scheja, Joerg Heeren **2020,** 88th Congress of the European Atherosclerosis Society (EAS), Geneva, Switzerland

- *The metabolic effects of the synthetic bile acid derivative norUDCA*
  Ioannis Evangelakos, Julia Rohde, Markus Heine, Anna Worthmann, Manka Fuh, Esther Verkade, Ludger Scheja, Folkert Kuipers,Tarek Moustafa, Joerg Heeren **2021**, 44th European Lipoprotein Club (ELC), Tutzing, Germany

1.4 Abstracts at national and international congresses

- *Activation of Type I Interferon Signaling Breaks Mitochondrial Bioenergetics and Drives Lethal Cardiomyopathy*
  Kumari M, Evangelakos I, Tian T, Rangrez A, Deshpande A, Scheja L, Rosen E, Heeren J. **2019**, American Heart Association Scientific Sessions, Philadelphia, USA

- *The Role of the Alternative Pathway-Derived Bile Acids in NAFLD Progression*
  Scheja L, Evangelakos I, Worthmann A, John C, Heeren J. **2020**, Keystone Symposia on “Obesity and NAFLD: Mechanisms and Therapeutics”, Banff, Canada

- *Bile Acids Prevent Hepatic Triglyceride Accumulation by Controlling Precursors for Lipid Synthesis in Liver and Adipose Tissue*
  Zaufel A, Silbert-Wagner D, Sommer J, Diwoky C, Reicher I, Prasch J, Trötzmüller M, Köfeler H, Kolb D, Vujic N, Evangelakos I, Willemsen N, Kratky D, Sattler W,

Bartelt A, Heeren J, Fickert P, Moustafa T. **2021**, 44th European Lipoprotein Club (ELC), Tutzing, Germany

Table of Contents

Abbreviations

22-HC	22 hydroxycholesterol
24s-HC	24s hydroxycholesterol
25-HC	25 hydroxycholesterol
27-HC	27 hydroxycholesterol
3β-HSD	3β-Hydroxysteroid dehydrogenase
AAV	Adenoassociated virus
ABCA1	ATP-binding cassette transporter A1
ABCB11	ATP-binding cassette sub-family B member 11
ABCB4	ATP Binding Cassette Subfamily B Member 4
ABCG1	ATP-binding cassette transporter G1
ABCG5	ATP-binding cassette transporter G5
ABCG8	ATP-binding cassette transporter G8
ACC	acetyl-CoA-Carboxylase
ACLY	ATP Citrate Lyase
ACTA2	actin alpha 2, smooth muscle
AKR1C4	Aldo-Keto Reductase Family 1 Member C4
AKR1D1	Aldo-Keto Reductase Family 1 Member D1
ALT	alanine aminotransferase
ANGPTL4	Angiopoietin Like 4
ANOVA	analysis of variance
Apo	apolipoprotein
ASBT	apical sodium dependent biel acid transporter
AT	atorvastatin
ATGL	adipose triglyceride lipase
ATP	adenine triphosphate
BA(s)	bile acid(s)
BAAT	BA-CoA:amino acid N-acyltransferase
BAT	brown adipose tissue
BHT	butylated hydroxytoluene
bp	base pairs
BSA	bovine serum albumin
BSEP	bile salt export pump
BSH	bile salt hydrolase
C4	7α-hydroxy-4-cholesten-3-one
CA	cholic acid
cAMP	cyclic adenosine monophosphate
CAR	constitutive androstane receptor
CBA	onjugated bile acids
CCK	cholecystokinin
CCL2	CC-chemokine ligand 2
CCL5	CC-chemokine ligand 5
CD25	cluster of differentiation 25
CD3	cluster of differentiation 3
CD36	cluster of differentiation 36

CD4	cluster of differentiation 4
CD68	cluster of differentiation 68
CD8	cluster of differentiation 8
CDCA	chenodeoxycholic acid
CDHFD	choline deficient high fat diet
CE	cholesteryl ester
CER	ceramides
CH25H	cholesterol 25-hydroxylase
ChIP	chromatin immunoprecipitation
Chol	cholesterol
ChREBP	carbohydrate response element binding protein
CoA	coenzyme A
COL1A1	alpha-1 type I collagen
CPT1	carnitine palmitoyltransferase I
CXCL1	C-X-C motif chemokine 1
CXCL10	C-X-C motif chemokine 10
CXCL9	C-X-C motif chemokine 9
CYP27A1	sterol 27-hydroxylase
CYP2C70	cytochrome P450 family 2 subfamily c polypeptide 70
CYP46A1	Cholesterol 24-hydroxylase
CYP7A1	cholesterol-7α-hydroxylase
CYP7B1	oxysterol-7α-hydroxylase
CYP8B1	sterol-12-α-hydroxylase
DAG	diacylclycerol
DAMP	damage associated molecular pattern
DC	dendritic cells
DCA	deoxycholic acid
DGAT	Diglyceride acyltransferase
DIO2	iodothyronine deiodinase 2
dl	deciliter
DMSO	Dimethyl sulfoxide
DNL	de novo lipogenesis
dpm	deconvolutions per minute
EchoMRI	echo magnetic resonance imaging
ECM	extracellular matrix
ELOVL 3	fatty acid elongase 3
ELOVL 6	fatty acid elongase 6
EMR1	adhesion G protein-coupled receptor E1
ER	Endoplasmic reticulum
EtOH	ethanol
EZ	ezetimibe
FA	fatty acid
FA	formic acid
FACS	Fluorescent activasted cell sorting
FASN	fatty acid synthase
FATP	fatty acid transport protein
FC	free cholesterol

FGF15/19	fiboblast growth factor 15/19
Foxp3	forkhead box P3
FPLC	fast performance liquid chromatography
FXR	farnesoid X receptor
g	gramm
G3P	glycerol-3-phosphate
GCA	glycocholic acid
GCDCA	clycochenodeoxycholic acid
GDCA	glycodeoxycholic acid
GLP-1	glucagon-like-peptide 1
GPBAR1	G-protein-coupled bile acid receptor 1
GPIHBP1	Glycosylphosphatidylinositol Anchored High Density Lipoprotein Binding Protein 1
gWAT	gonadal white adipose tissue
h	hours
HCC	hepatocellular carcinoma
HDL	high density lipoproteins
HE	haematoxylin - eosin
HFD	high fat diet
HMGCR	3-hydroxy-3-methyl-glutaryl-coenzyme A reductase
HNF4α	hepatocyte nuclear factor 4α
HPLC	ultra high-perfomance liquid chromatography
HSC	Hepatic stellate cells
Hsd11b1	Hydroxysteroid 11-Beta Dehydrogenase 1
HSD3B7	3 Beta-Hydroxysteroid Dehydrogenase Type 7
HSL	Hormone sensitive lipase
IBAP	intestinal bile acid binding protein
iBAT	interscapular brown adipose tissue
IFN	interferon
IL17	interleukin 17
IL1b	interleukin 1 beta
IL6	interleukin 6
iWAT	inguinal white adipose tissue
kBq	Kilobecquerel
KC	Kupffer cells
kg	Kilogramm
KO	knockout
l	Liter
LC	liquid chromatography
LCA	Lithocholic acid
LDL	low density lipoproteins
LDLR	LDL-Receptor
LIPE	Hormonal sensitive lipase
LIPG	Endothelial lipase
LPC	lysophosphatidylcholine
LPC	Lysophosphatidylcholine
LPE	lysophosphatidylethanolamine

LPE	Lysophosphatidyloethanolamine
LPL	Lipoprotein Lipase
LRH1	liver receptor homologue 1
LRP1	LDLR-related protein 1
LSEC	liver sinusoidal endothelial cells
LXR	liver X receptor
Ly6c	lymphocyte antigen 6 complex
M	molarity
m	murine
MAFLD	metabolic associated fatty liver disease
MCD	methionine choline deficient diet
MD-2	myeloid differentiation factor-2
MDR2	multidrug resistance protein 2
MDR3	multidrug resistance protein 3
MeOH	Methanol
mg	milligram
MGAT	Monoacylglycerol acyltransferase
MgCl2	magnesium chloride
MGL	Monoacylglycerol lipase
min	minutes
mL or ml	milliliter
MMP12	matrix metallopeptidase 12
MMP13	matrix metallopeptidase 13
MMP2	matrix metallopeptidase 2
MRM	multiple reaction monitoring
MRP2	multidrug resistance-associated protein 2
MRP3	multidrug resistance-associated proteins 3
MRP4	multidrug resistance-associated proteins 4
MS	mass spectrometry
MTP	microsomal TG-transfer protein
mU	milliunits
NAFLD	non-alcoholic fatty liver disease
NASH	non-alcoholic steatohepatitis
NEFA	non esterified fatty acid
NFκB	nuclear-factor κB,
ng	nanogram
NH4Ac	ammonium acetate
NK	natural killer cells
NKT	natural killer T cells
nmol	nanomole
NPC1L1	Niemann-Pick C 1-like 1
Nr0b2	Nuclear receptor subfamily 0 group B member 2
NTCP	Na+-taurocholate cotransporting polypeptide
OATP	organic anion transporters
OST	organic solute transporter
OXPHOS	Oxidative phosphorylation
PBS	phosphate buffered saline

PC	phosphatidylcholine
PCR	Polymerase chain reaction
PE	Phosphatidyloethanolamine
PFA	Paraformaldehyde
PKA	Proteinkinase A
PL	Phospholipids
Ppargc1a	Peroxisome proliferator-activated receptor gamma coactivator 1-alpha
PXR	pregnane X receptor
Q	Quadrupole
qPCR	quantitative PCR
QqQ	Triple-Quadrupole
RORα	retinoic acid receptor-related orphan receptor α
RORγt	RAR-related orphan receptor-γt
ROS	reactive oxygen species
rpm	revolutions per minute
RT	room temperature
s	seconds
SCAP	SREBP cleavage activating protein
scBAT	subscapular brown adipose tissue
SCD1	stearoyl-CoA-desaturase
SEM	standard error of the mean
SHP	small heterodimer partner
SM	sphingomyelin
SPE	solid phase extraction
SR-B1	scavenger receptor-BI
SREBP1c	sterol response element binding protein 1c
Sult2a1	Sulfotransferase Family 2A Member 1
Sult2b1	Sulfotransferase Family 2B Member 1
T2DM	type 2 diabetes mellitus
TAG	triglyceride
TBE	Tris-Borat-EDTA
TCA	tauroholic acid
TCDCA	taurodchenodeoxycholic acid
TDCA	taurodeoxycholic acid
TGF-β1	Transforming growth factor beta-1
TGR5	Takeda G Protein-Coupled Receptor 5
TH	T helper
THDCA	taurohyodeoxycholic acid
TIMP 1	tissue inhibitor of metalloproteinases 1
TLCA	taurolithocholic acid
TLR	toll-like receptor
TNF	Tumor necrosis factor
TOF	Time of flight
TREM	Triggering receptor expressed on myeloid cells
TRL	triglyceride-rich lipoproteins
TUDCA	tauroursodeoxycholic acid
T-α-MCA	tauro-α-muricholic acid

T-β-MCA	tauro-β-muricholic acid
U	units
UBA	unconjugated bile acids
UCP1	uncoupling protein 1
UDCA	Ursodeoxycholic acid
UPLC	Ultra perfomance liquid chromatography
VDR	Vitamin D receptor
VLDL	very low-density lipoproteins
WAT	white adipose tissue
WT	wild type
WTD	western type diet
α-MCA	α-muricholic acid
β-MCA	β-muricholic acid
µg	microgram
µl	microliter
µM	micromolar
ω-MCA	ω-muricholic acid

Part A: Summary

Cold exposure and the simultaneous brown adipose tissue (BAT) activation are important determinants of metabolic processes such as carbohydrate and lipid metabolism. Recently, a new interplay between BAT and the liver was identified under which increased lipoprotein processing in the thermogenic organ triggers the hepatic synthesis of bile acids via alternative synthesis pathway. This process relies on the cold-dependent upregulation of oxysterol 7-α hydroxylase (CYP7B1), which mediates the conversion of hepatic cholesterol excess into bile acids, subsequently influencing gut microbiome composition as well as thermogenic responses of the host. The purpose of this thesis was firstly to elaborate on the conditions as well as the factors that may contribute to this mechanism in mice. Acute cold exposure was identified insufficient of triggering the alternative synthesis pathway, as a minimum of 3-day acclimation was necessary to induce hepatic *Cyp7b1* expression. This induction was further found to be dependent on the magnitude of cold stress, as housing at both 6^{o}C and 16^{o}C efficiently promoted while mild cold-stress (22^{o}C) did not affect the levels of *Cyp7b1* after a short-time acclimation. Regarding the regulation of *Cyp7b1* upon cold exposure, fasting-refeeding studies as well as pharmacological inhibition of Niemann-Pick C1-Like 1 (NPC1L1) and 3-hydroxy-3-methyl-glutaryl-coenzyme A reductase (HMGCR) pointed towards a negligible role of insulin signaling and cholesterol absorption/synthesis, respectively. On the other hand, RAR-related orphan receptor alpha (RORα) agonism positively regulated *Cyp7b1* and increased bile acid synthesis upon cholesterol-enriched high-fat diet, but further investigation is required to delineate its importance for the enzyme's transcriptional activation during cold exposure. Additionally, this thesis studied the relevance of *Cyp7b1*-derived bile acids in systemic metabolism via organ uptake studies with radioactive tracers in wild type (WT) and *Cyp7b1*$^{-/-}$ mice housed at thermoneutral or cold environments. Diminished BAT uptake of ^{3}H-triolein and ^{14}C-choesterol in cold acclimated *Cyp7b1*$^{-/-}$ mice underscored the importance of bile acids derived from the alternative synthesis pathway in the activation and establishment of thermogenic responses.

In the context of chronic metabolic diseases, it is of note that ambient temperature, apart from being an important determinant of the alternative bile acid synthesis, largely affects the progression of metabolic-associated fatty liver disease (MAFLD). Therefore, the involvement of CYP7B1 in the etiology of MAFLD under conditions of low and high energy expenditure was finally investigated. For this purpose, two experimental approaches were followed, under which *Cyp7b1*$^{-/-}$ and wild type mice were fed with either a methionine-choline deficient (MCD) or a choline-deficient high-fat diet (CD-HFD) and were housed at 30 °C (thermoneutrality) or at 22 °C (mild cold stress). To study the disease phenotype and underlying mechanisms, plasma and organ samples were analyzed to determine metabolic parameters, immune cell infiltration by immunohistology and flow cytometry, lipid species including hydroxycholesterols, bile acids and structural lipids. During the MCD study, the chosen duration of mild cold exposure did not upregulate the alternative synthesis pathway, so we couldn't conclude on a significant role for CYP7B1 in relation to MAFLD-associated parameters. However, in the CD-HFD induced model, thermoneutral housing promoted MAFLD in both WT and *Cyp7b1*$^{-/-}$ mice, with the effect being more pronounced in CYP7B1-deficient mice. In these mice, we found higher plasma alanine aminotransferase activity, hyperlipidemia, hepatic accumulation of potentially harmful lipid species, aggravated liver fibrosis, increased inflammation and immune cell infiltration. Bile acids and hydroxycholesterols did not correlate with aggravated MAFLD in *Cyp7b1*$^{-/-}$ mice housed at thermoneutrality. Notably, an up-regulation of lipoprotein receptors was detected at 22 °C but not at 30 °C in livers of *Cyp7b1*$^{-/-}$ mice, suggesting that accelerated metabolism of lipoproteins carrying lipotoxic molecules counteracts MAFLD progression. In summary, these studies show the pathophysiological relevance of the CYP7B1-dependent alternative bile acid synthesis pathway for the progression of MAFLD.

Part B: Zusammenfassung

Kälteexposition und die gleichzeitige Aktivierung des braunen Fettgewebes (BAT) sind wichtige Determinanten von Stoffwechselprozessen wie dem Kohlenhydrat- und Fettstoffwechsel. Kürzlich wurde ein neues Zusammenspiel zwischen BAT und der Leber identifiziert, bei dem eine erhöhte Lipoproteinverarbeitung in dem thermogenen Organ die hepatische Synthese von Gallensäuren über den alternativen Syntheseweg auslöst. Dieser Prozess beruht auf der kälteabhängigen Hochregulierung der Oxysterol-7-α-Hydroxylase (CYP7B1), die die Umwandlung des hepatischen Cholesterinüberschusses in Gallensäuren vermittelt und in Folge die Zusammensetzung des Darmmikrobioms sowie die thermogenen Reaktionen des Wirts beeinflusst. Ziel dieser Arbeit war es zunächst, die Bedingungen sowie die Faktoren, die zu diesem Mechanismus bei Mäusen beitragen können, zu untersuchen. Es wurde festgestellt, dass eine akute Kälteexposition nicht ausreicht, um den alternativen Syntheseweg auszulösen, da eine mindestens dreitägige Akklimatisierung erforderlich war, um die hepatische *Cyp7b1*-Expression zu induzieren. Diese Induktion war außerdem vom Ausmaß des Kältestresses abhängig, da die Unterbringung bei 6ºC und 16ºC die Expression von *Cyp7b1* effizient förderte, während leichter Kältestress (22ºC) die *Cyp7b1*-Konzentration nach einer kurzen Akklimatisierung nicht beeinflusste. Hinsichtlich der Regulierung von *Cyp7b1* bei Kälteexposition wiesen Fasten-Fütterungs-Studien sowie die pharmakologische Hemmung von Niemann-Pick C1-Like 1 (NPC1L1) und/oder 3-Hydroxy-3-Methyl-Glutaryl-Coenzym-A-Reduktase (HMGCR) auf eine vernachlässigbare Rolle Insulin-abhängiger Signalwege bzw. der Cholesterinabsorption/-synthese hin. Andererseits induzierte die Supplementation eines spezifischen Agonisten für den nukleären Transkriptionsfaktor RORα die Expression von *Cyp7b1* und steigerte die Gallensäuresynthese bei cholesterinreicher, fettreicher Ernährung. Die transkriptionelle Aktivierung durch RORa war jedoch nicht für die kälteinduzierte Expression des Enzyms notwendig. Darüber hinaus untersuchte diese Arbeit die Bedeutung von *Cyp7b1*-abgeleiteten Gallensäuren im systemischen Stoffwechsel durch Organaufnahmestudien mit radioaktiven Tracern in Wildtyp (WT) und *Cyp7b1*$^{-/-}$-Mäusen, die in thermoneutraler oder kalter Umgebung untergebracht waren. Die verminderte Aufnahme von ^{3}H-Triolein

und ^{14}C-Cholesterin in der BAT von Kälte-akklimatisierten *Cyp7b1*$^{-/-}$-Mäusen unterstreicht die Bedeutung von Gallensäuren, die aus dem alternativen Syntheseweg stammen, für die Aktivierung und Etablierung thermogener Reaktionen.

Im Zusammenhang mit chronischen Stoffwechselerkrankungen ist es bemerkenswert, dass die Umgebungstemperatur nicht nur eine wichtige Determinante der alternativen Gallensäuresynthese ist, sondern auch das Fortschreiten der stoffwechselassoziierten Fettlebererkrankung (MAFLD) maßgeblich beeinflusst. Zu diesem Zweck wurden zwei experimentelle Ansätze verfolgt, bei denen *Cyp7b1*$^{-/-}$ und Wildtyp-Mäuse entweder mit einer Methionin-Cholin-defizienten (MCD) oder einer Cholin-defizienten fettreichen Diät (CD-HFD) gefüttert und bei 30 °C (Thermoneutralität) oder bei 22 °C (leichter Kältestress) untergebracht wurden. Zur Untersuchung des Krankheitsphänotyps und der zugrundeliegenden Mechanismen wurden Plasma- und Organproben analysiert, um Stoffwechselparameter, die Infiltration von Immunzellen mittels Immunhistologie und Durchflusszytometrie sowie Lipidspezies einschließlich Hydroxycholesterine, Gallensäuren und strukturelle Lipide zu bestimmen. In der MCD-Studie führte die gewählte Dauer der milden Kälteexposition nicht zu einer Hochregulierung des alternativen Synthesewegs, so dass wir nicht auf eine signifikante Rolle von CYP7B1 in Bezug auf MAFLD-assoziierte Parameter schließen konnten. Im CD-HFD-induzierten Modell förderte die thermoneutrale Unterbringung jedoch die MAFLD sowohl bei WT- als auch bei Cyp7b1-defizienten Mäusen, wobei der Effekt bei den Knockout-Tieren deutlich stärker ausgeprägt war. Bei diesen Mäusen fanden wir eine höhere Alanin-Aminotransferase-Aktivität im Plasma, Hyperlipidämie, eine hepatische Anhäufung potenziell schädlicher Lipidspezies, eine verschlimmerte Leberfibrose, verstärkte Entzündungen und eine Infiltration von Immunzellen. Gallensäuren und Hydroxycholesterine korrelierten bei *Cyp7b1*$^{-/-}$-Mäusen, die thermoneutral gehalten wurden, nicht mit einer Verschlimmerung der MAFLD. Bemerkenswert ist, dass eine Hochregulierung von Lipoproteinrezeptoren bei 22 °C, nicht aber bei 30 °C in den Lebern von *Cyp7b1*$^{-/-}$-Mäusen festgestellt wurde, was darauf hindeutet, dass ein beschleunigter Stoffwechsel von Lipoproteinen, die lipotoxische Moleküle tragen, dem Fortschreiten der MAFLD entgegenwirkt. Zusammenfassend zeigen diese Studien die pathophysiologische

Bedeutung des CYP7B1-abhängigen alternativen Gallensäuresynthesewegs für das Fortschreiten von MAFLD.

Part C: Introduction

1. Liver: organ architecture and metabolism

1.1 General

The liver is an organ responsible for various physiological processes and represents a major niche for metabolic reactions and energy homeostasis. Among other processes, it governs glucose, lipid and amino acid metabolism, and metabolically connects multiple other organs such as adipose tissues and muscles. Regarding its complex architecture, the organ's building block is the hepatic lobule, a characteristic hexagonal structure that is centrally penetrated by the central vein (Ishibashi et al. 2009). The lobules are comprised by diverse cell types with specific functions, which are mainly organized around distinct formations, the so-called hepatic sinusoids, which connect the central vein with the portal area. In the portal area a distinct structure called portal triad can also be identified, consisted of a portal vein, a portal artery and a bile duct.

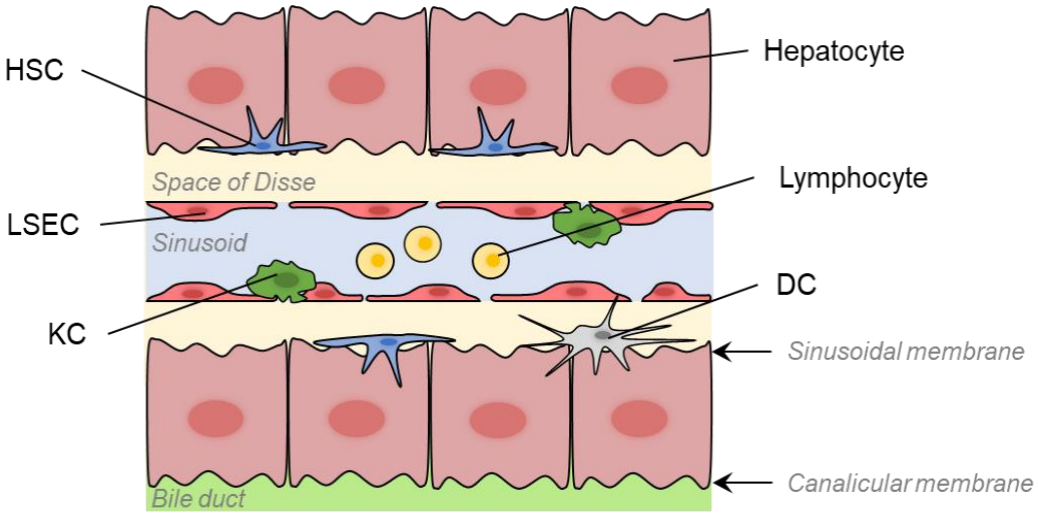

Figure 1. Schematic representation of the major liver cell types in the structure of a hepatic sinusoid. HSC; hepatic stellate cell, LSEC; liver sinusoidal endothelial cell, KC; Kupffer cell, DC; dendritic cell.

Liver parenchymal cells, or simply hepatocytes, account for ~70-80% of all liver cells and are carrying out crucial metabolic reactions related to glycogen

synthesis/degradation, gluconeogenesis/ glycolysis, fatty acid synthesis/oxidation, cholesterol metabolism and bile acid synthesis. The other cell types, the non-parenchymal fraction, comprises liver sinusoidal endothelial cells (LSECs), hepatic stellate cells (HSCs), biliary epithelial cells and various immune populations such as resident macrophages (Kupffer cells; KCs), lymphocytes and dendritic cells (DCs). Their spatial distribution around the hepatic sinusoid can be seen in Figure 1. At the sinusoidal membrane of the hepatocytes, the fenestrated LSECs form the functional sinusoid, which supports the blood flow from the portal circulation towards the central vein. The portal circulation connects the liver with the intestinal tract, as substances absorbed by the later can eventually be transferred to hepatocytes where they can be further metabolized or transformed. At their canalicular membrane and in parallel to the sinusoids, hepatocytes come in contact with the bile ducts, where secretion of bile components takes place.

1.2 Hepatic lipid and lipoprotein metabolism

In regards to lipid and lipoprotein metabolism, the liver exerts a crucial role as it is a major hub for *de novo* lipogenesis (DNL), fatty acid oxidation and secretion, lipoprotein uptake as well as cholesterol synthesis and conversion.

During DNL, carbohydrate sources can be converted to fatty acids (FAs) via a series of regulated enzymatic reactions. Briefly, carbohydrates such as glucose, besides to glycogen formation for energy storage in the liver, can be metabolized via the pathway of glycolysis to pyruvate, that is subsequently shuttled inside the mitochondria for the generation of citrate. The enzyme ATP citrate lyase (ACLY) is converting citrate, after its cytosolic release, to acetyl-CoA, thereby connecting carbohydrate metabolism with FA synthesis. Acetyl-CoA carboxylase (ACC) is converting acetyl-CoA to malonyl-CoA, which is further used as a substrate by fatty acid synthase (FASN) to generate FAs. The emerging FAs can be further elongated or desaturated via the action of elongation of very long chain fatty acids protein 6 (ELOVL6) and stearoyl-CoA desaturase 1 (SCD1), respectively. The key regulators of hepatic DNL and the implicated enzymes are the transcription factors sterol response element binding protein 1-c (SREPBP-1c) and the

carbohydrate response element binding protein (ChREBP), which are controlled in response to insulin and glucose, respectively (Foretz et al. 1999, Yamashita et al. 2001).

In addition to DNL, FAs present in the liver may result from the circulation following their uptake via specific transporters such as members of the fatty acid transport protein (FATP) family and cluster of differentiation 36 (CD36). Depending on the nutritional status, plasma FAs can either derive from adipose tissues, where prolonged fasting conditions mobilize their release to the circulation, or from ingested lipids during the postprandial state. Regardless of their source, hepatic FAs can be esterified and stored as triglycerides in lipid droplets, used as substrates for β-oxidation to fuel energy demands, or, again after their esterification to triglycerides can be packaged into very low-density lipoprotein (VLDL) particles and subsequently secreted. Esterification of FAs with glycerol-3-phosphate (G3P) or cholesterol generates triglycerides (TAGs) or cholesteryl esters (CEs), respectively. Under conditions of high energy demand, hepatic TGs can be hydrolyzed by various lipases (namely ATGL, HSL, MGL), ultimately leading to FA release. Free FAs can be then activated and upon translocation into the mitochondria via carnitine palmitoyltransferase 1 (CPT1), they are β-oxidized to sustain ATP production.

Incorporation of TG and CE into VLDL particles underscores the mechanism via which FAs can be secreted from the liver towards other peripheral organs such as muscle and adipose tissues. During VLDL assembly, microsomal triglyceride transfer protein (MTP) present in the endoplasmic reticulum (ER) assists the initial lipid loading onto ApoB-100 (Raabe et al. 1999). Further lipidation of the nascent particle by the cytosolic lipid droplets leads to the production of the mature VLDLs that can be excreted via Golgi-assembled vesicles. Important components for the assembly of VLDL particles are phospholipids, especially phosphatidylcholine (PC). Inability of PC synthesis has been connected to decreased hepatic VLDL secretion, that eventually promotes liver steatosis (Yao and Vance 1988). In fact, this is the rationale behind the commonly used choline-deficient diets in experimental feeding studies on fatty liver disease (Raubenheimer, Nyirenda, and Walker 2006).

The liver has an additional role in regards to lipoprotein uptake and endocytosis, hence controlling the homeostasis of circulating lipids. Low density lipoprotein receptor (LDLR) and its related protein 1 (LRP1) facilitate in a coordinated manner the endocytosis of ApoB-100 containing LDL particles in the liver, while the scavenger receptor class B member 1 (SR-B1) is mainly responsible for the uptake of apolipoprotein A1 (APOA1) rich high density lipoprotein (HDL) (van Berkel et al. 1995)(Acton et al. 1996). Among all tissues, LDLR is highly present in the liver where it facilitates LDL cholesterol uptake, providing hepatocytes with the crucial organic molecule for bile acid synthesis (discussed in section 2). On the other hand, efflux of cholesterol outside of the cell is mediated by ATP binding cassette transporter ABCG1 and ABCA1 (Cavelier et al. 2006).

Hepatocytes, as well as other mammalian cells, are capable of synthetizing cholesterol. When intracellular levels of cholesterol are high, SREBP cleavage-activating protein (SCAP) together with SREBP can remain anchored at the ER. When cholesterol levels are critically low, the complex can no longer be retained bound at the ER, so SREBP is proteolytically cleaved and its active form is entering the nucleus to drive the transcription of sterol response element (SRE)-containing target genes (Horton, Goldstein, and Brown 2002). These targets include LDLR and 3-hydroxy-3-methyl-glutaryl-coenzyme A reductase (HMG-CoA reductase or HMGCR), that are responsible for the hepatic cholesterol uptake and biosynthesis, respectively.

2. Cholesterol metabolism: bile acids and hydroxycholesterols

Cholesterol comprises a fundamental metabolic molecule for eukaryotes with multiple and unique functions due to its bipolar nature. First of all, its rigid chemical structure serves as a crucial component that supports the formation of eukaryote cellular and organelle membranes, while its concentration highly determines their permeability to other molecules. In addition, either *de novo* synthetized or diet-derived, cholesterol serves as a precursor for numerous other biological relevant molecules, including steroid hormones, vitamins and bile acids (Schade, Shey, and Eaton 2020). The cholesterol derivatives, including cholesterol itself, can regulate biological processes by activating a variety of membrane and nuclear receptors. Interestingly, bile acids and their intermediate

products i.e hydroxycholesterols influence a variety of metabolic and immune responses (Lefebvre et al. 2009)(Schroepfer and Wilson 2000), while in the context of related disorders, modulation of their synthesis and signaling is of particular scientific and clinical interest (Li and Chiang 2014)(Brown, Sharpe, and Rogers 2021).

2.1 Bile acid synthesis

The main pathway of cholesterol metabolism and excretion is the synthesis of bile acids and intermediates such as hydroxycholesterols (oxysterols), which facilitates the conversion of a highly insoluble molecule into metabolites with an amphipathic nature. In humans, approximately ~500 mg of cholesterol per day are converted to bile acids and upon production they are stored in the gallbladder. During the postprandial phase, their secretion to the intestinal lumen facilitates the emulsification and thus the catabolism of dietary fat and other fat-soluble nutrients such as vitamins. After a complete enterohepatic cycle, approximately 95% of bile acids is reabsorbed by the intestine and diverted back to the liver while the remaining 5% is excreted in the feces. This lost proportion can be compensated by *de novo* hepatic synthesis of bile acids and thus influences the cholesterol turnover (Kuipers, Bloks, and Groen 2014). These molecules with amphipathic nature can be found across all vertebrate species with common chemical structures. Namely they exist as 24-carbon or 27-carbon molecules.

Bile acids synthesis and the production of intermediate hydroxycholesterols are under a tight control of complex, multiple-step process, involving cytosolic, mitochondrial and peroxisomal enzymes, which are preferentially, or almost exclusively, expressed in the liver. They can be generated via two distinct routes, the classical (or neutral) and the alternative (or acidic) bile acid synthesis pathways as seen in Figure 2 (adapted from Evangelakos et al. 2021), both encompassing specific reactions such as cholesterol ring modification, oxidation and shortening as well as conjugation with amino acids such as taurine or glycine (Russell 2003). The enzyme cholesterol-7α-hydroxylase (CYP7A1) is a microsomal cytochrome P450 enzyme and the main regulatory enzyme of the classical

pathway, which catalyzes the 7α-hydroxylation of cholesterol, thus producing 7α-hydroxycholesterol (7α-HC) (Figure 2). CYP7A1 is the rate limiting enzyme as it determines the degree of cholesterol conversion, with its importance being highlighted in *Cyp7a1*-deficient mice that present a ~75% decreased bile acid pool size compared to

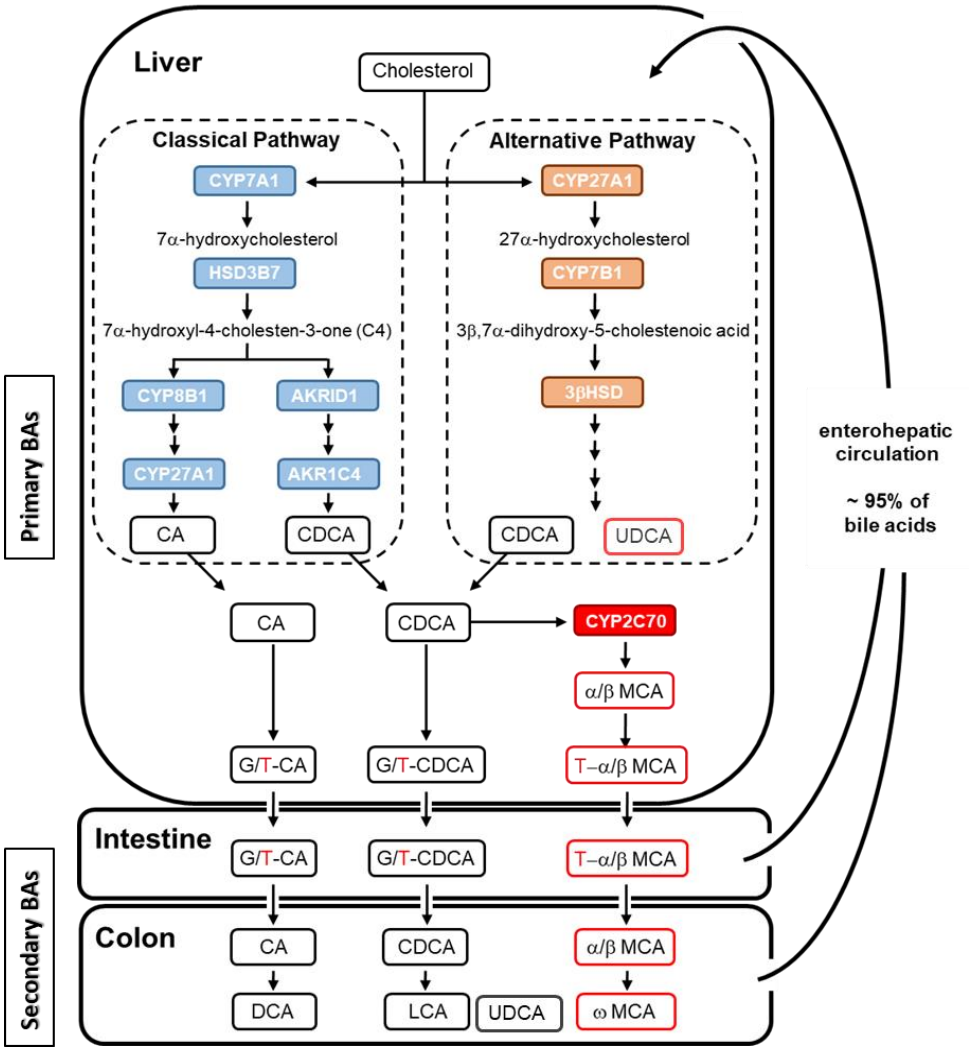

Figure 2: Generation of primary and secondary bile acids. Cholesterol is converted by a series of oxidative reactions to the primary bile acids, cholic acid (CA) and chenodeoxycholic acid (CDCA). In response to a meal, the conjugated forms of primary bile acids are released into the small intestine where they play an important role in digestion of dietary lipids. In the ileum of the intestine approximately 95% of bile acids are reabsorbed and return to the liver via the enterohepatic circulation. In the colon, primary bile acids are deconjugated and converted by a number of bacterial enzymes to secondary bile acids such as deoxycholic acid (DCA) or lithocholic acid (LCA), which can be excreted or follow the enterohepatic circulation. As indicated in red, in mice bile acids are primarily conjugated to taurine (T), while human bile acids are conjugated to glycine (G). Notably, murine bile acids known as muricholic acids (MCA) are generated by CYP2C70, an enzyme expressed in murine but not in human liver explaining the difference in the composition of human and murine bile acid species.

wild types (Schwarz et al. 2001). Following several steps of ring structure modification, 7α-hydroxy-4-cholesten-3-one (or C4) is produced, which is an intermediate of bile acid production and a reliable readout for CYP7A1 activity (Gälman et al. 2003). Crucial for the 12α-hydroxylation of C4 and the subsequent production of bile acids is the sterol 12α-hydroxylase (CYP8B1), a hepatic enzyme located at the ER. The alternative synthesis route is initiated by the enzyme sterol 27-hydroxylase (CYP27A1), a mitochondrial cytochrome P450 oxidase. Crucial for bile acid synthesis via the acidic route is the oxysterol-7α-hydroxylase (CYP7B1) which is responsible for the necessary 7α-hydroxylation of 27-HC as well as 25-HC.

The initial products of the synthesis pathways are the so-called primary bile acids, namely cholic acid (CA) and chenodeoxycholic acid (CDCA) in humans, while in mice CDCA is rapidly converted to ursdodeoxycholic acid (UDCA) as well as α/β-muricholic acids (α/βMCA). Bile acids can be conjugated with amino acids – most commonly glycine (G) and taurine (T) in humans and mice, respectively – ultimately leading to the production of bile salts. Bile acid-CoA:amino acid N-acyltransferase (BAAT) is the selective liver peroxisomal enzyme that mediates the conjugation reactions in both species. Bile acid conjugation increases their hydrophilicity, protects against their strong detergent effects of unconjugated bile acids while halt their passive diffusion through cellular membranes. As a result, several membrane transporters are required for their efficient transportation (Russell 2003). Hydrolysis of bile salts, the opposite reaction to conjugation, is mediated by bile salt hydrolases (BSHs). These enzymes are exclusively synthesized by gut microbes, emphasizing the important role of the gut microbiome for bile acid metabolism. An additional role of the gut flora during the bile acid synthesis is the conversion of primary to the so-called secondary bile acids such as deoxycholic (DCA) and lithocholic acid (LCA) in humans and additionally ωMCA in mice. It is so far visible that fundamental differences exist between human and murine bile acid composition while recent studies identified CYP2C70 as the responsible enzyme for the 6α-hydroxylation of bile acids and the production of α/βMCA, which are present only in mice (Takahashi et al. 2016, De Boer et al. 2020).

The alternative route is playing a significant role in regards to oxysterol synthesis, as several enzymes are implicated in cholesterol conversion to its oxygenated derivatives.

CYP27A1, which is responsible for the production of 27-hydroxycholesterol (27-HC) in the liver (Figure 2), is also present in extrahepatic tissues including the brain, the lungs and macrophages, underlining an important role for the respective oxysterol in various organs. Cholesterol 24-hydroxylase (CYP46A1) and cholesterol 25-hydroxylase (CH25H) are both present in the liver as well as brain and macrophages, mediating the production of 24-HC and the 25-HC, respectively (Lund, Guileyardo, and Russell 1999). In addition to their enzymatic production, oxysterols can be produced non-enzymatically via autoxidation to form 7α- and 7β-hydroxycholesterol as well 7-ketocholesterol (Iuliano 2011).

2.2 Enterohepatic circulation

Upon synthesis in hepatocytes, bile acids are actively transported across the canalicular membrane by the bile salt export pump (BSEP, encoded by *Abcb11*) and are then stored in the gallbladder. Other transporters which are present at the canalicular membrane are responsible for the transportation of cholesterol, organic ions (OA) and phospholipids (PL) into the bile (Figure 3). These include ATP Binding Cassette Subfamily G Members 5/8 (ABCG5/8), multidrug resistance-associated protein 2 (MRP2) and multidrug resistance protein 3 (MDR3), respectively (Halilbasic, Claudel, and Trauner 2013). When bile acid concentrations are passing a certain threshold inside the hepatocytes, they can be released basolaterally to the circulation in order to avoid bile hepatotoxicity. During this process, transport proteins such as multidrug resistance-associated protein 3 (MRP3) and 4 (MRP3) as well as organic solute transporters α/β (Ost α/β) are involved (Figure 3). During the postprandial phase, cholecystokinin (CCK), which is produced by the duodenal enteroendocrine cells, triggers gallbladder emptying in order to help the emulsification and digestion of dietary nutrients including lipids and fat-soluble vitamins. Upon release into the duodenum, bile acids are following their route through the gastrointestinal lumen, where they can be actively or passively absorbed by the different intestinal cells and be reverted back to the liver. Inside the enterocytes, apical sodium dependent BA transporter (ASBT) facilitates the active absorption of bile salts,

that can be subsequently bound to the intestinal bile acid binding protein (IBAP) until export to the portal circulation via Ostα/β heterodimers (Dawson et al. 2005, Dawson, Lan, and Rao 2009). Of importance is also the Niemann-Pick C1-like 1 (NPC1L1) transporter which is responsible for the absorption of dietary cholesterol by the gut. Some bile acids can reach the colon where they can be passively taken up by colonocytes and again be transported via Ostα/β heterodimers to the circulation. As already mentioned,

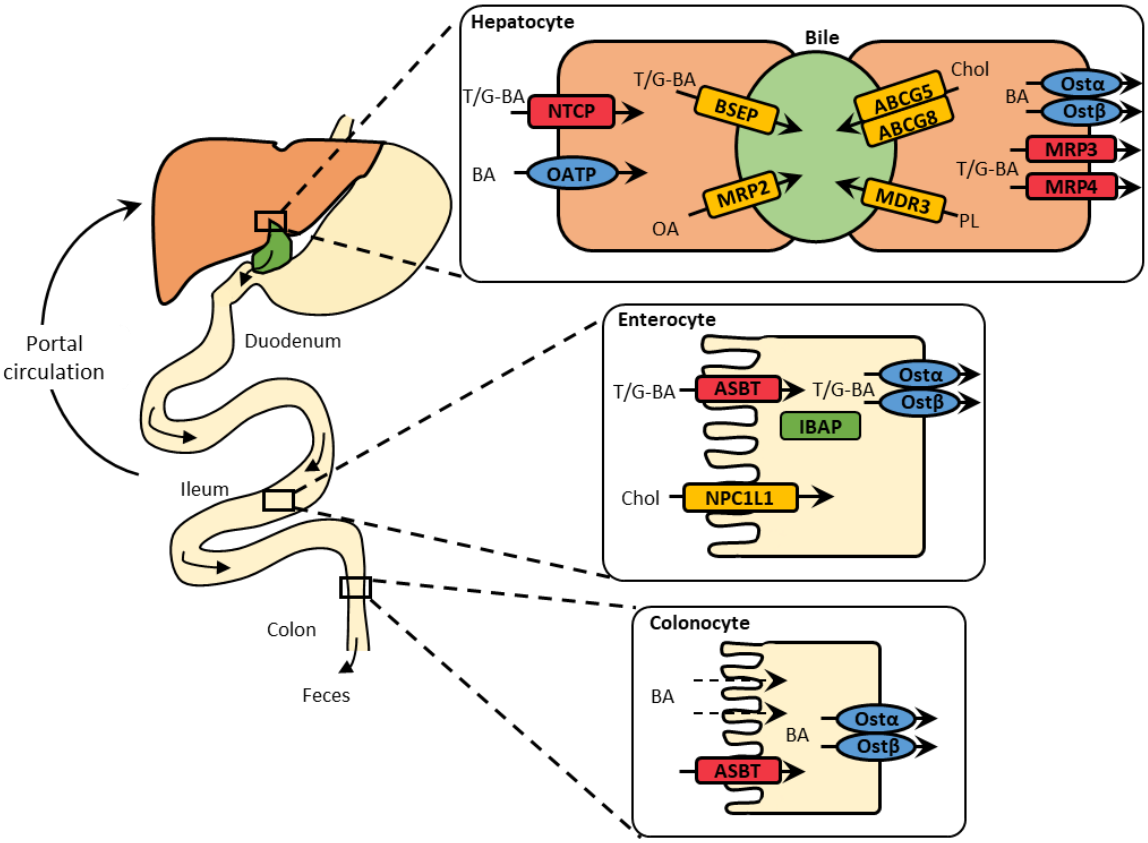

Figure 3: Major transport proteins involved in the enterohepatic circulation and hepatobiliary secretion of bile acids and other molecules. At the basolateral membrane of hepatocytes, NTCP facilitates the active transportation of conjugated bile acids (T/G-BA) inside the hepatocytes while members of the OATP family show specificity to unconjugated species. At the same time MRP3 and MRP4 together with Ostα/β mediate the secretion of BA into the circulation. At the canalicular membrane of hepatocytes several proteins are dedicated for the transportation of specific molecules: BSEP for T/G-BA, MRP2 for organic anions (OA), ABCG5/8 for cholesterol (Chol) and MDR3 for phospholipid (PL) secretion into the bile. Upon reaching the ileum, T/G-BA can be actively taken up via ASBT and can be attached IBAP and then released to portal circulation via Ostα/β heterodimers. NPC1L1 is responsible for cholesterol absorption at the apical membranes of enterocytes. Bile acids which escape uptake from enterocytes can be passively absorbed by colonocytes and excreted at the basolateral membrane again via Ostα/β. Finally, a portion of bile acids is escaping into the feces.

during the enterohepatic circulation ~95% of bile acids can be recycled (Figure 2) back to the liver, where specific proteins at the basolateral membrane such as Na+-taurocholate co-transporting polypeptide (NTCP) (Ananthanarayanan et al. 1994) and organic anion transporters (OATP) (Jacquemin et al. 1994) facilitate their internalization.

2.3 Bile acids and oxysterols in metabolic control

Along with their physiological role in regard to lipid emulsification and absorption as well as cholesterol homeostasis, many more functions have been attributed to these cholesterol derivatives during the recent years. Of note, bile acids can exert “hormone-like” functions by acting as ligands for several nuclear as well as membrane receptors. Table 1 (adapted from Evangelakos et al. 2021) summarizes the most significant bile acid receptors as well as their natural ligands and their cellular expression pattern. Two of the most studied bile acid receptors are the nuclear farnesoid X receptor (FXR, encoded by *Nr1h4*) and the transmembrane Takeda G protein-coupled receptor 5 (TGR5, encoded by *Gpbar1*). FXR is highly present in liver and intestine while TGR5 is expressed in non-parenchymal cells of the liver (Kupffer cells, endothelial cells, cholangiocytes etc) as well as thermogenic adipose tissues and enteroendocrine cells. Upon activation from bile acids, FXR drives the expression of small heterodimer partner (SHP, encoded by *Nr0b2*) which, together with liver receptor homologue 1 (LRH-1), suppresses the expression of *Cyp7a1* (Goodwin et al. 2000). Moreover, in a concerted action with hepatocyte nuclear factor 4α (HNF4α), SHP can also inhibit the expression of *Cyp8b1* (M. Zhang and Chiang 2001). As a consequence, bile acids regulate their own synthesis via FXR activation. Apart from that, FXR agonism has also been shown to decrease *Slc10a1* expression (encoding for NTCP) and to upregulate *Abcb11* (encoding for BSEP), ultimately leading to reduced hepatic uptake and increased excretion of bile acids, respectively (Calkin and Tontonoz 2012, Ananthanarayanan et al. 2001). In addition, intestinal FXR activation triggers fibroblast growth factor 15/19 (FGF15/19; FGF15 in mice and FGF 19 in humans), which upon secretion to the circulation and delivery to the liver via the portal vein, it

decreases the expression of *Cyp7a1* via binding to FGF receptor 4 (FGFR4) (Inagaki et al. 2005).

Table 1. Major nuclear (white) and membrane (pink) receptors of bile acids, their natural ligands and expression pattern.

Receptor	Natural bile acid ligands	Expression pattern	
		Liver/Gastrointestinal track	Immune cells
FXR (NR1H4, farnesoid X receptor)	CDCA > CA > LCA > DCA antagonists: MCAs, GUDCA	hepatocytes, Ito cells, Kupffer cells, cholangiocytes, Paneth cells, enterocytes	Macrophages, dendritic cells, NKT cells, T helper cells
PXR (NR1I2, pregnane X receptor)	LCA, CDCA,3-keto LCA	hepatocytes, enterocytes	not detected
CAR (NR1I3, constitutive androstane receptor)	CA, 6-keto LCA	hepatocytes	T cells
VDR (NR1I1, vitamin D receptor)	LCA metabolites, DCA	enterocytes	granulocytes, monocytes, macrophages, dendritic cells, T helper cells
RORγt (NR1F3, RAR-related orphan receptor-γ)	3,12-oxo LCA	not detected	T helper cells, innate lymphoid cells (ILC3)
TGR5 (Takeda G Protein-Coupled Receptor 5)	LCA > DCA > CDCA > UDCA > CA	Enterocytes, L cells, Paneth cells, cholangiocytes, Kupffer cells, Ito cells, liver sinusoidal endothelial cells,	monocytes/macrophages, dendritic cells, NKT cells

Next to the regulation of bile acid synthesis, activation of FXR is connected to glucose and lipid handling, energy metabolism, cellular proliferation, detoxification reactions as well as modulation of the immune system (Lefebvre et al. 2009, Ahmad and Haeusler 2019, Chiang and Ferrell 2019). For example, FXR activation reduces lipogenesis by regulating sterol regulatory element-binding protein 1c (SREBP1c) and carbohydrate-responsive element-binding protein (ChREBP), while it simultaneously controls gluconeogenesis and triggers glycogen synthesis (Molinaro et al., 2018, Caron et al., 2013). Interestingly, bile acids exert opposite effects regarding insulin signaling in the postprandial phase, as they can stimulate or inhibit GLP1 production in intestinal L cells,

via TGR5 or FXR activation, respectively (Shapiro et al. 2018). Brown adipose TGR5 plays an important role in energy metabolism as its activation by CA triggers the expression of *Dio2*, which converts T4 to T3, thereby increasing energy metabolism (Watanabe et al. 2006). This effect has been recently recapitulated in humans by CDCA supplementation (Broeders et al. 2015).

In the context of metabolic control, oxysterols do also play an important role as they can by serving as ligands for several nuclear receptors regulate the expression of several enzymes. It was very early reported that several oxysterols reduce the activity of HMGCR, thus mediating a feedback inhibition of cholesterol biosynthesis (Kandutsch and Chen 1973). On the contrary, low oxysterol levels can induce the enzyme's activity (Tamasawa et al. 1997). In addition, several oxysterols, including 25-HC, have been reported to affect cholesterol biosynthesis by SREBP processing (Janowski, Shan, and Russell 2001).

Oxysterols can also influence hepatic metabolism by activating nuclear receptors such as liver X receptors α and β (encoded by *Nr1h3* and *Nr1h2*, respectively), with 22-HC 24(S)-HC, 25-HC and 27-HC being major LXR ligands (Töröcsik, Szanto, and Nagy 2009). LXRs, by forming obligate heterodimers with RXRs, can regulate the expression of genes involved in lipid and cholesterol synthesis, therefore emphasizing the impact of oxysterols on lipid metabolism (Edwards, Kennedy, and Mak 2002). Of high importance is the LXR-driven induction of SREBP1c, a central activator of lipogenic genes (Repa et al. 2000). The fact that lipogenic induction was persistent upon LXR-agonism even in *Srebp-1c* null mice, led to the identification of ChREBP as a putative LXR target, which can drive lipogenesis in a SREBP1c-independent manner (Cha and Repa 2007). Among other LXR targets are genes of the ATP-binding cassette (ABC) receptor family such as ABCG5 and 8, which control biliary cholesterol excretion, as well as ABCA1 and ABCG1, which are involved in cholesterol efflux (Repa et al. 2002, Sabol, Brewer, and Santamarina-Fojo 2005). Additionally, LXRs can influence lipoprotein uptake and metabolism as they promote the expression of receptors such as LDLR and SR-BI (Ishimoto et al. 2006, Yu et al. 2004). Lastly, oxysterol signaling via LXR enhances *Cyp7a1* transcription, hence highlighting the antithetical regulatory mechanisms that oxysterols and bile acids exert regarding cholesterol homeostasis (Chiang, Kimmel, and Stroup 2001).

3. Metabolic associated fatty liver disease (MALFD)

As seen in Part C, section 1, the liver is a vital organ not only because it is implicated in processes of lipid metabolism and transportation but also by being a hub for numerous other functions including bile synthesis, iron metabolism, albumin synthesis, immune responses, detoxification and drug clearance (Trefts, Gannon, and Wasserman 2017). Therefore, abnormal organ homeostasis and hepatic function are related to the development of liver malignancies. As discussed in this section, this thesis focuses on metabolic-related liver disease.

3.1 Definition of MAFLD

Metabolic-associated fatty liver disease or MAFLD (a revised terminology for the commonly used term “non-alcoholic fatty liver disease” or NAFLD) (Eslam et al. 2020) is a rapidly emerging liver disease that already affects almost one fourth of the global population with an increased prevalence in the Western world. MAFLD is used as an umbrella term to describe a wide spectrum of related diseases that are mainly attributed to an imbalance between hepatic TG “gain” (via FA uptake and DNL) and “loss” (via FA oxidation in mitochondria and packaging on VLDL particles) (Berlanga et al. 2014). This hepatic disorder has been closely related to the development of obesity, insulin resistance, hyperglycemia and dyslipidemia (Yki-Järvinen 2014). Starting from simple hepatic steatosis, where more than 5% of hepatocytes show TG deposition in the form of lipid droplets, the disease can progress to steatohepatitis (known also as non-alcoholic steatohepatitis; NASH), which is characterized by additional hepatic injury, inflammation and fibrosis (Loomba and Sanyal 2013). Usually, If several control mechanisms are surpassed, the later may progress to cirrhosis or even hepatocellular carcinoma (HCC), and according to literature these conditions can occur up to the 10-30% of patients diagnosed with steatohepatitis (Cohen, Horton, and Hobbs 2011). Up to date, despite that a number of clinical trials have been completed or are still ongoing, there is no EMA- or FDA-approved drug for the treatment of steatohepatitis (Ratziu, Goodman, and Sanyal

2015). Therefore, lifestyle interventions, aiming at the reversible stage of steatosis, have been the most followed guidelines management of MAFLD.

3.2 Development of MAFLD

Despite the big scientific advances in understanding the pathogenesis of MAFLD, the mechanisms that drive the disease as well as the progression towards the inflammatory and fibrotic phenotype of steatohepatitis are still incompletely understood. The “two-hit” hypothesis was until recently a model that tried to explain how steatohepatitis occurs (Day and James 1998). According to this, hepatic steatosis, which is a result of excessive TG accumulation (“first-hit”), predisposes the liver for damage and injury that will eventually promote inflammation and fibrosis (“second-hit”). However, it has become clear that the disease is rather multifactorial as genetic predisposition, dietary habits and exercise may influence to a specific extend its development. On top of that, recent studies have highlighted that prolonged imbalance of glucose, lipid and cholesterol metabolism are important determinants of MAFLD (Bechmann et al. 2012). Regardless of progression towards steatohepatitis, cirrhosis or cancer, imbalance in TG metabolism is still considered the hallmark characterizing MAFLD establishment with three being the main reasons of fat accumulation: a) excess influx of non-esterified fatty acids (NEFA) from adipose tissues (AT) to the liver, b) increased uptake of dietary fat delivered by intestinal chylomicrons and c) high hepatic DNL. Impaired insulin signaling, a common characteristic of metabolic comorbidities such as obesity and type 2 diabetes mellitus (T2DM), is strongly associated with MAFLD in the form of insulin resistance and seems to play a crucial role both in adipose tissue as well as the liver (Anstee, Targher, and Day 2013). Under such conditions, insulin is not able to exert its physiological role, *i.e.* suppress the lipolytic processes in adipose tissue, but instead promote TG lipolysis and the concomitant flux of FAs from fat depots to the circulation. FAs are then delivered to the liver where they can be actively transported into hepatocytes via specific proteins such FATP2, FATP5 or CD36. Notably, CD36 levels positively correlate with the development of MAFLD (Inoue et al. 2005). Interestingly, murine studies of diet-induced

MAFLD have shown that mice lacking FATP5 display improvement of hepatic steatosis (Doege et al., 2008). The same results are acquired when caveolin-1 deficient mice are used (Mastrodonato et al. 2011). By being a membrane as well as cytosolic protein (Rudick and Anderson 2002), caveolin-1 plays an important role in lipid transport processes, as it directly interacts and carries cholesterol (Murata et al. 1995) and fatty acids (Trigatti, Anderson, and Gerber 1999) intracellularly. Additionally, dietary fats upon digestion are released from the intestine in the form of packed chylomicrons. After hydrolysis, by a process known as spill over the released fatty acids contribute to the circulating FA pool. Despite that these amounts account only for ~20% of FA found in the plasma (Ekstedt et al. 2006), they can still be taken up by the liver where due to an impairment of disposal mechanisms (e.g. β-oxidation, VLDL packaging) they promote hepatic steatosis. In addition, after peripheral lipolysis the remaining chylomicron remnants still contain significant amounts of triglycerides, which after receptor-mediated endocytosis deliver a surplus of dietary fat to the liver. Hepatic DNL is another factor that contributes to hepatic steatosis and is increased in patients as well as in mice with MAFLD (Lambert et al. 2014). The key enzymes that take part in hepatic FA synthesis, namely ACC and FASN, have been found upregulated in murine models of MAFLD as well as in human patients (Morgan et al. 2008, Kohjima et al. 2007, Eissing et al. 2013). As already mentioned in Part C, section 1.2, these enzymes are positively regulated in the transcriptional level by SREBP1c and ChREBP, which are in turn activated by insulin and glucose, respectively. Reasonably, a diet rich in carbohydrates such as glucose and fructose accelerates DNL and is associated with MAFLD (Moore, Gunn, and Fielding 2014). LXR also positively regulate the induction of SREBP1c while FXR inhibits both LXR and SREBP1c, ultimately leading to reduced hepatic steatosis (Yang, Shen, and Sun 2010). Notably, FXR seems to be a crucial regulator of hepatic lipid metabolism while modulation of its signaling is an attractive target for liver disease. As a result, bile acids, by being natural ligands for FXR, as well as the enzymes implicated in bile acid synthesis are gaining a lot of attention in the race to combat MAFLD development.

3.3 Development of inflammation and fibrosis

As mentioned before, the “two-hit” hypothesis model of steatohepatitis establishment that puts TG accumulation as the first incidence is more complicated in reality. In fact, FA incorporation into TG is considered to be rather hepatoprotective, while free FA metabolites emerge as the actual lipotoxic biomolecules (Neuschwander-Tetri 2010). Of note, inhibition of TG synthesis via DGAT deletion - a crucial enzyme for their synthesis - resulted in exacerbation of liver damage and fibrosis in a mouse model of diet-induced steatohepatitis (Yamaguchi et al. 2007). Particularly free FA can activate cellular apoptotic cascades by activating surface molecules including Toll-like receptors (TLRs) or interfering with the integrity of cellular and organelle membranes (Fessler, Rudel, and Brown 2009). Cellular responses to FA overload include their increased oxidation as well as the upregulation of mitochondrial respiratory chain. Under such conditions overproduction of ROS is occurring and if specific antioxidant mechanisms fail to eliminate them, their accumulation fires oxidative stress that promotes MAFLD to steatohepatitis progression. Accumulated free FA as well as free cholesterol in the liver

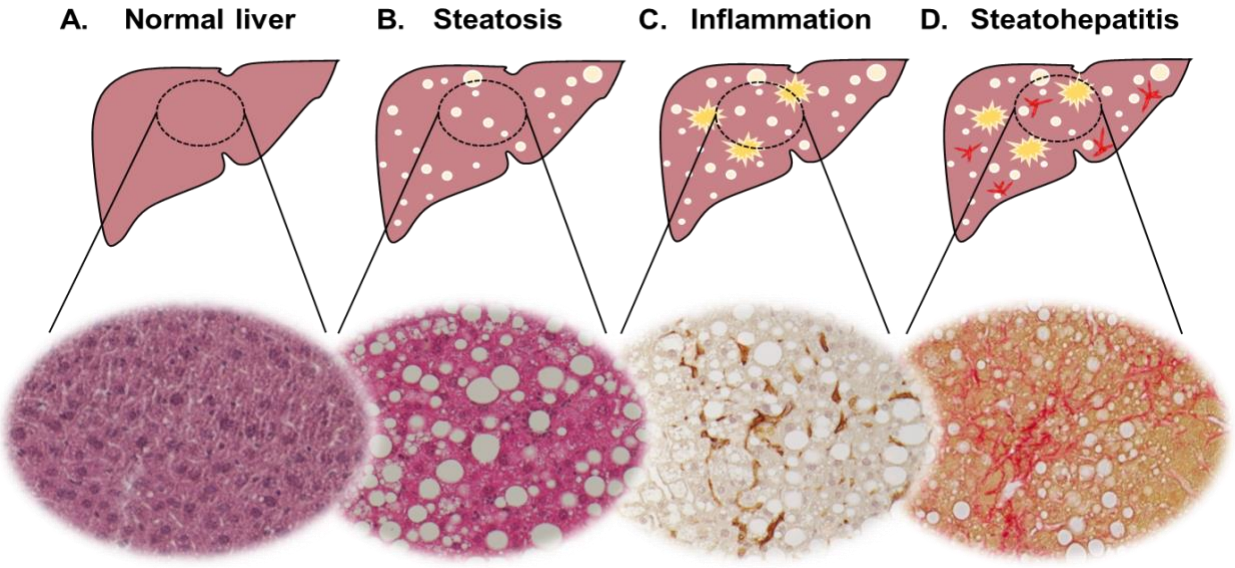

Figure 4. Schematic representation of the different hepatic stages during the progression of MAFLD to steatohepatitis. During MAFLD establishment, the intact morphology of the healthy liver (A) is progressively lost as fat is accumulating (B), infiltration of immune cells and activation of resident Kupffer cells promote inflammation (C) and collagen deposition due to the activation of HSCs (D).

are considered pro-inflammatory, since they can trigger TNFα-mediated liver damage (Feldstein et al., 2004, Marí et al., 2006), ER stress and DNA instability. As a result, hepatocytes undergo activation of specific cellular cascades (e.g. activation of stress kinases like JNKs) while at the same time release factors that promote inflammation and recruitment of immune cells in the liver (Lade, Noon, and Friedman 2014). If such inflammation and hepatocyte damage become chronic, HSCs can be activated by neighboring KCs. The activated HSCs synthesize extracellular matrix (ECM) proteins including collagen, ultimately leading to hepatic fibrosis and further tissue deterioration (Schuppan, Surabattula, and Wang 2018). A subsequent increase of matrix metalloproteinases (MMPs) is ensued with some members described of having pro- and others anti-fibrotic effects (Naim, Pan, and Baig 2017). Alterations of their levels have been associated with MAFLD to steatohepatitis progression (Okazaki et al. 2014) while their inhibitor TIMP-1 is significantly upregulated as well (Thiele et al. 2017).

3.4 Immune cells in MAFLD progression

Adaptive as well as innate immune responses are orchestrating the hepatic immunological phenotype during MAFLD progression and as mentioned in 3.3, hepatic infiltration of immune cells is an important determinant of steatohepatitis development. As MAFLD advances, damage associated molecular patterns (DAMPs) released by the damaged hepatocytes can activate KCs to produce a variety of proinflammatory cytokines such as TNFα and IL6, the levels of which are found elevated in the circulation and the liver in both murine models as well as human patients with steatohepatitis (Tilg 2010,Krenkel and Tacke 2017). In addition to KCs, other cell types such as damaged hepatocytes produce large amounts of the potent chemoattract CC-chemokine ligand 2 (CCL2) which positively correlates with the grade of steatohepatitis and in turn promotes the recruitment of monocytes, neutrophils and natural killer (NK) cells within the inflamed regions of the liver (Krenkel et al. 2018). Apoptotic hepatocytes can also produce pro-inflammatory cytokines of the CXC motif ligand family including CXCL10 that has been also found increased in both human and murine steatohepatitis and mediates monocyte recruitment (X. Zhang et al. 2014). Next to the innate immune cell infiltration, evidence

shows that adaptive immunity plays an equally significant role for the disease development (Sutti and Albano 2020). Studies in mice have shown that CD4+ and CD8+ lymphocytes as well as B cells infiltrate into the liver and worsen hepatic injury and inflammation (Sutti *et al.*, 2014, Wolf *et al.*, 2014). Interestingly, polarization of CD4+ T cells towards IFNγ-T helper 1 (T_H1) as well as IL-17-producing T populations (T_H17) has been reported in patients with steatohepatitis (Inzaugarat *et al.*, 2011, Rau *et al.*, 2016). Similarly, in mice, elevated hepatic IL-17 levels aggravated inflammation in a model of diet-induced MAFLD (Tang et al. 2011), while ablation of IL-17 signaling in rodents fed with the MCD diet resulted in diminished steatohepatitis (Harley et al. 2014). Cytotoxic CD8+ T cells, which are chemoattracted by IFNα-signaling, have been also found elevated in mice and humans with progressive MAFLD (Ghazarian et al. 2017) while ablation of their populations adequately attenuates steatohepatitis in mice fed with a high caloric diet (Bhattacharjee et al. 2017).

4. Bile acids and MAFLD

Regulation of bile flow and composition is a major hepatic function, so irregularities in biliary homeostasis can affect liver function and/or its patho-physiology. In the following section, current knowledge regarding the interplay between bile acids and MAFLD is discussed.

4.1 MAFLD-associated alterations in bile acids/oxysterols

As mentioned above (see Part C, section 2.3), a series of metabolic processes that could be involved in the development of MALFD and steatohepatitis can be regulated by bile acids and/or the intermediate oxysterol products. A number of studies have reported distinct differences in bile acid levels and composition in various biological samples of murine models as well as patients with MAFLD or steatohepatitis. For instance, taurine-conjugated βMCA (T-β-MCA) together with taurocholate (TCA) were specifically increased in the serum of a methionine-choline deficient diet (MCD) fed mice, an

established model to induce fatty liver in rodents, while after methionine or choline supplementation, their levels were normalized (Tanaka et al. 2012). Recently, it was reported that total circulating bile acids are elevated in mice with diet-induced steatohepatitis and are associated with the degree of fibrosis (Suga et al. 2019). Next to observations in animal models, human studies have uncovered important changes in bile acid homeostasis in relation to MAFLD. Of note, postprandial as well as fasting bile acid levels have been found to be significantly elevated in the serum of adult patients with steatohepatitis and relate with its severity (Ferslew et al. 2015)(Bechmann et al. 2012)(Dasarathy et al. 2011). A recent study, however, claimed that elevated serum bile acids are present in patients with steatohepatitis that exert simultaneously insulin resistance, therefore limiting their liability as ubiquitous biomarkers of steatohepatitis (Grzych et al. 2021). Nevertheless, these studies argue towards a systemic exposure to potentially cytotoxic bile acid species, which could eventually trigger liver injury and/or mediate the pathogenesis of the MAFLD. In an effort to identify differences on bile acid species level, a metabolomic analysis of a steatohepatitis cohort revealed increased levels of serum TCA, GCA and GDCA in comparison to healthy individuals (Kalhan et al. 2011). Circulating TCA and GCA, along with both CDCA conjugates, were also elevated in biopsy-proven MAFLD as well as steatohepatitis patients (Puri et al. 2018). In line with the previous observations, Nimer et al. recently described that in a cohort of MAFLD patients, plasma TCA and GCA are positively associated with increasing grades of inflammation and fibrosis, respectively (Nimer et al. 2021). Interestingly, despite the fact that bile acid measurements in liver tissue revealed characteristic changes during MAFLD to steatohepatitis progression, reported outcomes were quite contradictory (Aranha et al. 2008) (Lake et al. 2013). The rationale between these disparities could be attributed to technical limitations of the studies, since bile acids were extracted from whole hepatic tissues. Instead, a compartmentalized analysis of blood-, biliary- or intracellular concentrations is needed in order to identify bile acid alterations in the liver that might be correlated with MAFLD/steatohepatitis. Next to primary bile acid species-related changes, specific alterations between primary and secondary bile acids have been identified in steatohepatitis patients, suggesting dynamic changes in the gut microbiota during the establishment of the disease. The ratio of primary to secondary bile acids is higher in steatohepatitis patients while the ratio of conjugated to unconjugated seem to be relatively

unaffected (Puri et al. 2018)(Mouzaki et al. 2016). However, Legry et al. underlined an association of increased primary bile acids with insulin resistance, but not with hepatic necroinflammation in a biopsy-proven steatohepatitis cohort of obese individuals (Legry et al. 2017). Another study in MAFLD patients revealed specific changes of the gut microbiome and an increase of fecal bile acid concentrations that were related to the degree of hepatic fibrosis in non-obese individuals, but not in obese subjects (Lee et al. 2020). The authors argue that finding no relation between fibrosis and bile acid alterations in the obese state might be explained by a masking effect that obesity already manifests as a significant determinant of commensal microbiota and bile acid synthesis.

Despite that oxysterols are not so extensively investigated in the context of MAFLD and steatohepatitis progression, some interesting data have gathered during the last years. In a small human trial, the LXRα ligands 25- and 27-HC where significantly elevated in the serum of patients with MAFLD patients (Ikegami et al. 2012). A strong induction of serum 27-HC has been observed in genetic murine models of obesity as well (Guillemot-Legris et al. 2016). A recent study showed that hepatic oxysterols levels are elevated in patients as well as a diet-induced mouse model of steatohepatitis, with 7α-HC, 7β-HC and 24-HC being positively correlated to the disease severity. However the same study showed no correlation of hepatic 25- and 27-HC in both species (Raselli et al. 2019). Interestingly, 27-HC was rather reported beneficial for steatohepatitis in mice as its administration reduced hepatic inflammation, via a proposed mechanism that halts lysosomal cholesterol accumulation in KCs (Bieghs et al. 2013).

In summary, the implication of cholesterol metabolites in MAFLD development and progression is increasingly acknowledged, while differential activation or modulation of their receptors for potential therapeutic interventions are still under investigation (Arab et al. 2017).

4.2 Bile acid/oxysterol synthesis enzymes and their receptors in MAFLD

The foundation of bile acid alterations during MAFLD development has extensively been studied in humans and mice, primarily focused on the hepatic expression of bile

acid synthesis-related genes as well as their targets within the enterohepatic circulation (De Boer et al. 2018). The expression of CYP7B1 has been found elevated in patients with steatohepatitis. Notably, CYP8B1 was rather found downregulated, suggesting a possible shift towards the alternative pathway of bile acid synthesis during disease progression (Lake et al. 2013). Of note, knockdown of *Cyp8b1* in mice fed with a high cholesterol diet was reported protective against the progression of MAFLD, an effect that was largely attributed to the remodeling of the BA pool (Chevre et al. 2018). In contrast to patients with steatohepatitis, in a murine model of HFD-induced steatohepatitis, *Cyp7b1* was down-regulated but when *Cyp7b1*$^{-/-}$ mice were given the same diet, no significant differences were observed in relation to the steatohepatitis score, rendering the alternative pathway still ambiguously involved in MAFLD progression (Raselli et al. 2019). Nevertheless, *Cyp7b1* expression has been found significantly reduced in mice and humans with metabolic comorbidities such as obesity and diabetes (Wei et al. 2020, Chen et al. 2016, Worthmann et al. 2017), implying a possible role of the alternative pathway of bile acid synthesis especially during the onset of metabolic diseases. This could be related with the elevated levels of oxysterols, particularly 25-HC, 24-HC and 27-HC, which are substrates of CYP7B1 and accumulate in the liver due its downregulation. The striking result of *Cyp7b1* deficiency in humans was reported in a newborn child, which presented accumulation of hepatotoxic mono-hydroxy bile acids and respective oxysterols that resulted in hepatic inflammation and fatal cirrhosis within the first year of life (Setchell et al. 1998). A later study showed that *Cyp7b1* deletion is firstly implicated with the presence of hepatic fat that promotes steatosis and subsequently MAFLD (Dai et al. 2014).

Many studies, on the other hand, have reported that CYP7A1 expression is increased in MAFLD patients, suggesting that the classical pathway of bile acid synthesis can be also activated (Legry *et al.*, 2017, Jiao *et al.*, 2018). Recently, Govaere et al. conducted a transcriptomic analysis of liver biopsies in patients with MAFLD that were categorized according to disease severity and based on histopathological evaluation (Govaere O et al. 2020). It could indeed be validated that CYP7A1 is up-regulated in all MAFLD stages, with its expression reaching a peak early upon the onset of the disease but progressively decreasing as steatohepatitis advanced. These findings imply that changes in bile acid

synthesis occur very early, so that treatments designed to target bile acid synthesis could be considered even at primary stages of the disease. However, it is still not clear whether the up-regulation of CYP7A1 and its respective products mediate the development or act protectively against some features of the disease. For example, *Cyp7a1*$^{-/-}$ mice presented greater hepatic inflammation, fibrosis and lipid accumulation upon an MCD diet than wild-type controls, while AAV-mediated overexpression of CYP7A1 reversed these detrimental effects (Liu et al. 2016). Therefore, CYP7A1-mediated cholesterol conversion to bile acids could potentially reduce intrahepatic cholesterol accumulation and/or produce ligands for FXR or TGR5.

The bile acid receptors have been also associated with anti-inflammatory responses, while numerous studies highlight important alterations in the bile acid pool size and their enterohepatic circulation during inflammatory diseases such as steatohepatitis (Tanaka et al. 2012). The hepatoprotective activity of FXR has been supported by several animal studies performed in mice lacking FXR and TGR5, which present augmented MAFLD and steatohepatitis-related features (Bjursell *et al.*, 2013, Ferrell *et al.*, 2019). Interestingly, a study comparing liver versus intestine-specific *Fxr*$^{-/-}$ mice underlined that the protective effect against lipid accumulation was mainly attributed to the hepatic presence of FXR and was rather independent of intestinal FGF15 activation (Schmitt et al. 2015). In parallel, since *Tgr5*$^{-/-}$ mice are prone to LPS-induced inflammation (Y. D. Wang et al. 2011), it is postulated that TGR5 could exert significant anti-inflammatory properties during MAFLD and steatohepatitis, but this remains to be elucidated.

The LXR anti-inflammatory properties have been extensively studied in the past (Joseph et al. 2003), rendering its natural ligands oxysterols as attractive targets for inflammatory diseases (Fessler 2018). However, and as already mentioned in section 2.3, LXR activation by various oxysterols can upregulate important genes - including SREBP1c, FASN and ACC - that drive hepatic lipogenesis and eventually steatosis (Griffett et al. 2013). Of note, its inhibition by inverse agonists attenuates hepatic fat accumulation and fibrosis in mice (Griffett et al. 2015). However, it was recently reported that the levels of LXR are not only correlated with hepatic steatosis but also with the degree of hepatic inflammation in patients with advanced steatohepatitis (Ahn et al.

2014). As a result, the role of LXR in steatohepatitis remains contradictory and thus targeting the receptor against the disease faces many challenges.

5. Housing temperature, thermoregulation and metabolic diseases

Since its discovery in mammals, and especially after its detection in humans during the last decades, brown adipose tissue has gained a lot of scientific attention as its activation has been proven beneficial for systemic metabolism and might serve a putative target for related disorders such as obesity (Cypess et al. 2009). On that note, β3-adrenergic stimulation by cold acclimation has been widely used to activate this adipose depot in mice (Cannon and Nedergaard 2004). Therefore, differential housing temperature is a useful intervention to study how metabolic related functions and/or phenotypes are affected by thermogenic responses and *vice versa*. In the following section, the importance of brown adipose tissue as well as recent data on the interplay between thermogenic responses and bile acid metabolism are discussed.

5.1 Thermogenic adipose tissues

Brown adipose tissue (BAT) is an organ with a critical thermoregulatory function at low ambient temperatures as it produces heat by non-shivering thermogenesis with uncoupling protein-1 (UCP1) playing a key role in this process (Cannon and Nedergaard 2004). The activation of BAT has a profound influence on systemic energy metabolism and thus determines plasma glucose, triglyceride and cholesterol levels (Bartelt *et al.*, 2011, Bartelt *et al.*, 2017). Activation of BAT leads to FA mobilization from intracellular stored TGs, which are diverted and metabolized into the mitochondria via the oxidative phosphorylation reactions. The mitochondrial respiratory chain produces a proton gradient from the inner mitochondrial membrane towards the intermembrane space, required for ATP production. UCP1 is a unique protein that uncouples the respiratory chain from this ATP production as it shuttles the protons back to mitochondrial matrix, ultimately leading to the generation of heat. BAT is highly vascularized and innervated by sympathetic nerves and brown adipocytes express β-3 adrenergic receptors. These can

be activated by norepinephrine which is released upon different stimuli such as cold exposure. Physiologically, low temperatures are sensed by thermoreceptors located on the skin and transmit the signal via the central nervous system to the BAT. Intracellularly, upon the release of norepinephrine by the sympathetic nervous system and the concomitant β-3 adrenoreceptor stimulation, G_s-coupled signaling cascades lead to the production of cyclic AMP (cAMP), activation of protein kinase A (PKA) and phosphorylation of various substrates such as mitogen activated protein kinases (MAPK) and cAMP response element-binding protein (CREB). These factors promote the expression of thermogenesis-related markers including UCP1, iodothyronine deiodinase 2 (or DIO2, encoded by *Dio2*) and peroxisome proliferator-activated receptor gamma coactivator 1-alpha (or PGC1a, encoded by *Ppargc1a*). Both PGC1a and DIO2 further contribute to adaptive thermogenesis as they promote *Ucp1* expression (Bartelt and Heeren 2014).

5.2 Ambient temperature and metabolic-associated diseases

The activation of thermogenic adipose tissues and the adaptive thermogenesis are taking place when the environmental temperature is critically below the thermoneutral zone. The thermoneutral zone is described as the ambient temperature where an organism does not need to dispense additional energy to maintain its body temperature. Recent studies have highlighted the difference of human and mouse thermoneutral zones, that are considered to be ~30ºC for mice and ~24ºC for humans (Fischer, Cannon, and Nedergaard 2018a). While humans are usually creating a micro-environment devoid of cold stress, maintenance of mice under housing conditions standard in most animal facilities (*i.e.,* ~22ºC) is exposing the animals to a mild cold stress that can activate adaptive responses. As a result of the thermogenic adipose tissues activation, the metabolic rate and the turnover of energy-containing substrates (such as lipids and carbohydrates) is accelerated. This is of particular importance when studying metabolic-associated diseases as the results from murine studies may not be translated accurately to the human state (Seeley and MacDougald 2021). As reported by several studies, the constant cold stress caused by housing at sub-thermoneutral environments has beneficial

effects against metabolic disorders as it halts their full establishment. On the other hand, thermoneutral housing better recapitulates their complete metabolic-related phenotypes. For example, in obesogenic diet-fed *ApoE*$^{-/-}$ mice being housed under thermoneutral conditions, *i.e.* 30^{o}C, the onset of metabolic inflammation as well as atherosclerosis development are augmented (Tian *et al.*, 2016, Giles *et al.*, 2016). On the other hand, activation of BAT by β3-adrenergic receptor agonism in APOE*3-Leiden.CETP mice, increases energy expenditure and reduces associated hyperlipidemia and hypercholesterolemia, ultimately protecting from atherosclerosis progression (Berbeé et al. 2015). Of great interest for this particular thesis, is one study reporting that thermoneutral housing (30^{o}C) exacerbates the development of MAFLD, since markers for hepatic damage, inflammation and fibrosis are elevated in HFD-fed mice (Giles et al. 2017). At the same time, sub-thermoneutral housing at 22^{o}C impedes the disease progression as most of the associated markers are significantly lower. These observations pinpoint the importance of thermoneutral housing in metabolic disease-related studies performed in rodents, especially when the final goal is translatability to the human state and uncovering of potentially unappreciated key mediators.

5.3 Ambient temperature and cholesterol metabolism: the role of CYP7B1

As already mentioned, cold exposure or β3-adrenergic stimulation triggers the activation of BAT and enhances the lipoprotein processing into this thermogenic organ. Under such conditions, despite the increased cholesterol intake and its uptake into the liver due to higher energy demands, intrahepatic cholesterol is not accumulating due to its conversion to bile acids, mediated by a new mechanism uncovered by a recent study conducted (Worthmann et al., 2017). Specifically, under conditions of cold exposure and cholesterol enriched-diet feeding, a specific upregulation of *Cyp7b1* and hence the alternative synthesis pathway of bile acids is converting the excess of hepatic cholesterol to bile acids (Worthmann et al. 2017) which are subsequently excreted into the feces. Overall, activation of BAT and upregulation of *Cyp7b1* stimulate cholesterol turnover and the production of metabolites that can potentially enhance thermogenic responses

(Kuipers and Groen 2017). In fact, when *Cyp7b1*$^{-/-}$ mice were housed under cold conditions (6^{o}C), bile acid production and excretion were strikingly diminished and the animals exerted impaired adaptive thermogenesis. These systemic adaptations to increased energy expenditure are accompanied by distinct changes in gut microbiota, decreased hepatic lipid accumulation and increased heat production, suggesting an important role of bile acids generated by the alternative synthesis route for steatosis or even MAFLD prevention.

Part D: Aims of the study

Earlier studies in the group of Prof. Heeren (included in the PhD thesis of Dr. rer. nat. Anna Worthmann as well the respective publication Worthmann et al. 2017) showed that housing temperature affects BAT function and determines cholesterol metabolism via a previously unappreciated mechanism. Specifically, cold exposure and the concomitant BAT activation induce cholesterol conversion to bile acids via the upregulation of CYP7B1 and the alternative synthesis pathway. Despite the high fat and increased cholesterol consumption needed to fuel adaptive thermogenesis, cold exposure led to a higher synthesis of bile acids in mice, which could be effectively secreted into the feces and maintain overall cholesterol homeostasis. However, the exact mechanism behind this induction remains elusive. Therefore, the goal of the first part of the thesis was to identify potential factors that are responsible for the upregulation of CYP7B1 observed at lower ambient temperatures.

Secondly, since bile acids are important regulators of lipid metabolism, it was hypothesized that cholesterol derivatives produced via the alternative synthesis pathway may influence systemic metabolism in the context of minimal or increased BAT activity. For this reason, radioactive uptake studies as well as chylomicron production assays were conducted in wild type and CYP7B1-deficient mice that were housed under thermoneutral (30^{o}C) or extreme cold conditions (6^{o}C).

Thirdly, since bile acids and oxysterols are potent ligands for several receptors that regulate metabolic and inflammatory processes, we asked whether the CYP7B1-derivatives may influence MAFLD and the progression towards steatohepatitis in mice. Substantial for this question were previous publications from Fischer et al. 2018 and Giles et al. 2017, which proved that conventional temperatures for humans (around 22^{o}C) are considered suboptimal for animal housing and in fact delay the development MAFLD, possibly via activation of BAT and increase of their energy expenditure. Given the temperature-dependent regulation of CYP7B1, the hypothesis that was tested was whether CYP7B1 prevent the progression of MAFLD to steatohepatitis progression under conditions of low BAT activation. Therefore, in this last part of this thesis, experimental

murine steatohepatitis studies were used to investigate whether CYP7B1 and its related metabolites exert an important role for the MAFLD progression in environments that accurately reflect thermoneutrality for mice and better resemble the human state.

Part E: Materials and Methods

1. Experimental animal models, diets and interventions

1.1 Mouse models and housing

All mouse experiments were approved by the Animal Welfare Officers of University Medical Centre Hamburg-Eppendorf (UKE) and Behörde für Gesundheit und Verbraucherschutz Hamburg. *Cyp7b1*$^{-/-}$ mice were bred and housed in the animal facility of the UKE at 22^{o}C under a day-night cycle of 12 h and *ad libitum* access to drinking water. For our studies, group-caged and age-matched *Cyp7b1*$^{-/-}$ or wild type (WT) male mice (10-12 weeks-old in the beginning of the experiments) were fed with specific diets based on the respective research questions and the designed experimental interventions. At the end of the feeding studies, tissue and blood collections were performed after a 4 h fasting period. Mice were anesthetized with a lethal dose (150µL/g mouse bodyweight) of a mixture containing Ketamin (25mg/mL)/Xylazin (0.2%) in 0.9% NaCl. Systemic blood was withdrawn by cardiac puncture with syringes containing 5µL 0.5M EDTA (Sigma-Aldrich) and portal blood directly by the portal vein with syringes congaing 2µL 0.5M EDTA. Subsequently, the animals were perfused with PBS (unless differently mentioned) and their harvested tissues were immediately either conserved in TriFast reagent (Peqlab) for RNA analysis and in 3.7% formaldehyde solution for histology or stored at −80 °C for further processing. Body weight was monitored once per week throughout the studies and body composition analysis was performed 1 week before the end of the experiments using an EchoMRI Body Composition Analyzer.

1.2 Diets

Before starting the specific diet interventions, mice were fed with a regular chow diet (P1324, Altromin, Germany). The following custom diets were used for our studies:

- Western Type-Diet (WTD) (Ssniff TD88137, 21% butter, 0.2% Cholesterol) for a period of 7-10 days

- Choline deficient high fat diet (CD-HFD, Research Diets; D05010402) for a period of 32 weeks
- Methionine/choline deficient diet (MCD, Envigo Teklad Diets; TD.90262) for a period of 4 weeks

1.3 Interventions

1.3.1 Brown adipose tissue activation after cold exposure

To activate the brown adipose tissue, the animals were kept in individual cages at 6°C for a period of 4-7 days while the corresponding control groups were also kept in individual cages at room temperature (22^{o}C) or thermoneutrality (30°C), all according to individual experimental setups.

1.3.2 Postprandial lipid uptake studies and organ distribution

To analyse lipid uptake upon different ambient temperatures, WT and *Cyp7b1*$^{-/-}$ mice were fed a WTD diet + 0.2% cholesterol for a total period of 10 days, and only during the last 7 days they were housed either under thermoneutral (30^{o}C) or cold conditions (6^{o}C). Mice were fasted for 4 h and then gavaged with 200µL corn oil traced with [9, 10-^{3}H (N)]-triolein (185kBq/mouse) and [4-^{14}C]-cholesterol (32kBq/mouse). Two hours after oral administration, mice were anaesthetized with ketamine/rompun and were transcardially perfused with PBS containing 10U/mL heparin. Organs were collected, weighted and solubilized in Solvable (Perkin Elmer, 0.1mL per 10 mg organ) at 60°C. Scintillation fluid (Aquasafe 500 Plus, Zinsser Analytic) was added to 400µL of tissue lysate or 10µL plasma and radioactivity was measured in a liquid scintillation counter (Perkin Elmer Tricarb). Radioactivity was calculated as dpm per mg organ or µL plasma. For total organ uptake, calculations were adjusted using the equivalent organ weights.

1.3.3 Intestinal chylomicron production studies

To determine intestinal lipoprotein production upon different ambient temperatures, WT and *Cyp7b1*$^{-/-}$ mice were fed a WTD diet + 0.2% cholesterol for a total period of 10

days, and only during the last 7 days they were housed either under thermoneutral (30°C) or cold conditions (6°C). Mice were fasted for 4 h and then intravenously injected with Triton WR 1339 (Tyloxapol, Sigma-Aldrich) as a 10% solution in NaCl, at a dose 0.5mg/g bodyweight, in order to inhibit the enzymatic activity of LPL. Immediately after, mice were gavaged with 200μL corn oil traced with [9, 10-^{3}H (N)]-triolein (185kBq/mouse) and [4-^{14}C]-cholesterol (32kBq/mouse). Plasma was collected by tail bleeding 0, 15, 30, 60, 120 and 240min after lipid gavage and chylomicron production was determined by measuring plasma cholesterol and TGs. Four hours after the oral administration, mice were anaesthetized with ketamine/rompun and were transcardially perfused with PBS containing 10U/mL heparin. Organs were collected, weighted and solubilized in Solvable (Perkin Elmer, 0.1mL per 10 mg organ) at 60°C. Scintillation fluid (Aquasafe 300 Plus, Zinsser Analytic) was added to 400μL of tissue lysate or 10μL plasma and radioactivity was measured in a liquid scintillation counter (Perkin Elmer Tricarb). Radioactivity was calculated as dpm per mg organ or μL plasma. For total organ uptake, calculations were adjusted using the equivalent organ weights.

1.3.4 Fasting-refeeding studies

For refeeding studies, WT and *Cyp7b1*$^{-/-}$ mice that were kept only at cold conditions (6°C) were initially fasted for 6h and then given access to food for the last 2h before the organ harvest.

1.3.5 Atorvastatin/Ezetimibe treatment

To inhibit cholesterol production in the liver, the drug atorvastatin (AT) was administered to the animals. AT, like all statins, blocks the enzyme HMG-CoA reductase, which is responsible for cholesterol production. To inhibit dietary cholesterol absorption in the intestine, the drug ezetimibe (EZ) was administered to the animals. EZ inhibits the absorption of cholesterol by blocking the clathrin-AP2 mediated endocytosis of cholesterol-bound to Niemann-PickC1-like1 (NPC1L1) and thus its internalization (Ge et al. 2008). The daily administration of (0.0036% w/w) AT (Trade name Atorvastatin HEXAL®) and (0.006% w/w) EZ (Trade name Ezetrol®) was performed orally via the diet. For this, ½ Atorvastatin HEXAL® tablet (20mg AT) and 3⅓ Ezetrol® tablets (33.3mg EZ) were crushed and dissolved in 20ml of pure EtOH. Subsequently, 556g of WTD were

soaked with the AT/EZ solution and the food was shaken until the EtOH was completely evaporated.

1.3.6 RORa agonist/inverse agonist injections

To activate RORα, the organic compound SR1078 (TOCRIS) was used as a specific agonist of retinoic acid receptor-related orphan receptors. The mice received daily intraperitoneal SR1078 injections (diluted in 10% DMSO in NaCl) at a dose of 10mg/kg for a total period of 7 days before the organ harvest. Control mice were injected only with a 10% DMSO in NaCl solution. To inhibit RORα activity, the synthetic RORα selective inverse agonist SR3335 (Cayman Chemical) was used (Kumar et al. 2011). The mice received twice a day intraperitoneal SR3335 injections (diluted in 10% DMSO in NaCl) at a dose of 15mg/kg for a total period of 4 days before the organ harvest.

2. Genotyping

2.1 DNA isolation

To isolate DNA from tail biopsies, they were first digested overnight at 37°C using 700µL STE buffer to which 10µL proteinase K was added. After addition of 70µL 10% SDS and 270µL 5M NaCl to the lysate, the precipitated proteins were pelleted by centrifugation at RT for 10 min 13.000g. 450µL of the DNA-containing supernatant was washed in 900µL 70% EtOH, and the DNA was then pelleted by centrifugation at 4°C for 30 min at 13.000g. The excess EtOH was removed and the DNA pellet was dried for 2 hours at 42°C and 300 rpm. DNA was taken up in 50µL ddH_2O.

2.2 PCR Reaction

The following were mixed for each PCR reaction:

Table 2. PCR reaction for Cyp7b1

Material	Amount (µL)
ddH20	18.00
10XPCR-Buffer GREEN	2.50
10 mM dNTP	0.50
10 µM Primer 6s	1.00
10 µM Primer 3UTRas	1.00
10 µM Primer SI-75	1.00
Taq-Polymerase (5 U/µl)	0.03
DNA	1.0
Total Reaction	25.0

Table 3. PCR primer sequences from 5’ to 3’

Primer	Sequence
6s	ACAGGAAGCCTATAGGGCTAAATCACAGTC
3UTRas	AACAAGAGTAGCGGTTGCATTTGGGGGAGT
SI-75	GATTGGGAAGACAATAGCAGGCATGC

The PCR reactions were briefly centrifuged down in the table centrifuge and the PCRs were carried out according to the following programs:

Table 4. PCR program

Step	Temperature	Time
1	95°C	5min
2	95°C	30sec
3	60°C	20sec
4	72°C	30sec
	Repeat steps 2-4 for 35 cycles	
5	72°C	5min
6	4°C	oo

The PCR products were separated in or 2.5% agarose gels (2.5 agarose, 100 ml TBE buffer, 5 µl Roti®-GelStain) by means of gel electrophoresis at a current of 120 mA for 60 min. 5 µl of GeneRuler ™ DNA Ladder Mix were applied as a marker. The bands were made visible under UV light and photographed. For the *Cyp7b1* PCR, the wild-type (WT) (+/+) band was 195 bp and the KO (d/d) band was 140 bp in size.

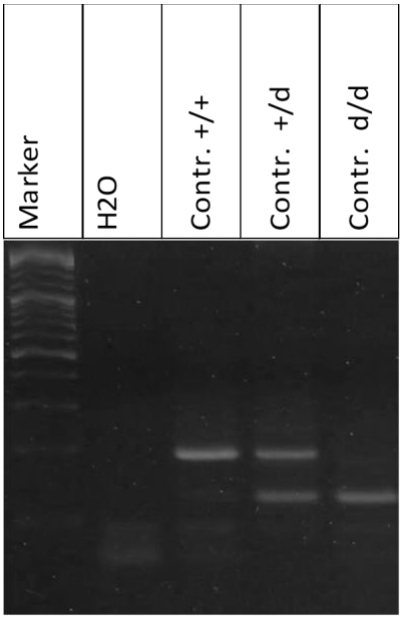

Figure 5. Exemplary PCR results from the *Cyp7b1* PCR. In addition to the marker, the gel picture shows the PCR products of homozygous WT (+/+), heterozygous (+/d) as well as KO samples (d/d).

3. Blood and plasma parameters

3.1 Blood glucose measurement

Glucose was determined in a drop of the animals' tail blood using Accu-Check Aviva test strips and the associated test device.

3.2 Plasma collection

To obtain blood plasma from whole blood, blood was collected either from the tail vein using EDTA-coated Microvettes® or from the heart as described in 1.1. After the heart blood was transferred to a reaction tube, both tail and heart blood were stored on ice until further processing. To separate the cellular blood components, the whole blood was centrifuged at 4 °C for 10 min at 10.000 g. The plasma was then transferred to a new reaction tube and was stored at -80 °C if it not directly analysed.

3.3 Determination of plasma Triglycerides, Cholesterol and NEFAs

Plasma cholesterol and triglycerides were determined using commercial colorimetric kits (Roche) that were adapted to 96-well microtiter plates with Precipath (Roche) as standard. In each case, 100 µL Precipath or sample diluted with PBS was mixed with 200 µL reagent in a microtiter plate and incubated at 37 °C for 10 minutes. The absorbance of the resulting reaction product was determined photometrically at 540 nm. Linear regression of the absorbances of different dilutions of the standard series was used to calculate the lipid concentrations of the samples. Free fatty acids (FFAs) were determined photometrically using the NEFA-HR(2) Assay (FUJIFILM).

3.4 Lipoprotein profiling

Plasma was combined in equal amounts for each experimental group. To separate the individual lipoprotein classes, 200 µL of the plasma pool was separated by fast-performance liquid chromatography (FPLC) on a Superose 6 Increase 10/300 GL (GE Healthcare) at a flow rate of 0.4mL/ min. FPLC buffer was used as the running medium. Using a fraction collector, 40 fractions with a volume of 0.5 mL were collected in a MegaBlock® plate and the cholesterol and triglyceride content of each fraction was determined as described in 3.3.

3.5 Insulin measurement

Plasma insulin levels were measured with an ELISA kit (ChrystalChem), following a low-range assay according to the manufacturers protocol.

3.6 Plasma activity of alanine aminotransferase

For assessment of liver damage, we determined plasma activity of alanine aminotransferase (ALT) using a photometric ALT Activity Assay (Sigma-Aldrich), following the manufacturer's protocol.

4. Enzymatic determination of total lipid content in liver tissue

Using a metal ball, approximately 100 mg of liver tissue were homogenized in PBS (10 µL/mg). After dilution, the lysate was used directly to measure triglyceride concentration as described in 3.3. For the determination of cholesterol concentration, 50 µL of the lysate were extracted with a solution of chloroform/methanol (8/5, v/v). For this purpose, lysate and solvent were first mixed vigorously and then precipitated proteins were separated by centrifugation for 5 minutes at 13.000 g. 200 µL of the supernatant were transferred to a new reaction tube and dried at 80°C. The lipid film was taken up in 200 µL PBS and homogenized for 20 min at 50°C and 600 rpm. Amplex Red reaction mixture (Amplex Red: 1/67, Horseradish peroxidase:1/100, cholesterol oxidase:1/100, cholesterase: 1/100 in PBS) was added to 50 µL of the homogenate as well as Precipath® and incubated for 30 min at 37°C. Fluorescence was measured at an excitation wavelength of 515 nm and emission of 570 nm. The lipid concentrations obtained were normalized to the protein content of each liver. Protein concentration in the liver was performed according to the method of Lowry. For this purpose, the protein standard (various dilutions of a BSA solution) and 10 µL of the lysate prepared above (1/25 diluted with PBS) were added to 40 µL of 0.1 M NaOH and 500 µL of a mixture of Lowry solution A and Lowry solution B (50/1, v/v) in a MegaBlock® plate, mixed, and incubated for 10 minutes in the dark. Then 50 µL of Folin reagent was added to each well and incubated again for 20-30 minutes in the dark. The absorbance of the resulting reaction product was

measured at a wavelength of 740 nm, and the protein concentration was determined via linear regression of the standard curve.

5. Histology – Immunohistochemistry

For hepatic histological analysis liver tissues were first fixed in 3.7% formaldehyde solution after perfusion and then embedded in paraffin. Hematoxylin/Eosin, Sirius Red as well as immunohistochemistry (IHC) stainings were performed on 4µm sections of the paraffin-embedded tissues using standard procedures. For IHC stainings we used rat-anti-Ly6c (abcam) and rat-anti-F4/80 (BIORAD) primary antibodies, all in a dilution of 1:200 in 3% BSA (Sigma). Horseradish peroxidase (HRP) coupled donkey-anti-rat (Jackson Immunoresearch) was used as secondary antibody. Images were taken using a NikonA1 Ti microscope equipped with a DS-Fi-U3 brightfield camera. For fibrosis quantification, the Sirius Red-positive area was quantified in at least 6 fields per section using Adobe Photoshop and ImageJ in a blinded fashion as previously described (Pradere et al. 2013). Ly6c positive cells were quantified by counting the number of stained cells in at least 6 fields per section in a blinded manner.

6. Western blotting

For SDS–PAGE protein analysis, samples were homogenized in a tissue lyser (Qiagen) by adding a 10x (v/w) RIPA buffer (50 mM Tris-HCl pH 7.4, 5 mM EDTA, 150 mM sodium chloride, 1 mM sodium pyrophosphate, 1 mM sodium fluoride, 1 mM sodium orthovanadate, 1 % NP-40) supplemented with cOmplete Mini Protease Inhibitor Cocktail Tablets (Roche) and Phosphatase Inhibitor Cocktail (Bimake.com). Lysates were centrifuged at 16.000 g for 10 min, the clear soluble middle layer without the fat was taken, and protein concentration was determined using a Lowry method. 20 µg of total protein in NuPAGE reducing sample buffer (Invitrogen) were denatured at 60°C for 10 min and separated on 10% SDS-polyacrylamide Tris-glycine gels. Transfer to nitrocellulose membranes was performed in a wet blotting system, membranes were stained with Ponceau S (Serva) to confirm equal loading, washed twice in TBS-T (20 mM Tris, 150

mM sodium chloride, 0.1 % (v/v) Tween 20) and blocked in 5% milk powder (Sigma) in TBS-T or ROTI®Block (Roche) for 1 hour at room temperature. Primary antibody incubation (5% BSA in TBS-T) was performed overnight at 4°C. Secondary antibodies were diluted in 5% milk powder in TBS-T, and detection was performed with enhanced chemiluminescence using an Amersham Imager 600 (GE Healthcare). The following primary antibodies were used: γ-Tubulin (rabbit monoclonal; 1:2000; cat. No. ab179503, abcam), AKT (rabbit polyclonal; 1:1000, cat#9272, cell signaling), phospho-AKT-(Ser473) (rabbit polyclonal; 1:1000, cat#9272, cell signaling), LPL (goat polyclonal; 1:2000, self-made), FASN (mouse monoclonal; 1:1000, cat#610962BD Biosciences), phospho-(Ser/Thr) PKA Substrate (rabbit polyclonal; 1:1000, cat#9621, cell signaling), total OXPHOS cocktail (mouse monoclonal; 1:25000, cat#ab110413, abcam), GPIHBP1 (rat monoclonal; 1:1000, self-made), LDLR (rabbit monoclonal antibody; 1:1000, cat# ab52818, abcam), CYP7B1 (rabbit monoclonal antibody; 1:1000, cat# ab138497, abcam). The following secondary antibodies, in a dilution of 1:5000, were used: HRP goat anti-rabbit (cat# 111-035-144, Jackson ImmunoResearch Labs), HRP goat anti-mouse (cat#115-035-003, Jackson ImmunoResearch Labs), HRP donkey anti-rat (cat#712-035-150, Jackson ImmunoResearch Labs) HRP mouse anti-goat (cat# 205-035-108, Jackson ImmunoResearch Labs).

7. Gene Expression Analysis

7.1 RNA isolation - Reverse transcription

To isolate RNA from liver tissue, a piece of liver was firstly mixed with peqGOLD TriFast™ or TRIzol™ Reagent and then homogenized using metal beads and shaking in tissue lyser (Qiagen). Chloroform was added to the lysate in a 5:1 ratio and then homogenized again. A centrifugation at 13.000 g for 15 minutes was then performed for phase separation. The RNA contained in the upper phase was carefully removed and precipitated in a fresh reaction tube containing 70% EtOH. Using the commercially available NucleoSpin® RNA II kit (Macherey & Nagel), the RNA was purified according to the manufacturer's instructions and finally dissolved in ddH_2O. RNA concentration was

determined with NanoDrop and 400 ng of RNA were used for reverse transcription into cDNA by using the High-Capacity cDNA Reverse Transcription Kit, according to manufacturer's protocol.

7.2 Quantitative real time PCR

Quantitative real time PCR (qPCR) was performed to quantify gene expression. For this purpose, TaqMan Assay-on-Demand™ primer sets (Table 5) and Universal PCR MasterMix (Applied Biosystems) were mixed with the cDNA to be analysed. For specific reactions, SYBR™ Green PCR Master Mix was used in combination with custom designed primers from Eurofins (Table 6). The qPCR reaction and quantification of the reaction product were performed using the ABI Prism 7900HT Sequence Detection System or the QuantStudio™ 5 Real-Time PCR System. Measured values were normalized to TATA-box binding protein (*Tbp*) housekeeper gene as described before and relative gene expression was calculated via the 2-ΔΔCt-method (Livak and Schmittgen 2001). The following TaqMan Assay-on-Demand™-Primer were used:

Table 5: Gene names and TaqMan Assays-on-Demand™

Gene name	Assay-on-Demand™	Gene name	Assay-on-Demand™
Tbp	Mm00446973_m1	*Hmgcr*	Mm01282499_m1
Abca1	Mm00442646_m1	*Hsd11b1*	Mm00476182_m1
Abcb11	Mm00445168_m1	*Il1b*	Mm00434228_m1
Abcg1	Mm00437390_m1	*Il6*	Mm00446190_m1
Abcg5	Mm00446249_m1	*Infg*	Mm00801778_m1
Abcg8	Mm00445970_m1	*Ldlr*	Mm00440169_m1
Acta2	Mm00725412_s1	*Lipe*	Mm00495359_m1
Baat	Mm00476075_m1	*Lipg*	Mm00495368_m1
Ccl2	Mm00441242_m1	*Lpl*	Mm00434764_m1
Ccl5	Mm01302428_m1	*Lrp1*	Mm00464608_m1
Cd4	Mm00442754_m1	*Mmp12*	Mm00500554_m1

Cd36	Mm00432403_m1	*Mmp13*	Mm00439491_m1
Cd68	Mm03047343_m1	*Nr0b2*	Mm00442278_m1
Cd8b1	Mm00438116_m1	*Pnpla2*	Mm00503040_m1
Chrebp-beta	AIVI4CH	*Ppargc1a*	Mm00447183_m1
Col1a1	Mm00801666_g1	*Scd1*	Mm00772290_m1
Cxcl1	Mm00433859_m1	*Slc27a1*	Mm00449511_m1
Cxcl10	Mm00445235_m1	*Slc27a4*	Mm01327405_m1
Cxcl9	Mm00434946_m1	*Slc27a5*	Mm00447768_m1
Cyp27a1	Mm00470430_m1	*Slc2a1*	Mm00441480_m1
Cyp7a1	Mm00484150_m1	*Slc2a4*	Mm01245502_m1
Cyp7b1	Mm00484157_m1	*Sult2a1*	Mm04205657_mH
Cyp8b1	Mm00501637_s1	*Sult2b1*	Mm00450550_m1
Dio2	Mm00515664_m1	*Tgfb1*	Mm00441724_m1
Elovl3	Mm00468164_m1	*Timp1*	Mm00441818_m1
Fasn	Mm00662319_m1	*Tnf*	Mm00443258_m1
Foxp3	Mm00475156_m1	*Trem2*	Mm00451744_m1
Gpihbp1	Mm01205849_g1	*Ucp1*	Mm00494069_m1

Table 6: Gene names and custom designed primers

Gene name	FW primer sequence	REV primer sequence
Cd9	TGCTGGGATTGTTCTTCGGG	GCTTTGAGTGTTTCCCGCTG
Gpnmb	GAGCACAACCAATTACGTGGCT	GGTGATATTGGAACCCACCAGA

8. Bile acid measurements

Bile acids were quantified by HPLC coupled to electrospray ionization tandem mass spectrometry (John et al. 2014). Briefly, portal plasma samples were spiked with internal standards and bile acids were extracted using a simple methanol liquid-liquid extraction. Quantitative measurement of bile acids was performed using a LC-ESI-QqQ system run multiple reaction monitoring (MRM) mode. HPLC analysis was performed using NEXERA

X2 LC-30AD HPLC PUMP (Shimadzu, Tokyo, Japan) equipped with a Kinetex C18 column (100 Å, 150 mm × 2.1 mm i.d., Phenom-enex, Torrance, CA, USA) coupled to QqQ: Q trap 5500 System (SCIEX, Darmstadt, Germany), with mobile phase A consisting of water and mobile phase B consisting of acetonitrile methanol (3/1 v/v) both enriched with 0.1% formic acid and 20mM NH_4Acetate. Peaks were identified and quantified by comparing retention times, as well as MRM transitions and peak areas, respectively, to particular corresponding standard chromatograms.

9. Liver lipid analysis

For lipid analysis of structural and storage lipids, snap frozen liver samples were homogenized and extracted using MTBE/methanol. Lipidyzer™ Internal Standards (SCIEX) were added to all samples during lipid extraction. Lipid extracts were concentrated and reconstituted in running buffer containing 10mM ammonium acetate, dichloromethane / methanol (50/50). Lipid species were quantified using an ESI-QqQ system in multiple reaction monitoring (MRM) mode (QTRAP® 5500; SCIEX) employing the Lipidyzer™ software.

10. Liver hydroxycholesterol analysis

Hepatic hydroxycholesterols were analyzed after derivatization with Girard P reagent as previously described (Meljon et al. 2012). Targeted analysis by HPLC coupled to electrospray ionization tandem mass spectrometry was subsequently performed. Briefly, liver samples (approx. 100-150mg) were homogenized in chloroform/methanol (1:1, v/v) and the resulting extract was vacuum dried. After resuspension in ethanol, samples were fractionated using reversed phase solid phase extraction (SPE) to enrich oxysterols devoid of cholesterol (Sep-Pak cartridges, Waters, Milford, MA, USA). Subsequently oxysterols were derivatized with Girard P reagent followed by another SPE clean-up to deplete excess Girard P reagent. Oxysterols were separated on a hypersil GOLD reversed phase column (50 x 2.1 mm, 1.9 µm; Thermo Fisher Scientific) using 49.9%

H2O, 33.3% MeOH, 16.7% acetonitrile and 0.1% formic acid as mobile phase A and 4.9% H2O, 63.3% MeOH, 31.7% acetonitrile and formic acid 0.1% as mobile phase B. The HPLC (NEXERA X2 LC-30AD HPLC PUMP; Shimadzu, Tokyo, Japan) was coupled to a QqQ: Q trap 5500 System (SCIEX, Darmstadt, Germany) run in MRM mode and quantification was achieved by comparing retention times, MRM transitions and peak areas, respectively, to particular corresponding standard chromatograms.

11. Immune cell isolation – FACS analysis

Spleen immune cells and liver lymphocytes were isolated as described previously (Schwinge et al. 2015). Briefly, spleens were meshed through a 100 µm cell-strainer in order to get a single cell suspension. Erythrocytes were lysed by short-term incubation of spleen cells in ACK-buffer. For the isolation of liver non-parenchymal cells (NPCs), mouse livers were perfused with PBS and mechanically dissected trough a 100 µm cell-strainer. Hepatocytes and debris were pelleted twice at 40xg and non-parenchymal cells were re-covered by centrifugation over a 35% Optiprep (Sigma-Aldrich, Taufkirchen, Germa-ny) gradient at 400xg. Immunofluorescence surface staining was performed with anti-bodies against CD3, CD4, CD8, NK1.1, CD45.2, CD11b, CD11c, Ly6C, Ly6G (all Bio-Legend, Koblenz, Germany). Dead cells were stained with Pacific Orange™ Succin-imidyl Ester (Thermo Fisher Scientific, Germany) and excluded from further analysis. For intracellular cytokine staining, cells were restimulated with PMA (10 ng/ml) and ionomycin (1 µg/ml, both Sigma-Aldrich, Germany) in the presence of GolgiPlug™ (1 µl/ml, BD Biosciences, USA) for 4 h. Cells were PFA fixed and perforated in PBS con-taining 0.5% saponine and 2% BSA and stained for IL-17, IFNgamma and TNF (all Bio-Legend, Koblenz, Germany). Flow cytometry was performed using a BD LSR II cytome-ter (BD Biosciences, Heidelberg, Germany) and data were analyzed with FACS DIVA software.

12. Statistics

Data are presented as mean ± s.e.m. Statistical analysis were made in Microsoft Excel 2013 and Graph Pad Prism 8.0, where either two-tailed unpaired T-Test, one-way ANOVA or two-way ANOVA were conducted, depending on the groups and parameters which were compared at each experiment. No statistical method was used to predetermine sample size. The statistical parameters (i.e., p values, numbers of biological repeats) can be found in the figure legends. No exclusion or inclusion criteria were used for data analyses. $P < 0.05$ was considered significant.

Part F: Results

1. Regulation of *Cyp7b1* expression upon cold exposure

1.1 Time- and temperature-dependent hepatic expression of *Cyp7b1*

After unravelling that the hepatic expression of *Cyp7b1* is induced by a 7-day cold stimulus in mice fed with a WTD, we aimed to investigate if such a response is already triggered at a shorter period of cold stimulation. For this reason, we housed wild type mice at a cold environment (6°C) for 1 and 3 three days and compared them with thermoneutral-housed littermates (30°C). We could show that the upregulation of *Cyp7b1* occurs already after 3 days of cold acclimation while 1 day of cold stimulus is rather insufficient to promote this effect (Figure 6A). Further, since temperatures below 30°C are considered sub-thermoneutral and expose mice to a mild-cold stress, we wanted to investigate how *Cyp7b1* expression is affected under different housing temperatures. For this reason, we housed wild type mice for a period of 4 days at thermoneutrality (30°C, control) and at conditions of mild (22°C) and more severe (16°C and 6°C) cold exposure. Significant upregulation of hepatic *Cyp7b1* was already observed upon housing at 16°C

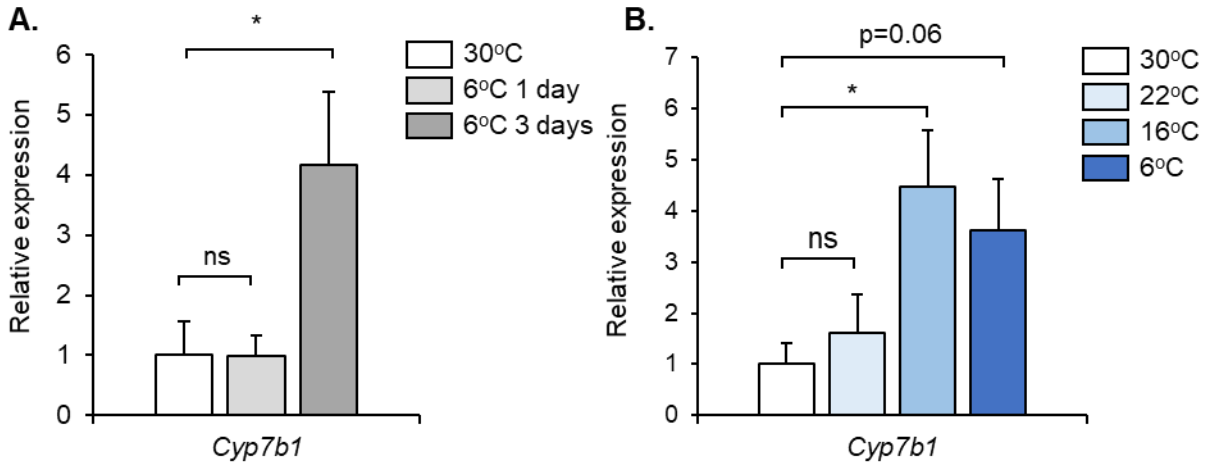

Figure 6. Effect of cold exposure duration and housing temperature on *Cyp7b1* expression. Hepatic expression of *Cyp7b1* in wild type mice fed with a WTD and housed under A) differential duration of cold exposure (6°C) or B) different ambient temperatures for 4 days. Data are shown as mean values ± SEM with N=3-4 mice/group. Bars represent relative expression with *Tbp* as a house-keeper. Statistics are performed with one way-ANOVA.

while housing under the conventional temperature of 22°C showed a trend towards the same effect, yet not significant, for the given time point of 4 days (Figure 6B).

1.2 Insulin signaling is not responsible for *Cyp7b1* induction upon cold

While various factors have been postulated to affect the differential expression of *Cyp7b1*, the mechanism that drives its upregulation after cold exposure in mice fed with a WTD is still not clear. A previous study showed that the LIRKO mouse model, which lacks the insulin receptor specifically in the liver. This liver-specific deletion causes hepatic insulin resistance and a disrupted insulin signalling (Michael et al. 2000). These LIRKO mice exert significantly lower expression of *Cyp7b1* after feeding a lithogenic diet (Biddinger et al. 2008). Accordingly, we asked whether insulin signalling is an important determinant for the cold-induced *Cyp7b1* expression in mice fed a WTD. A common experimental procedure to promote insulin secretion, and as a result insulin signalling in the responsive organs such as the liver, is fasting and refeeding (Agouni et al. 2010). In our previous animal studies, the conditions that induced a robust increase in *Cyp7b1*

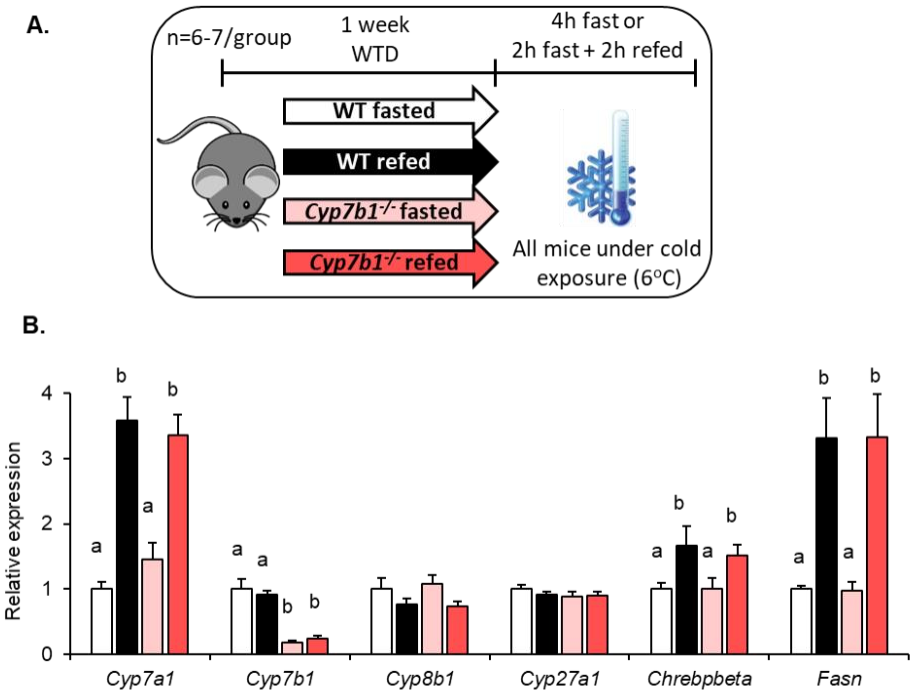

Figure 7. Effect of refeeding on Cyp7b1 regulation upon cold exposure. A) Experimental setup scheme, B) hepatic gene expression of fasted vs refed wild type mice, all housed at extreme cold conditions (6°C) and fed with a WTD for a week. Data are shown as mean values ± SEM with N=6-7 mice/group. Bars represent relative expression with *Tbp* as a house-keeper. Different letters indicate significant differences between groups ($p<0.05$) determined by two-way ANOVA.

expression were WTD feeding and housing at severe cold conditions (6^{o}C) for a week. Here, we employed a similar study setup, but the animals were either completely fasted for 4 hours or only for 2 hours that were followed by a refeeding intervention for additional 2 hours. The goal for the last condition was to promote an insulin response, as depicted in the experimental setup scheme (Figure 7A). Hepatic expression analysis showed that under both fasting and refed conditions, *Cyp7b1* levels were comparable, while not detectable in our knockout mice (Figure 7B). On the other hand, mRNA levels of *Cyp7a1* and known insulin-responsive genes such as carbohydrate-responsive element-binding protein beta (*Chrebpbeta*) and fatty acid synthase (*Fasn*) were positively regulated by refeeding conditions regardless of the mouse genotype (Figure 7B). These results indicate that refeeding and a concomitant insulin response are not, at least alone, responsible for the hepatic *Cyp7b1* upregulation after cold stimulus.

1.3 Cholesterol absorption or synthesis are dispensable for *Cyp7b1* induction upon cold

It has been observed that *Cyp7b1* and the alternative BA synthesis pathway are induced after cold exposure when mice are fed with a WTD that contains 0.2% cholesterol but not a chow diet (data not shown). Cholesterol is the initial substrate for BA synthesis but data so far are inconclusive regarding its potential role for *Cyp7b1* regulation. One study showed that the enzyme's activity was increased after cholesterol addition in primary rat hepatocytes (Pandak et al. 2002). Another study pointed towards a minimal influence on rat *Cyp7b1* activity when cholesterol was supplemented in the diet (Ren et al. 2003). Nevertheless, little is known regarding the implication of this sterol for the transcriptional control of *Cyp7b1*. Since conditions of cold exposure are translated to higher energy demands, which results due to accelerated flux to increased cholesterol transport to the liver (Bartelt et al., 2017), the next question to be examined was whether cholesterol is the key factor of the WTD that drives *Cyp7b1* induction. During the experimental approach, wild type mice were fed with a WTD and housed either under thermoneutral (30^{o}C) or cold environments (6^{o}C). In order to block cholesterol synthesis and uptake, half of the groups were treated with a combination of Ezetimibe (EZ) and Atorvastatin (AT) (Figure 8A). Under these conditions *Cyp7b1* was upregulated even after AT/EZ treatment, despite not reaching statistical significance due to higher standard

deviation (Figure 8B). Other genes related to bile acid synthesis and transport like *Cyp27a1, Cyp7a1, Cyp8b1, Baat and Nr0b2* were largely unaffected by the AT/EZ treatment. Therefore, we concluded that cholesterol absorption or *de novo* synthesis have both a rather minor impact on the induction of *Cyp7b1* and the alternative synthesis pathway under conditions of increased energy expenditure.

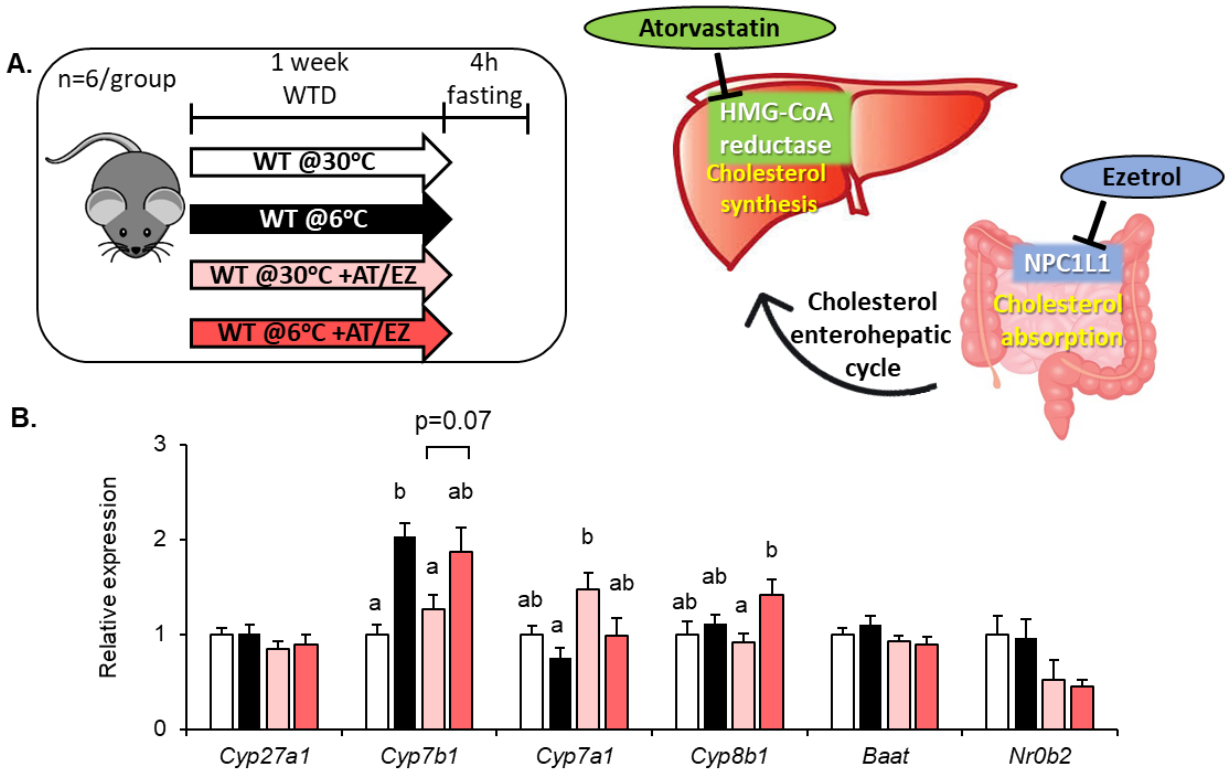

Figure 8. Effect of cholesterol synthesis/absorption on *Cyp7b1* regulation upon cold exposure. A) Experimental setup scheme and AT/EZ functions, B) hepatic gene expression. Data are shown as mean values ± SEM with N=6-7 mice/group. Bars represent relative expression with *Tbp* as a house-keeper. Different letters indicate significant differences between groups ($p<0.05$) determined by two-way ANOVA.

1.4 RORα agonism triggers *Cyp7b1* expression and bile acid alterations under thermoneutral housing

Since the induction of *Cyp7b1* occurs at the transcriptional level after cold exposure (Figure 6A), to the next aim was to identify potential transcriptional factors that may drive its expression under the given experimental conditions. RAR-related orphan receptor alpha (RORα or NR1F1) was recently described as a positive regulator of *Cyp7b1* in mice (Wada et al. 2008), which triggered the question of whether this factor can drive the

enzyme's expression under conditions of high energy expenditure and increased cholesterol intake. Firstly, in order to delineate whether RORα activation can trigger *Cyp7b1* expression solely upon a WTD feeding, wild type mice fed with the regimen were housed under thermoneutral conditions (30°C) for a week and were daily injected intraperitoneally with SR1078, a synthetic agonist for RORα (Y. Wang et al. 2010) (Figure 9A). Hepatic expression analysis revealed that *Cyp7b1* was the only upregulated among all bile acid-related genes that were measured (Figure 9B). Additionally, this led to an upregulation of the alternative synthesis pathway of bile acids depicted in the higher levels of CDCA and UDCA as well as their taurine conjugated forms, TCDCA and TUDCA, respectively (Figure 9C). This proved that RORα activation leads to *Cyp7b1* induction and triggers specific changes in the bile acid pool in mice which were fed a WTD and were housed under thermoneutral conditions (30°C).

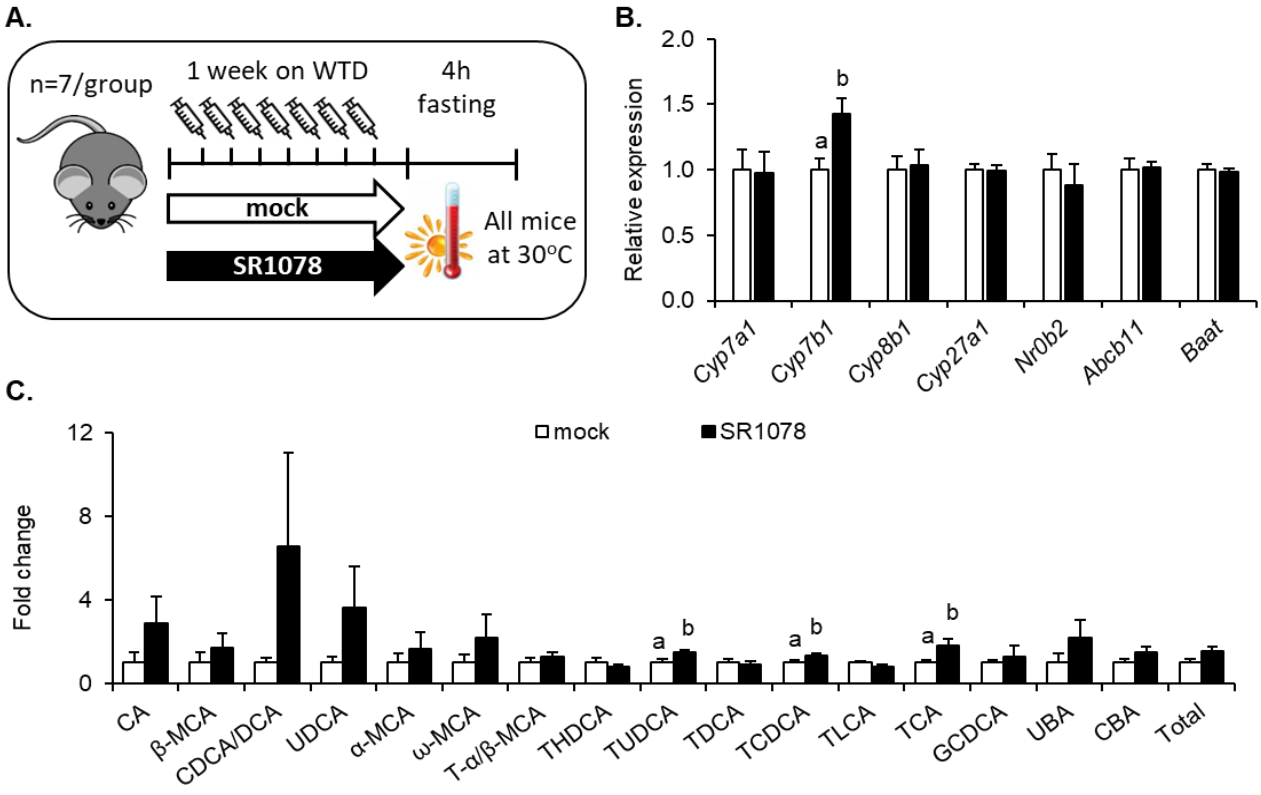

Figure 9. Effect of RORα agonism on *Cyp7b1* regulation at thermoneutrality. A) Experimental setup scheme, B) hepatic gene expression and C) fold change of hepatic bile acid species. Data are shown as mean values ± SEM with N=7-8 mice/group. Bars represent either relative expression to the house-keeper *Tbp* or relative fold change of bile acid levels compared to mock. Different letters indicate significant differences between groups ($p<0.05$) determined by unpaired T-test.

1.5 RORα antagonism and *Cyp7b1* upregulation upon cold stimulus

Since RORα was verified as a positive regulator of *Cyp7b1* under the given experimental conditions, the next step was to assess whether its inhibition upon cold exposure hampers the enzyme's transcriptional upregulation. For this reason, wild type mice were fed for a week with a WTD and housed either under thermoneutral (30ºC) or cold conditions (6ºC) in order to promote *Cyp7b1* expression. At the same time, half of the groups received intraperitoneal injections of SR3335, a synthetic RORα selective inverse agonist (Kumar et al. 2011), to block the transcriptional activity of RORα (Figure 10A). The food intake, and hence the cholesterol intake, were increased as expected in the cold exposed groups. SR3335 did not influence cumulative food consumption (Figure 10B). Here, cold exposure triggered a robust increase of *Cyp7b1* expression regardless of the SR3335 injection, while other bile acid-related genes were not affected (Figure 10C). However, known RORα target genes were transcriptionally unaffected (Figure 10D), pointing towards technical limitations of the experimental approach (e.g. insufficient

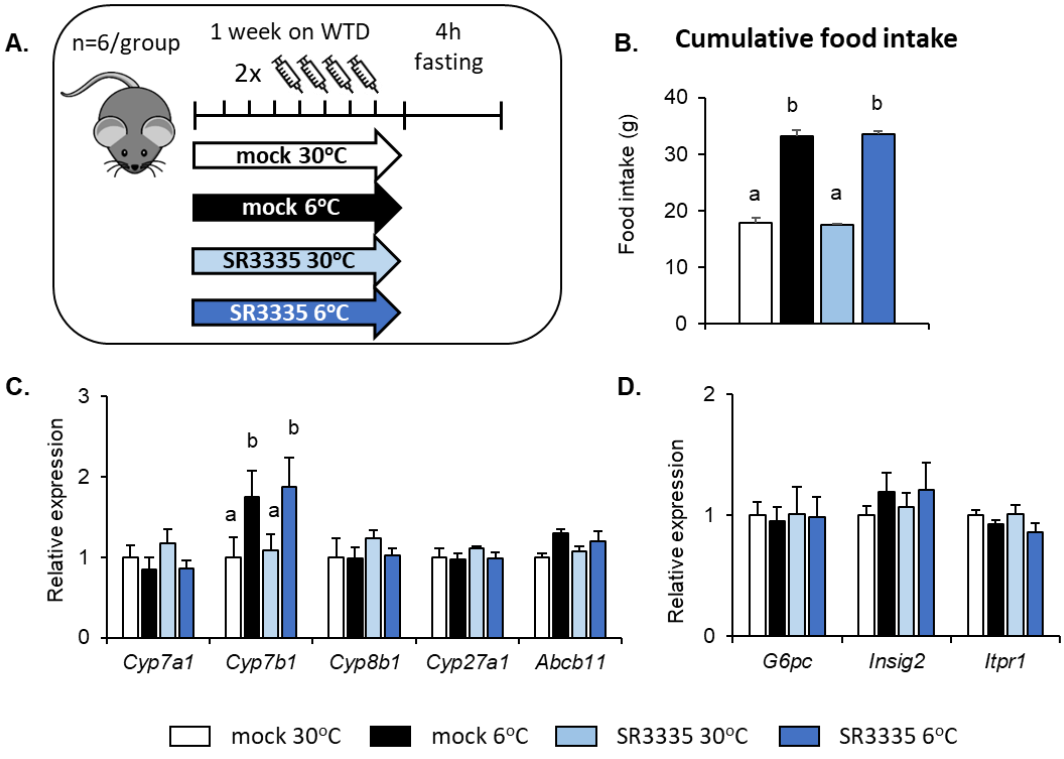

Figure 10. Effect of RORα inhibition on *Cyp7b1* regulation upon cold exposure. A) Experimental setup scheme, B) cumulative food intake and C) and D) hepatic gene expression. Data are shown as mean values ± SEM with N=7 mice/group. Different letters indicate significant differences between groups ($p<0.05$) determined by two-way ANOVA

dose or duration of the injections). Therefore, since the transcription factor's activity was likely not inhibited, solid conclusions about RORα-mediated regulation of *Cyp7b1* upon cold exposure could not be drawn.

2. Relevance of *Cyp7b1*-derived bile acids in brown adipose tissue activation and systemic metabolism

2.1 *Cyp7b1* depletion affects brown adipose tissue responses

Physiologically, bile acids are important for the digestion of fat and lipid-based nutrients (e.g. vitamins) as they mediate their emulsification in the intestinal tract. At the same time, they regulate systemic responses via activation of their respective receptors in the several organs such as white and brown adipose tissues as well as cardiac and skeletal muscles. In our recent study (Worthmann et al. 2017), it was observed that after cold exposure mice devoid of the alternative bile acid synthesis pathway, due to *Cyp7b1* deletion, display decreased energy expenditure and reduced expression of thermogenic marker genes (*Ucp1*, *Ppargc1a*, *Elovl3*, *Dio2*) in BAT. To get a deeper understanding why *Cyp7b1*$^{-/-}$ mice exert an attenuated activation of the thermogenic brown adipose tissue, wildtype (WT) and *Cyp7b1*$^{-/-}$ mice were housed at thermoneutral (30° C) or cold (6° C) conditions for a week and fed a WTD (Figure 11A). Here, and in line with the previous report, a significant upregulation of hepatic *Cyp7b1* expression was observed in WT mice kept at 6° C, while very low *Cyp7b1* transcripts were detected in the *Cyp7b1*$^{-/-}$ mice both at 30° C and at 6° C (Figure 11B). Expression of *Cyp27a1*, another critical component of the alternative BA synthesis pathway was higher in WT mice after cold exposure and also higher in *Cyp7b1*$^{-/-}$ mice (Figure 11B). Other mediators of BA synthesis (*Cyp7a1* and *Cyp8b1*) were neither affected by cold nor by *Cyp7b1* deficiency (Figure 11B). According to gene expression analysis, CYP7B1 protein levels were higher in cold-exposed WT mice while almost no protein was detected in the *Cyp7b1*$^{-/-}$ mice (Figure 11C, D). Importantly, in WT mice, higher hepatic *Cyp7b1* expression upon cold-housing translated into higher plasma BA levels, an effect that was blunted in *Cyp7b1*$^{-/-}$ mice (Figure 11E).

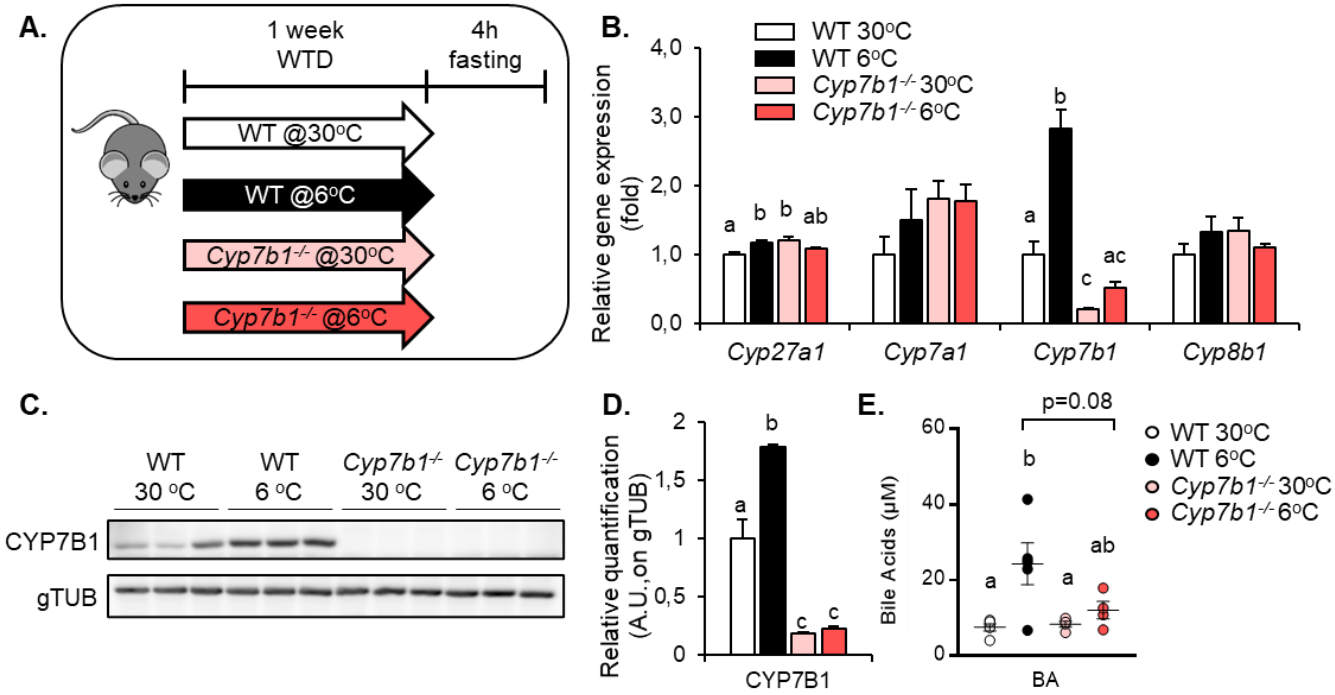

Figure 11. Deletion of *Cyp7b1* attenuates the cold-induced bile acid (BA) synthesis. A) Experimental setup scheme, B) hepatic gene expression, C) hepatic protein levels of CYP7B1 with D) relative quantification and E) circulating bile acid levels. Data are shown as mean values ± SEM with N=3-4 mice/group. Different letters indicate significant differences between groups ($p<0.05$) determined by two-way ANOVA

BA have been shown to activate BAT via TGR5 (Watanabe et al. 2006, Broeders et al. 2015), followed by a signalling cascade that involves elevated levels of cyclic adenosine monophosphate (cAMP) and activation of protein kinase A (PKA) (Thomas et al. 2008). However, and as expected, the levels of pPKA-substrates were reduced in cold exposed *Cyp7b1*$^{-/-}$ mice (Figure 12A, B), arguing towards attenuated activation of the respective kinase. In addition, altered protein levels of OXPHOS complexes were detected in cold-housed *Cyp7b1*$^{-/-}$ mice. While complexes III-V were only mildly affected, a significant lower abundance of complex I and II was observed (Figure 12A, B). In line with the previous report, these data support that *Cyp7b1* deletion and reduced BA levels compromise BAT thermogenic responses.

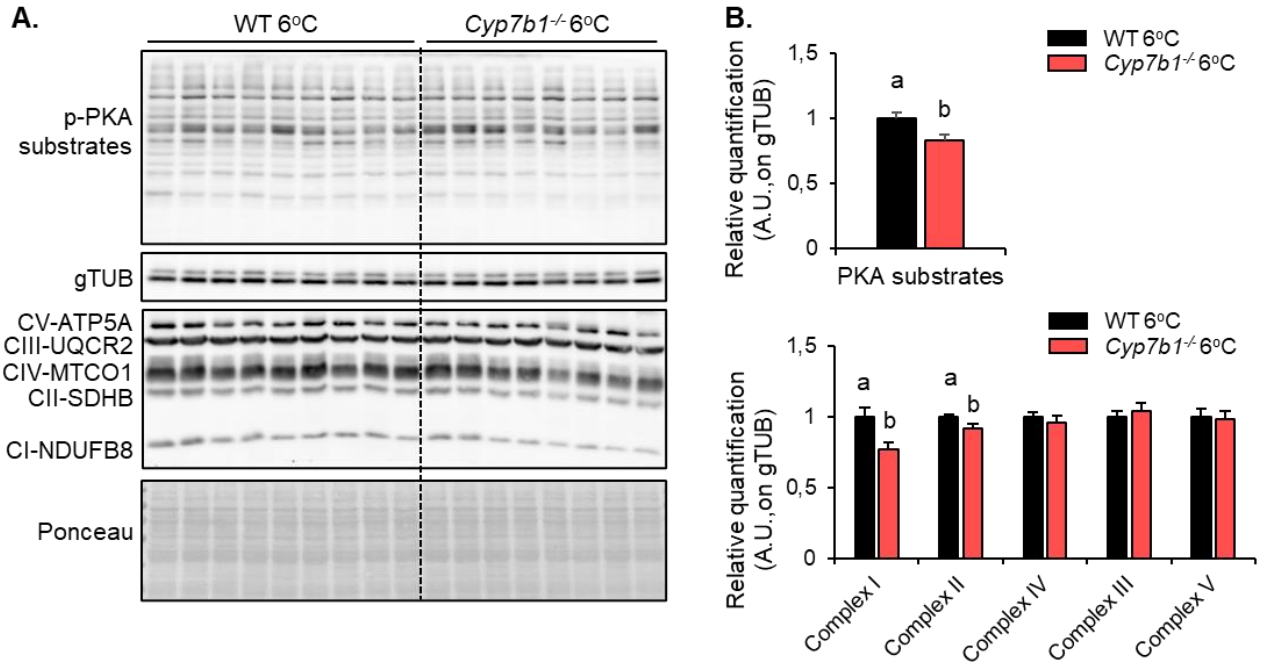

Figure 12. Deletion of *Cyp7b1* correlates with compromised brown adipose tissue (BAT) responses. A) Representative Western blotting of pPKA-substrates and OXPHOS complexes in BAT and (B) relative quantification of cold exposed WT vs *Cyp7b1*$^{-/-}$ mice (N=8-9/group). Quantification data are shown as mean values ± SEM. Different letters indicate significant differences between groups ($p < 0.05$) determined by Student's T-test.

2.2 *Cyp7b1* deletion affects cold-induced systemic lipoprotein metabolism: radioactive tracer uptake studies and organ distribution

As mentioned in Part C section 5.1, cold exposure critically determines systemic energy metabolism by enhancing TRL as well as well as cholesterol uptake by BAT, while a compromised activity of the later could in turn affect postprandial lipid metabolism. The observations in Part F section 2.1 were the reason to investigate whether the absence of CYP7B1 and the respective bile acids influence lipid handling in adipose tissues, as well as other peripheral organs, under conditions of high energy demand caused by cold exposure. For this purpose, an oral fat tolerance test was performed to evaluate organ distribution in *Cyp7b1*$^{-/-}$ and wild type (WT) mice that were fed with a WTD and housed either at thermoneutral (30ºC) or cold conditions (6ºC) for one week (Figure 13A). After a 4h-fasting period, mice were orally administered with corn oil spiked with radioactively-labelled ^{3}H-triolein and ^{14}C-cholesterol and blood clearance as well organ uptake was followed after 120 minutes (Figure 13A). Employment of these radiotracers enables for monitoring of vascular lipoprotein processing via the uptake of free fatty acids (^{3}H-label)

as well as the uptake of total lipoproteins (^{14}C-label) at the same time. In this experiment, cold exposure resulted in higher food consumption, decreased body weight and white adipose tissue depots but slightly increased heart volumes, all largely independent from the genotype (Figure 13B, 13C and 13D). However, no significant weight changes of other organs were observed, including the thermogenic BAT (Figure 13D). As expected, in all groups, postprandial plasma triglyceride (TG) levels were increased in response to the oral lipid gavage (Figure 14A) following a 120 min-post administration period. In agreement with previous findings, despite that TG levels doubled over time in both warm-housed groups, these raises were only moderate in cold-housed mice. After 120 min, plasma TG levels were significantly lower in cold-housed WT mice compared to warm-housed WT mice, while this effect was blunted in *Cyp7b1*$^{-/-}$ mice (Figure 14A). In line, higher amounts of ^{3}H-radioactivity were detected in the BAT of cold-housed WT mice

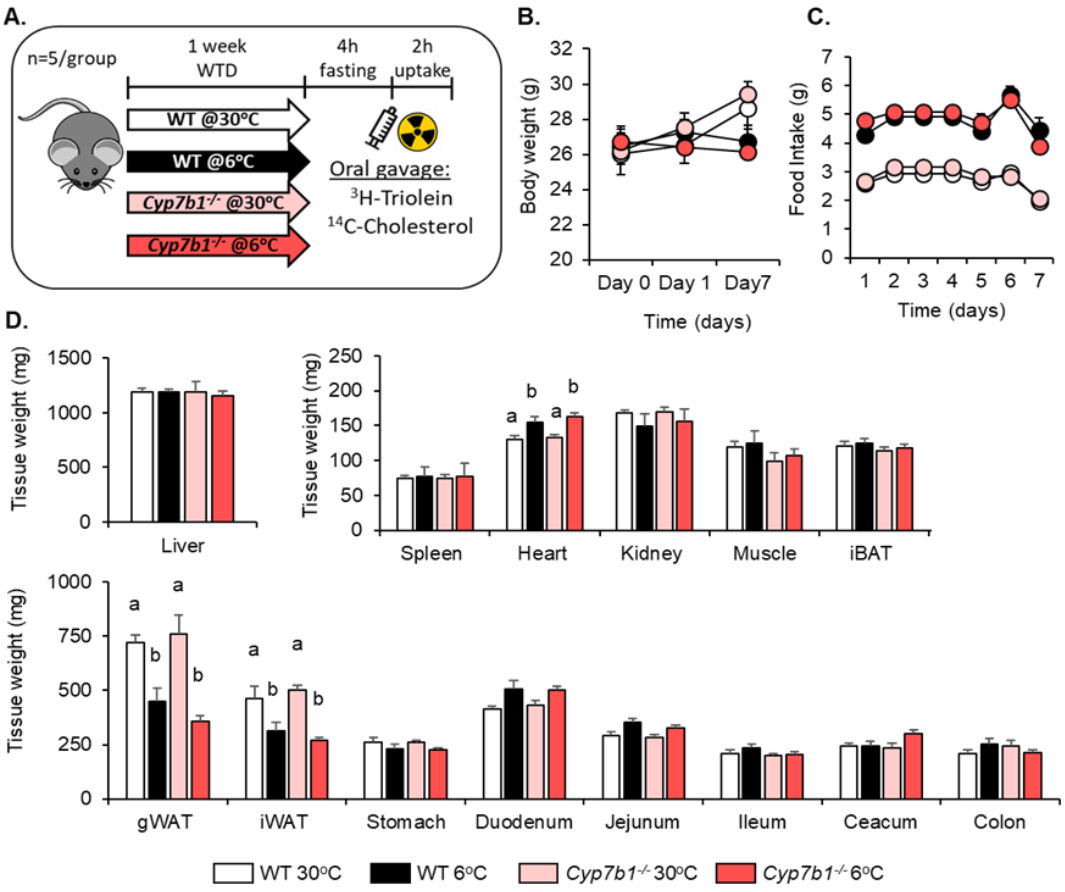

Figure 13. Turnover studies in *Cyp7b1*$^{-/-}$ mice housed at thermoneutral or cold environment. A) Experimental setup scheme, B) body weight change, C) food intake and D) organ weights of *Cyp7b1*$^{-/-}$ vs WT mice. Data are shown as mean values ± SEM with N=5 mice/group. Different letters indicate significant differences between groups ($p<0.05$) determined by two-way ANOVA.

compared to their warm littermates, while this effect was significantly diminished in *Cyp7b1*$^{-/-}$ mice (Figure 14B). Nevertheless, compared to both warm-housed groups, the amount of ^{3}H-triolein derived fatty acids in BAT was still higher in cold-housed *Cyp7b1*$^{-/-}$ mice (Figure 14B). These data indicate that the cold-induced increase in vascular lipoprotein processing is compromised in *Cyp7b1*$^{-/-}$ mice. Triolein uptake into the heart was enhanced after cold-treatment but not affected by loss of *Cyp7b1* (Figure 14D), while it remained unaffected in the gonWAT (Figure 14C), the spleen, kidney, muscle (Figure 14D), liver (Figure 14E) and most of the intestinal parts (Figure 14F). Interestingly, the ^{3}H-triolein counts were slightly higher in the stomach of *Cyp7b1*$^{-/-}$ mice compared to WT

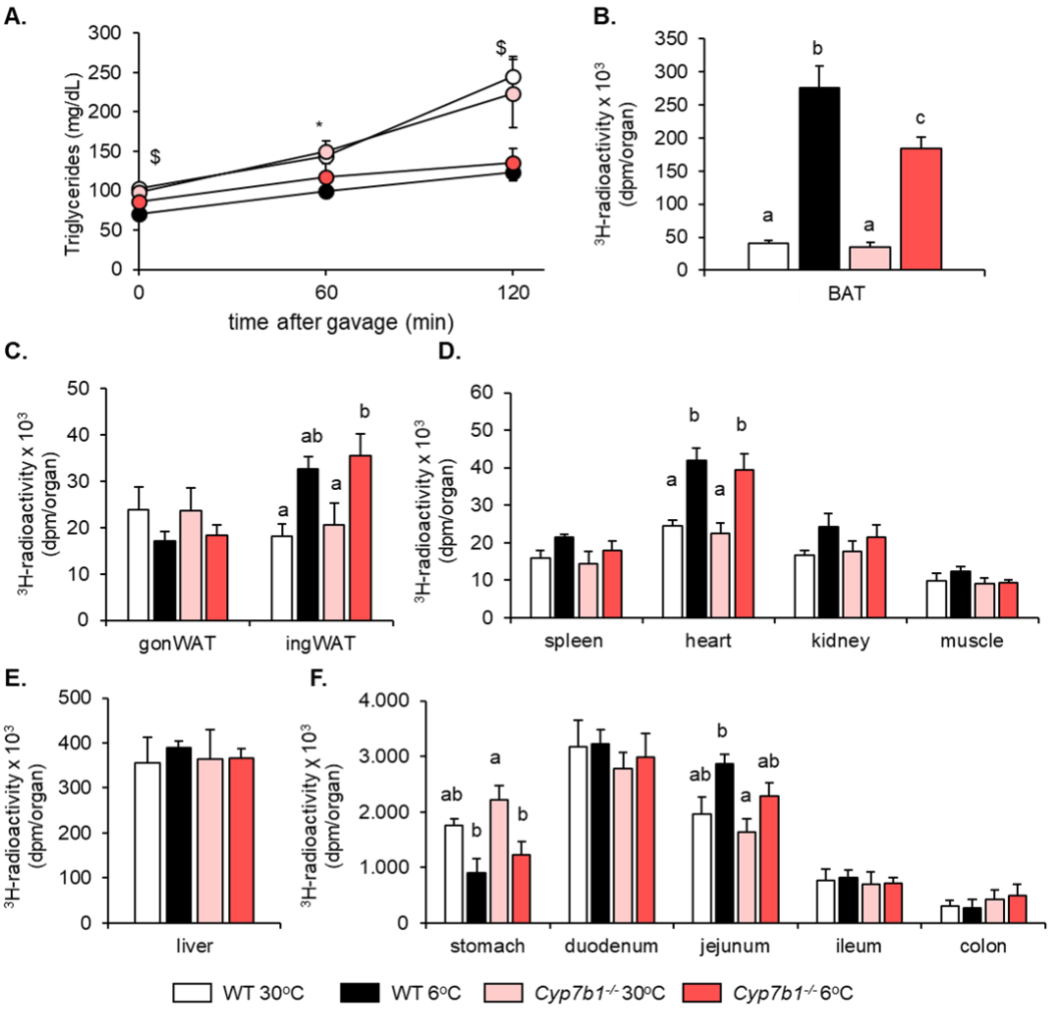

Figure 14. *Cyp7b1* deletion compromises cold-induced fatty acid uptake into BAT. (A) Plasma triglyceride levels, B) total uptake of ^{3}H-triolein in brown or C) white adipose tissue depots and D, E, F) other metabolic organs (N=5/group). Data are shown as mean values ± SEM. For A) p values lower than 0.05 were considered statistically significant and are indicated as follows: $ =WT30 vs WT 6; * =WT 6 vs KO 30; # =WT 30 vs KO 6; & =KO 30 vs KO 6; For C-F): Different letters indicate significant differences between groups ($p < 0.05$) determined by two-way ANOVA.

mice housed at 30°C (Figure 14F), but were unaffected at 6°C. This indicates that the postprandial lipid digestion might be slower under thermoneutral conditions when the alternative pathway derived bile acids are missing, but not under cold exposure.

Plasma cholesterol levels remained similar before and 120 min after the oil-gavage in all groups (Figure 15A). Of note, in agreement with recent reports, total plasma cholesterol levels in cold-housed mice were significantly lower than in warm-housed mice. This was not affected by the absence of *Cyp7b1* (Figure 15A). In accordance with what was observed for the ^{3}H-label, significantly higher amounts of ^{14}C-cholesterol were detected in iBAT of both WT and *Cyp7b1*$^{-/-}$ mice (Figure 15B). However, ^{14}C- tracer levels were reduced in cold-housed *Cyp7b1*$^{-/-}$ mice compared to their WT counterparts (Figure 15B). Similar to the uptake of radiolabelled fatty acids, cholesterol uptake into other

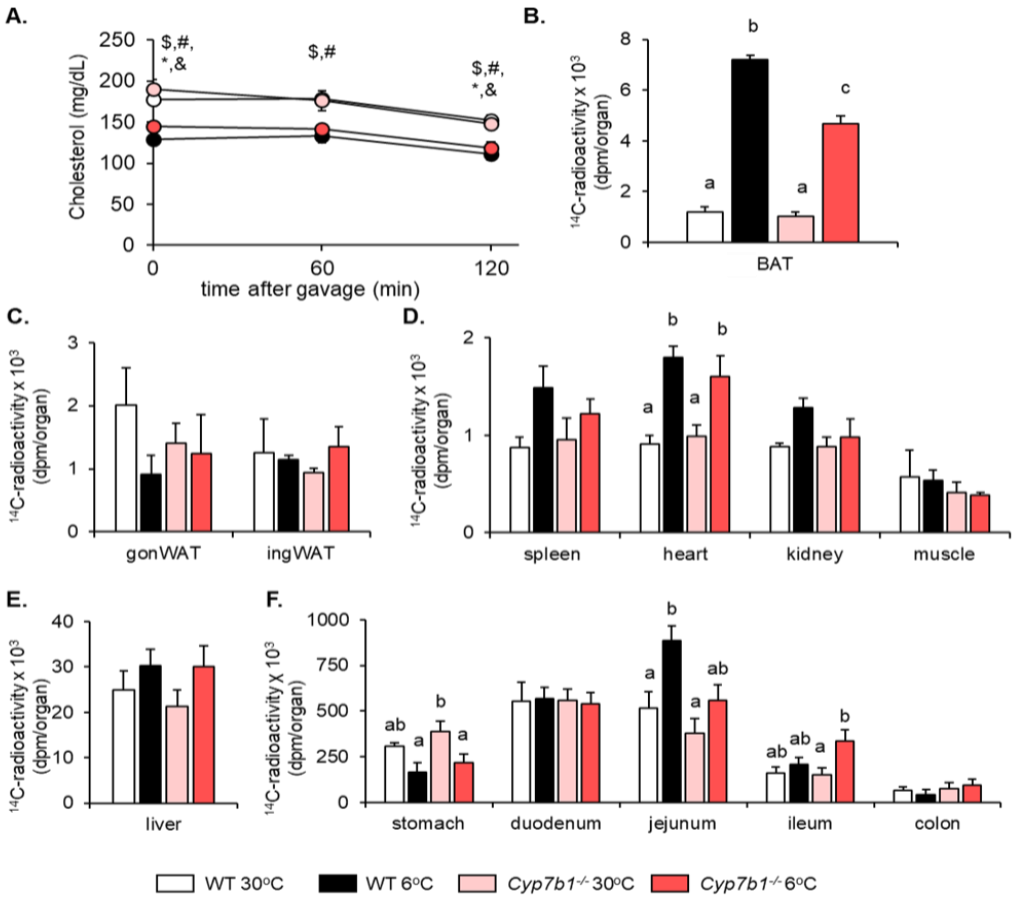

Figure 15. *Cyp7b1* deletion compromises cold-induced lipoprotein uptake into BAT. A) Plasma cholesterol levels, total uptake of ^{14}C-cholesterol in B) brown or C) white adipose tissue depots and D, E, F) other metabolic organs (N=5/group). Data are shown as mean values ± SEM. For A) p values lower than 0.05 were considered statistically significant and are indicated as follows: $ =WT30 vs WT 6; * =WT 6 vs KO 30; # =WT 30 vs KO 6; & =KO 30 vs KO 6; For B-F): Different letters indicate significant differences between groups ($p < 0.05$) determined by two-way ANOVA.

organs (ingWAT, gonWAT, spleen, kidney, muscle, liver) remained unchanged (Figure 15C-E). Under cold exposure, ^{14}C-cholesterol levels were reduced in the stomach but increased in the jejunal and ileal parts of the intestinal tract (Figure 15F) in both genotypes. However, the *Cyp7b1*$^{-/-}$ mice presented slightly elevated levels of the radioactive tracer in the ileum (Figure 15F) and together with the reduced ^{14}C-cholesterol counts in proximal parts of these mice, this could argue towards a quicker sterol digestion. Again, irrespective of genotype, we detected increased amounts of ^{14}C-cholesterol in the heart of cold-exposed mice (Figure 15D). Altogether, these data suggest that the uptake of fatty acids (^{3}H-label) and entire lipoprotein particles (^{14}C-label) into BAT is attenuated in cold-housed *Cyp7b1*$^{-/-}$ mice.

2.3 *Cyp7b1* depletion does not affect intestinal lipoprotein secretion in response to cold treatment

Postprandial lipoprotein processing does not only depend on clearance by metabolic tissues such as adipose tissues, heart and muscle, but is also dependent on intestinal lipid uptake and lipoprotein assembly. Ingestion of exogenous lipids leads to the intestinal production of triglyceride rich lipoproteins (TRLs), the chylomicrons (CM). Especially lipid ingestion is mediated by BA and since absence of the alternative synthesis pathway and the respective bile acids affected systemic lipid metabolism, the next question was whether deletion of *Cyp7b1* affects the processing and packaging of lipids into chylomicrons as well. In order to rule out any effects of *Cyp7b1* on intestinal lipid ingestion and lipoprotein secretion, a radioactive ^{3}H-triolein/^{14}C-cholesterol tracing experiment was performed using WTD-fed *Cyp7b1*$^{-/-}$ and WT mice which were housed at thermoneutral (30^{o}C) or cold conditions (6^{o}C) for a week. This time, mice were orally administered with the fat load in the presence of the detergent Triton WR-1339 (Figure 16A). This compound inhibits lipases and thus blocks intravascular hydrolysis of lipoproteins. This leads to the accumulation of triglyceride-rich lipoproteins in the circulation and enables tracking of the postprandial intestinal CM production. Blood was withdrawn by tail vein puncture every hour for a total of 4 hours, and the amount of radioactivity was measured in the plasma. As expected, upon blocking intravascular hydrolysis of lipoproteins, plasma triglyceride levels raised dramatically over time and accumulated in a range of 2000-3000mg/dL after

240 min (Figure 16B). Of note, at 240 min we did not detect any significant differences regardless of genotype or housing temperature (Figure 16B). In line, also plasma levels of ^{3}H-triolein and ^{14}C-choleterol strongly increased over the 4 h period of the experiment but after 4 hours, no differences were detected between the groups (Figure 16C-D).

Together, these data indicate, that neither cold-housing nor loss of *Cyp7b1* affect intestinal chylomicron production. Accordingly, the higher postprandial lipoprotein levels observed in *Cyp7b1*$^{-/-}$ mice are rather dependent on BAT-mediated lipoprotein clearance.

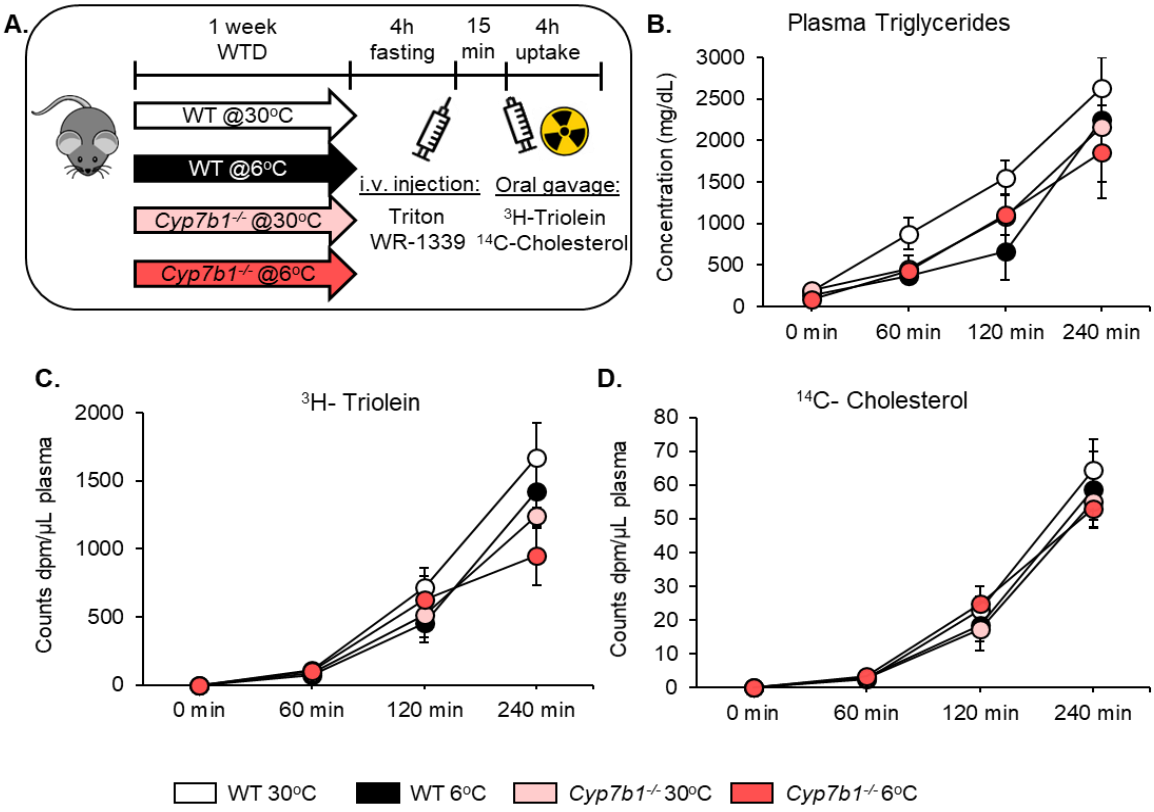

Figure 16. *Cyp7b1* deletion does not affect intestinal chylomicron production in response to cold exposure. A) Experimental setup, B) triglyceride, C) ^{3}H-triolein and D) ^{14}C-cholesterol levels in the plasma between 0- and 240-min post gavage (N=5/group). Data are shown as mean values ± SEM. Different letters indicate significant differences between groups ($p < 0.05$) determined by two-way ANOVA.

2.4 *Cyp7b1* depletion alters machinery for intravascular lipoprotein clearance in response to cold treatment

To get a deeper understanding on how the loss of *Cyp7b1* may interfere with lipoprotein clearance by BAT mechanistically, gene expression analysis was performed in BAT samples from cold-housed WT and *Cyp7b1*$^{-/-}$. In line with the reduced uptake of lipoproteins into BAT of *Cyp7b1*$^{-/-}$ mice in Part F section 2.2, lower copy numbers of genes encoding proteins mediating intravascular processing and uptake of lipoproteins were detected. Specifically, gene expression (Figure 17A) of the lipases endothelial lipase

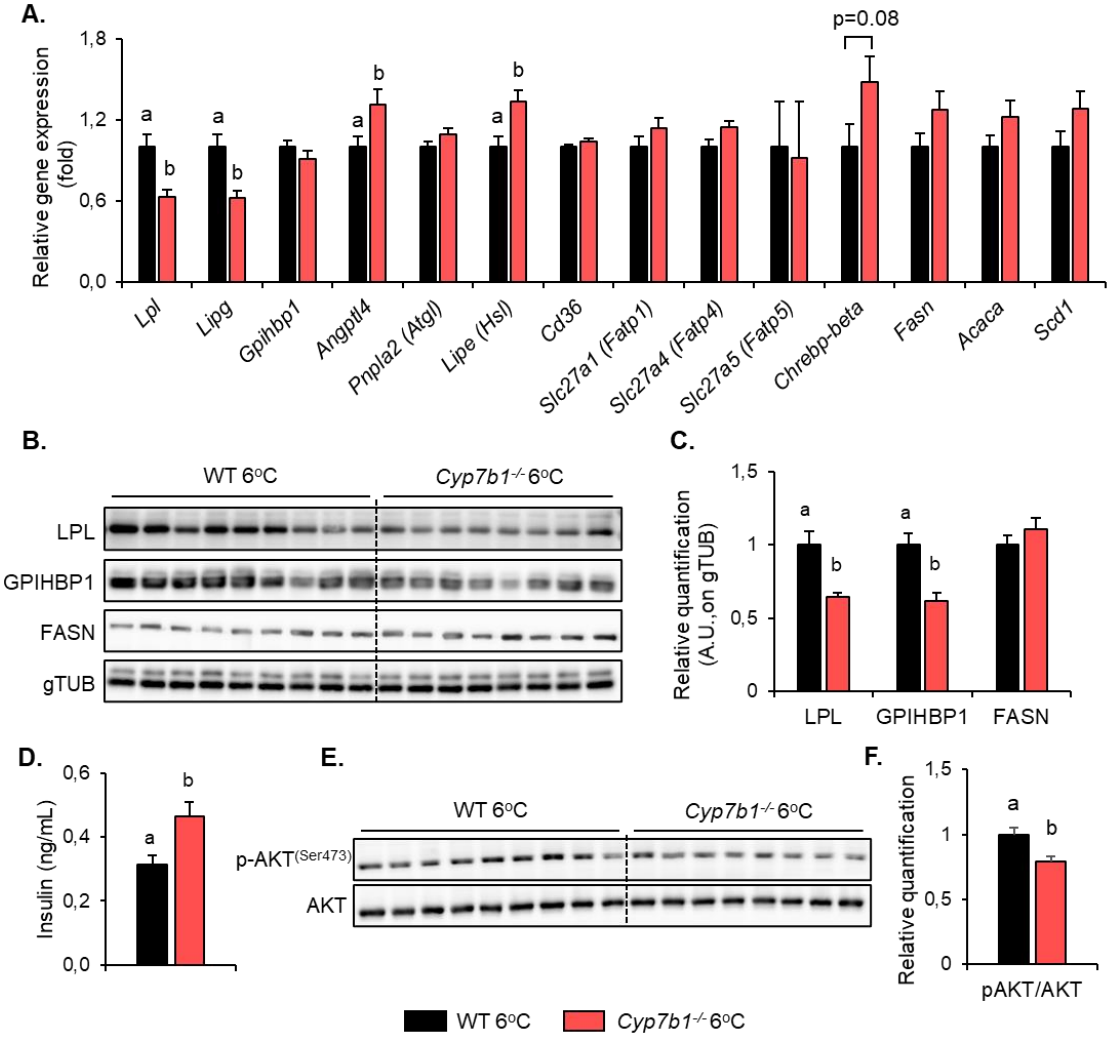

Figure 17*. Cyp7b1* deletion impairs BAT lipoprotein processing responses during cold exposure. A) BAT relative gene expression of lipoprotein processing/uptake, glucose uptake and *de novo* lipogenesis markers (measurements performed by Anastasia Kuhl), B) protein levels of LPL, GPIHBP1, FASN with C) relative quantification, D) plasma insulin levels, E) BAT protein levels of p-AKT and AKT with F) relative quantification (N=8-9/group). Data are shown as mean values ± SEM. Different letters indicate significant differences between groups ($p < 0.05$) determined by Student's T-test.

(encoded by *Lipg*) and lipoprotein lipase (encoded by *Lpl*) were decreased in *Cyp7b1*$^{-/-}$ mice, while the gene expression of LPL's negative regulator angiopoietin like 4 (*Angplt4*) was increased (Figure 17A). This was also translated into reduced LPL protein levels (Figure 17B). Additionally, glycosylphosphatidylinositol-anchored high density lipoprotein binding protein 1 (*Gpihbp1*), which is important for intravascular localization of LPL, was slightly decreased on transcript level (Figure 17A) and even significantly reduced on protein level after loss of *Cyp7b1* (Figure 17B, C). Of note, expression of fatty acid receptors and transport proteins (*Cd36*, *Slc27a1, Slc27a4*, *Slc27a5*) (Figure 17A) remained unchanged. Interestingly, expression of genes involved in lipolysis (hormone-sensitive lipase encoded by *Lipe* and adipose triglyceride lipase encoded by *Pnpla2*) (Figure 17A) and *de novo* lipogenesis (carbohydrate response element binding protein 1 beta (*Chrebp1b*), fatty acid synthase (*Fasn*) (Figure 17A-C), acetyl-CoA carboxylase alpha (*Acaca*), stearoyl-CoA desaturase-1 (*Scd1*) (Figure 17A) trended to be increased as well. The next aim was to explore how lower expression of lipases and especially *Lpl* might be regulated in BAT of cold-housed *Cyp7b1*$^{-/-}$ mice. As *Lpl* is activated by insulin, both plasma insulin levels and BAT insulin signaling were assessed in WT and *Cyp7b1*$^{-/-}$ mice. In comparison to WT mice, cold housed *Cyp7b1*$^{-/-}$ mice had significantly higher levels of plasma insulin (Figure 17D). In addition, insulin-mediated phosphorylation of protein kinase B at serine 473 (pSer473) was assessed by Western blot a surrogate marker for insulin action. The levels of pAKT in the BATs of *Cyp7b1*$^{-/-}$ mice were significantly lower (Figure 17E, F). Thus, despite hyperinsulinemia, insulin signaling was lower in *Cyp7b1*$^{-/-}$ mice suggesting that these mice were insulin resistant. To conclude, reduced intravascular lipoprotein processing and hydrolysis in *Cyp7b1*$^{-/-}$ mice might be dependent on reduced activity of LPL and other lipases as a result of impaired insulin-mediated activation of LPL.

3. The role of *Cyp7b1*-derived metabolites in MAFLD and steatohepatitis

To investigate the role of CYP7B1 and its derived metabolites in MAFLD and steatohepatitis in the context of different housing conditions and energy expenditure, diet-induced MAFLD/steatohepatitis studies were performed in mice lacking CYP7B1 and littermate controls. In the first approach, mice were fed a methionine-choline deficient diet (MCD) for 2 weeks while in the second approach a choline deficient high fat diet (CD-HFD) was employed. Both regimens have been widely used for the disease's experimental setup (Anstee and Goldin 2006, Wolf et al. 2014). During both feeding studies, *Cyp7b1*$^{-/-}$ mice and their wild type littermates were housed either at thermoneutral (30^{o}C) or conventional housing environment (22^{o}C), which is considered as mild cold exposure for rodents.

3.1 The role of *Cyp7b1* in methionine-choline deficient diet (MCD)-induced MAFLD/steatohepatitis

For the MCD-induced model the intervention had to be terminated after 2 weeks (Figure 18A) as all animal groups were losing body weight significantly throughout the duration of the study (Figure 14B). Plasma and hepatic triglycerides were slightly elevated in all mice housed at 30^{o}C but no difference was attributed to CYP7B1 deficiency (Figure 18C, 18F). Plasma and hepatic cholesterol were only slightly elevated in the 30^{o}C-housed WT mice, but no other group (Figure 18D, 18G). Interestingly, alanine aminotransferase activity was elevated in the plasma of all mice housed under mild cold exposure, indicative of increased liver damage in the respective groups (Figure 18E). However, liver tissue weights were comparable between all mice (Figure 18H). Adipose tissue depots were smaller in mice housed under mild cold conditions, yet comparable between genotypes, (Figure 18H), supporting the notion that conventional temperature leads to metabolic adaptations due to excess of energy expenditure (Figure 18H).

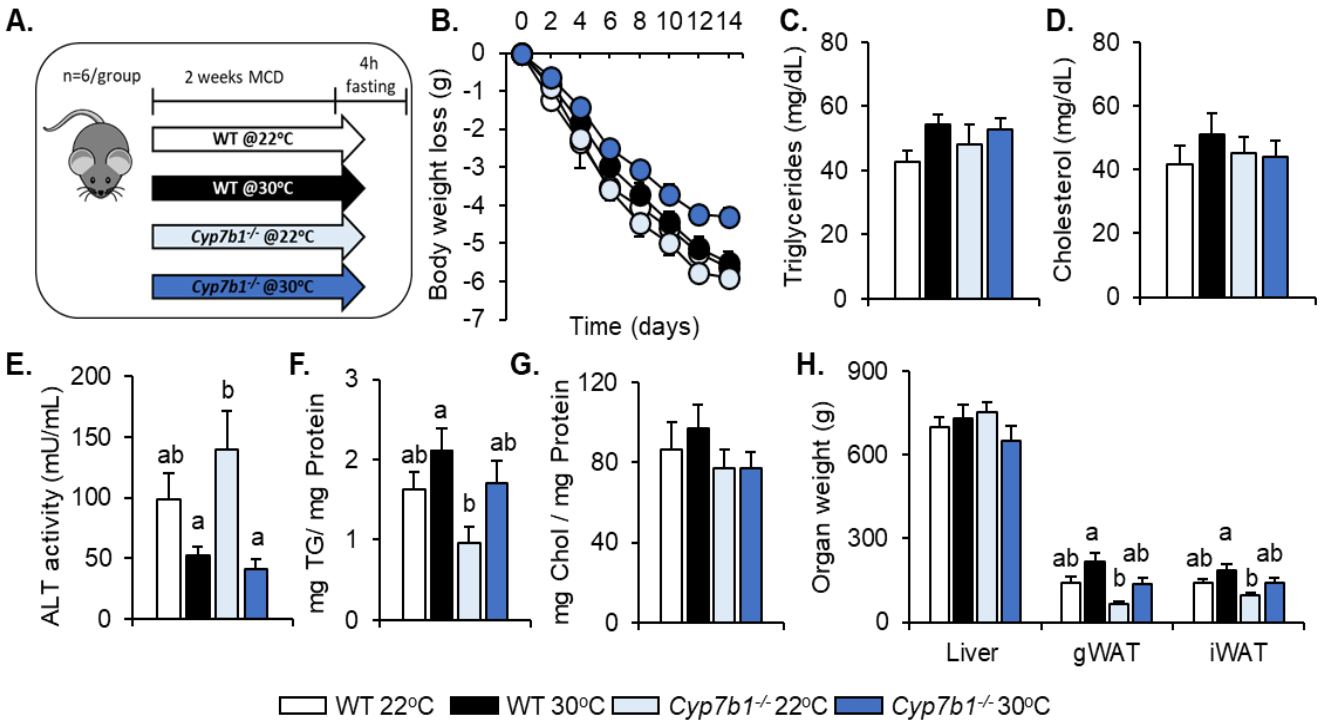

Figure 18. Role of CYP7B1 in MCD-induced MAFLD/steatohepatitis. A) Experimental setup scheme, B) body weight change, C) plasma triglycerides, D) plasma cholesterol, E) plasma ALT activity, F) hepatic triglycerides, G) hepatic cholesterol, H) organ weights of *Cyp7b1*$^{-/-}$ vs WT mice housed either at 30°C or 22°C. Data are shown as mean values ± SEM with N=5 mice/group. Different letters indicate significant differences between groups ($p<0.05$) determined by two-way ANOVA.

Common bile acid synthesis-related genes showed no significant alterations among the groups, while in the *Cyp7b1*$^{-/-}$ mice a truncated form was most likely detected with our *Cyp7b1* assay (Figure 19A). While fibrotic gene markers were not differentially expressed between genotypes and housing temperatures (Figure 19B), hepatic staining with Sirius Red revealed slightly elevated collagen deposition in mice that were housed under thermoneutrality (Figure 19C, 19D). However, *Cyp7b1* deletion did not affect fibrosis progression or hepatic inflammatory gene expression in comparison to the wild type state (Figure 19D, 19E). In summary, CYP7B1 did not influence MAFLD and steatohepatitis development in the MCD model in the context of differential housing conditions.

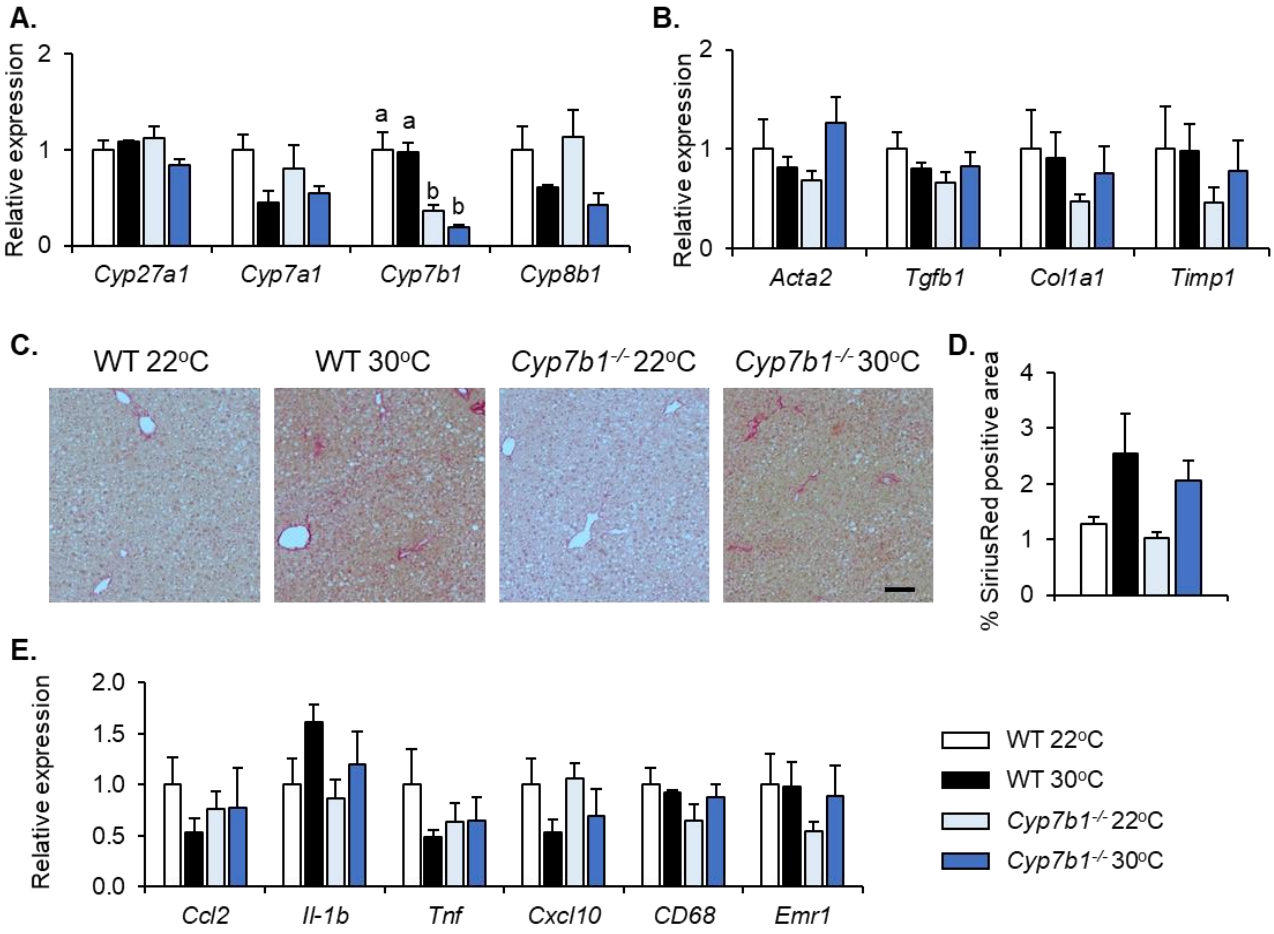

Figure 19. Role of CYP7B1 in MCD-induced MAFLD/steatohepatitis. Relative hepatic gene expression of A) bile acid related genes, B) fibrotic markers, E) inflammatory markers, C) representative microscopic pictures of Sirius Red staining and D) respective quantification of *Cyp7b1*$^{-/-}$ vs WT mice housed either at 30ºC or 22ºC. Data are shown as mean values ± SEM with N=6 mice/group. Different letters indicate significant differences between groups ($p<0.05$) determined by two-way ANOVA. Scale bar 100µM.

3.2 The role of *Cyp7b1* in choline deficient high fat diet (CD-HFD)-induced MAFLD/steatohepatitis

To investigate whether CYP7B1 affects progression to steatohepatitis in an obesity-triggered model of MAFLD, wild type (WT) and *Cyp7b1*$^{-/-}$ mice were fed a choline-deficient high fat diet (CD-HFD). In this model diet-induced steatohepatitis is usually observed after a feeding period of 8 months (Wolf et al. 2014a). To elucidate whether housing temperature modulates the role of CYP7B1 during disease's progression, littermates from both groups were housed either at room temperature (22°C) or at thermoneutrality (30°C).

Despite all groups started with similar body weights, mice housed at 30°C initially gained more weight than those at 22°C (Figure 20A). After 32 weeks of the CD-HFD intervention, body weight was still different between the two groups of *Cyp7b1*$^{-/-}$ mice but not the WT mice (Figure 20B). EchoMRI body composition analysis revealed that this was attributed to both fat and lean mass (Figure 20B). Plasma triglycerides were significantly higher in both WT and *Cyp7b1*$^{-/-}$ mice housed at 30°C compared to the 22°C-housed littermates (Figure 20C), an effect likely attributed to reduced lipid clearance by less active brown adipose tissue (Bartelt et al. 2011, Heine et al. 2018). Plasma free fatty acids

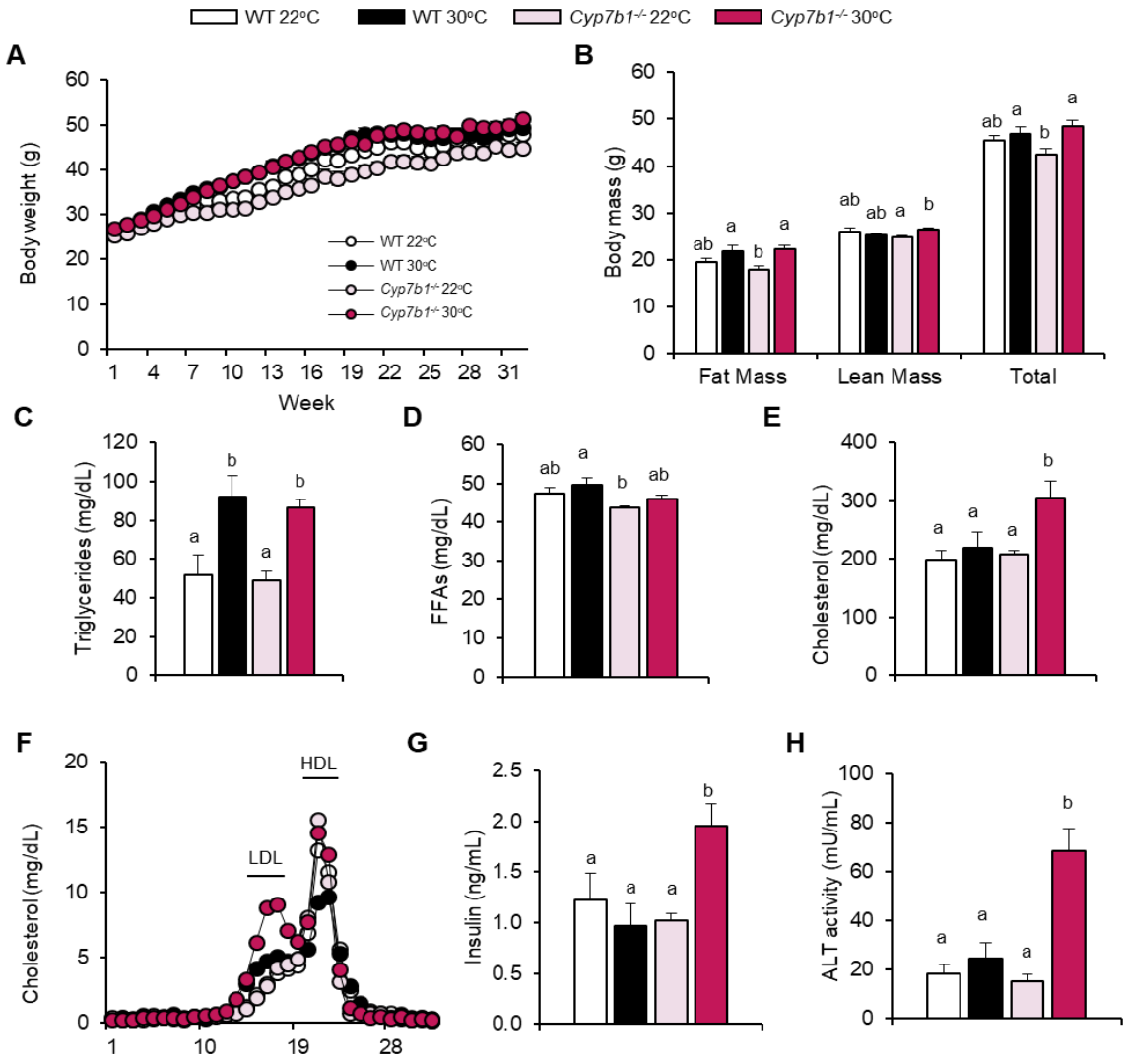

Figure 20. Metabolic and plasma parameters after 8-months of CD-HFD. (A) Body weights, (B) body composition analysis by EchoMRI, (C) triglycerides, (D) free fatty acids (FFA), (E) cholesterol, (F) cholesterol in FPLC fractions, (G) insulin and (H) alanine aminotransferase (ALT) activity in plasma of *Cyp7b1*$^{-/-}$ and WT littermates housed under 22°C or 30°C. Data are shown as mean values ± SEM with N=9-16 mice/group. Different letters indicate significant differences between groups ($p<0.05$) determined by two-way ANOVA.

followed a similar, yet not significant, trend as triglycerides and were slightly higher at thermoneutrality (Figure 20D). Notably, plasma cholesterol levels were significantly higher in thermoneutral housed *Cyp7b1*$^{-/-}$ but not WT mice (Figure 20E). FLPC analysis showed that this was attributed mainly to the LDL lipoprotein fraction (Figure 20F). Similarly, thermoneutral housed *Cyp7b1*$^{-/-}$ had elevated insulin (Figure 20G) and plasma alanine aminotransferase (Figure 20H). In addition, gene expression analysis of brown adipose tissues showed that *Ucp1* and *Elovl3* transcript levels were significantly lower in both genotypes upon thermoneutral housing (Figure 21), while for *Dio2* and *Ppargc1a* this effect of thermoneutrality was only observed in *Cyp7b1*$^{-/-}$ mice (Figure 21). Diminished BAT activity at 30°C was in accordance with the lower circulating TG levels observed in Figure 20C, supporting the notion that thermogenic responses are attenuated under thermoneutral housing. Together, plasma parameters indicate that at thermoneutral but not at conventional housing temperature CYP7B1 deficiency enhances insulin resistance, dyslipidemia and liver damage in mice fed with a CD-HFD.

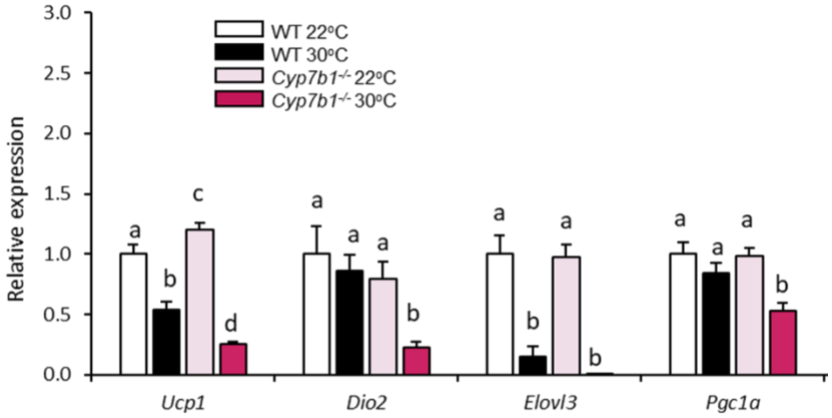

Figure 21. Brown adipose tissue expression after 8 months of CD-HFD. Gene expression in interscapular brown adipose tissue (iBAT) of *Cyp7b1*$^{-/-}$ and WT littermates housed under 22°C or 30°C. Data are shown as mean values ± SEM with N=8 mice/group. Bars represent relative expression with Tbp as a house-keeper. Different letters indicate significant differences between groups ($p<0.05$) determined by two-way ANOVA.

Next, the pathophysiological consequences of housing temperature and CYP7B1 deficiency for the liver were studied. Notably, *Cyp7b1*$^{-/-}$ mice housed at 30°C but not 22°C had higher liver weights in comparison to WT mice (Figure 22A). As determined by targeted lipidomics, hepatic triglyceride content was higher in mice housed at 30°C compared to 22°C, independent of the genotype (Figure 22B). In contrast, the content of cholesteryl esters (Figure 22C) and diacylglycerols (Figure 22D) was exclusively elevated in livers of *Cyp7b1*$^{-/-}$ mice at thermoneutrality. Despite that most of the phospholipid classes including lysophosphatidylcholine (LPC), lysophosphatidylethanolamines (LPE), phosphatidylethanolamines (PE) and sphingomyelins (SM) remained unchanged between the groups, phosphatidylcholines (PC) trended to be decreased in both groups housed at 22°C (Figure 22D). Deeper lipidomic analysis of the significantly altered hepatic cholesteryl esters and diacylglycerol lipid classes revealed that *Cyp7b1*$^{-/-}$ mice housed at thermoneutrality displayed distinct increases of species containing mono- and saturated-

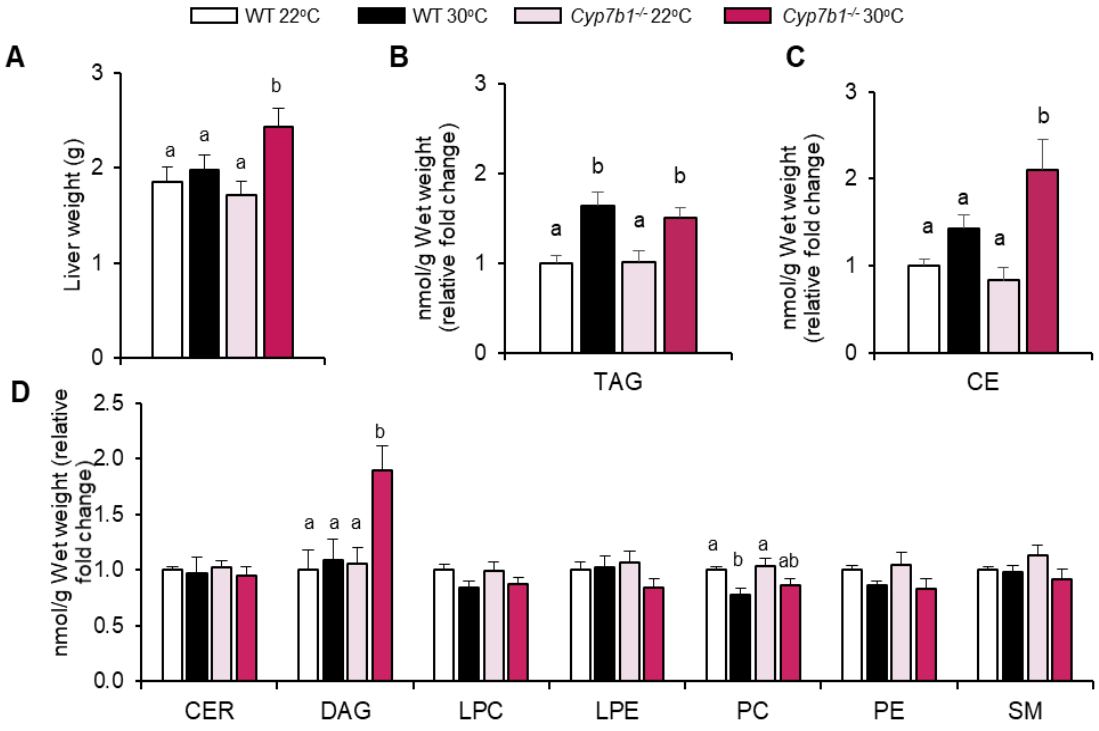

Figure 22. Hepatic lipid profiling after 8 months of CD-HFD. (A) Liver weight and relative levels of hepatic (B) triglycerides (TAG), (C) cholesteryl esters (CE) and (D) other lipid species of *Cyp7b1*$^{-/-}$ and WT littermates housed under 22°C or 30°C. Data are shown as mean values ± SEM with N=8 mice/group. Different letters indicate significant differences between groups ($p<0.05$) determined by two-way ANOVA. ceramides (CER), diacylglycerols (DAG), lysophosphatidylcholines (LPC), lysophos-phatidylethanolamines (LPE), phosphatidylcholines (PC), phosphatidylethanolamines (PE), sphingomyelins (SM).

fatty acids like 16:0, 18:0, 16:1 and 18:1 (Figure 23A, 23B) in comparison to all other groups. However, in line with Figure 22, WT and *Cyp7b1*$^{-/-}$ mice displayed higher content of hepatic triglyceride fatty acids when housed at 30ºC in comparison to 22ºC, but no significant differences were attributed to *Cyp7b1* deletion (Figure 23C).

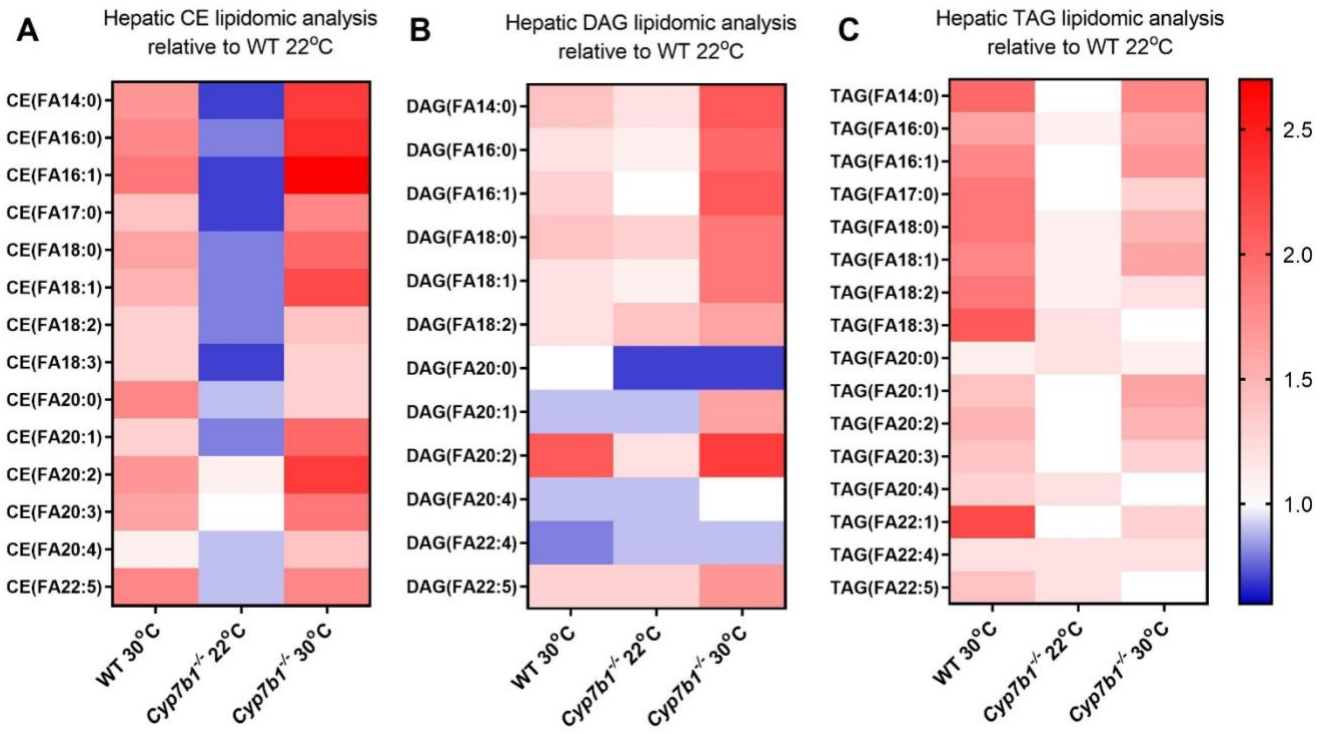

Figure 23. Fatty acid concentration of the significantly altered hepatic lipid species. Lipidomic analysis of A) cholesterol esters (CE), B) diacylglycerol (DAG) and C) triglycerides (TAG) of *Cyp7b1*$^{-/-}$ and WT littermates housed under 22°C or 30°C. Heat maps represent fold change of mean values relative to WT 22ºC (control) with N=8 mice/group.

Consistent with the hepatic triglyceride levels (Figure 22B), *Cyp7b1*$^{-/-}$ and WT mice housed at 30°C exhibited a higher content of liver lipid droplets, as assessed by histology (Figure 24A). Hepatic collagen deposition, as evaluated by Sirius Red staining (Figure 24B), was higher in mice housed at thermoneutrality, although the difference reached statistical significance only in *Cyp7b1*$^{-/-}$ mice (Figure 24C). At transcriptional level, several fibrosis-related markers including *Timp1*, *Mmp2*, *Mmp12* and *Mmp13* exhibited highest expression in the 30°C-housed *Cyp7b1*$^{-/-}$ mice (Figure 24D). Collectively, under thermoneutral housing CYP7B1-deficient mice exhibited signs of increased MAFLD-related fibrosis and accumulated liver lipids like cholesterol esters (CE), diacylglycerols (DAG) as well as triglycerides (TAG), that have been previously associated with

inflammation and insulin resistance (Walenbergh and Shiri-Sverdlov 2015, Petersen and Shulman 2018).

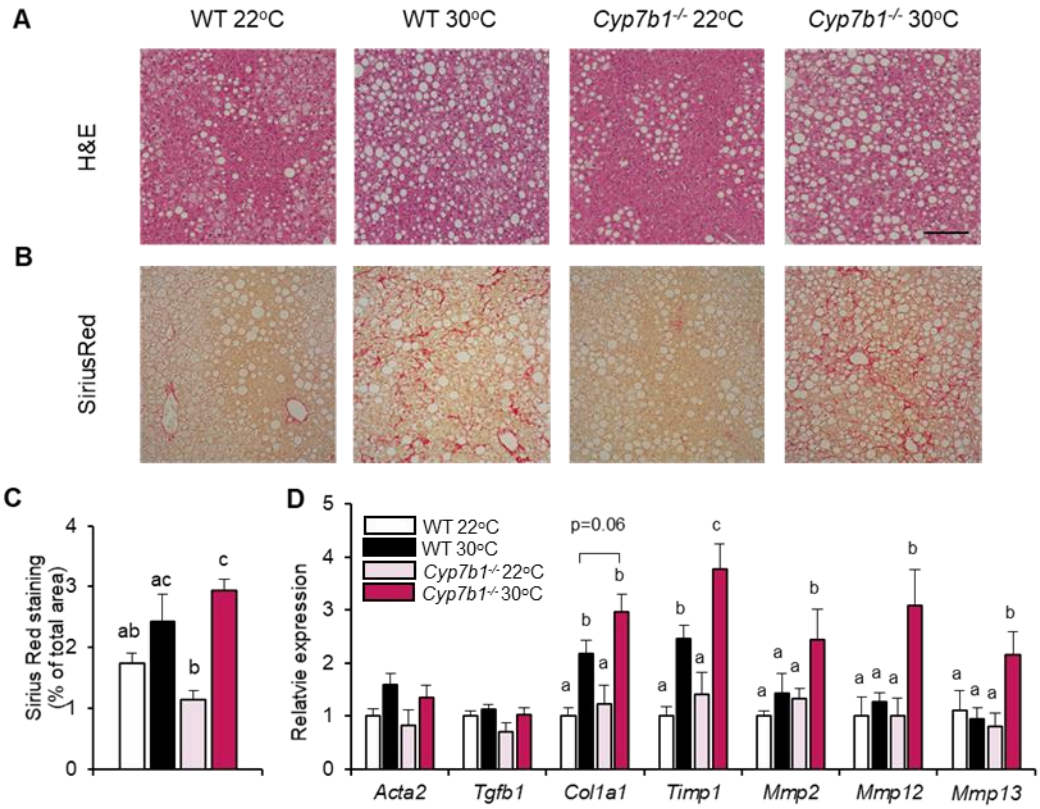

Figure 24. Hepatic histology and fibrotic markers after 8 months of CD-HFD. Representative images of (A) HE and (B) Sirius red stained liver sections, (C) quantification of fibrotic areas (N=9-16/group) and (D) hepatic expression of fibrosis-related genes normalized to *Tbp* as housekeeper (N=8/group). Data are shown as mean values ± SEM. Different letters indicate significant differences between groups ($p<0.05$) determined by two-way ANOVA.

CYP7B1 is a critical enzyme in the alternative bile acid synthesis pathway and affects the biosynthesis of several hydroxycholesterols. Therefore, the influence of its deficiency on hepatic markers, related to the metabolism of bile acids and hydroxycholesterols, was investigated by gene expression analysis. The expression of the bile acid synthesis genes *Cyp7a1*, *Cyp7b1*, *Cyp27a1* and *Cyp8b1* was lower in WT mice housed at 30°C compared to 22°C (Figure 25A).

In the *Cyp7b1* knockout mice, where a truncated *Cyp7b1* mRNA was detected at lower levels but no CYP7B1 protein (Figure 25B), a similar trend was observed for

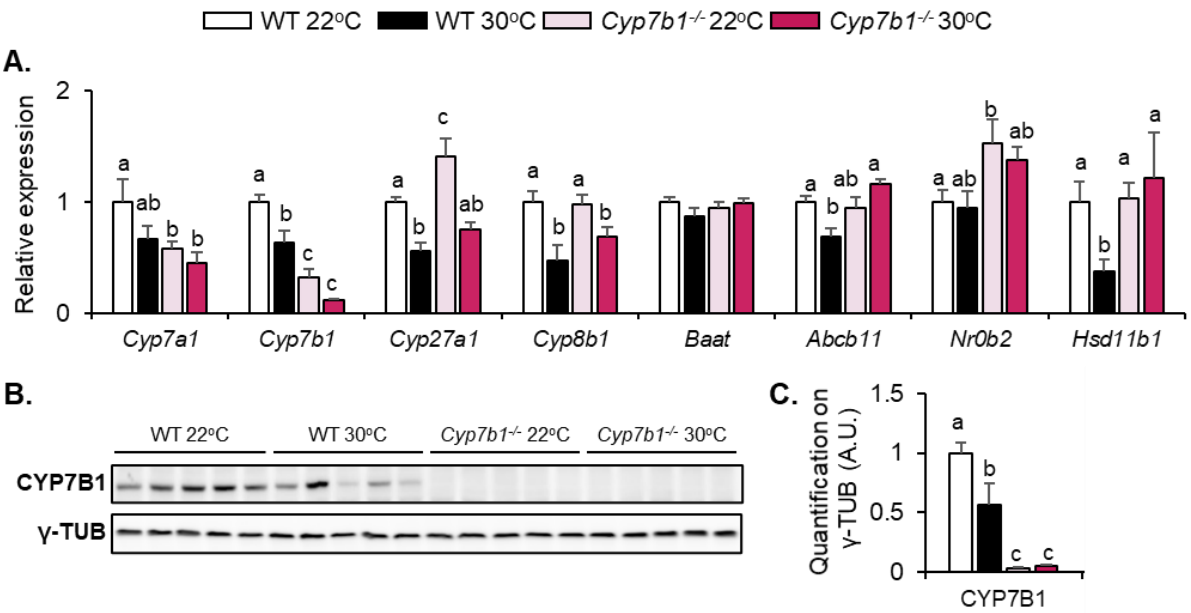

Figure 25. Changes in bile acid synthesis related markers after 8 months of CD-HFD. (A) Relative hepatic expression of bile acid- and oxysterol-related genes (N=8), (B) Western blot analysis of hepatic CYP7B1 and the loading control gamma tubulin (γ-TUB), (C) relative change of portal bile acid levels in comparison to WT 22°C mice (N=9-16) of *Cyp7b1*$^{-/-}$ and WT littermates housed under 22°C or 30°C. Data are shown as mean values ± SEM. Different letters indicate significant differences between groups ($p<0.05$) determined by two-way ANOVA.

Cyp27a1 and *Cyp8b1*. In addition, at 22°C *Cyp7a1* exhibited lower expression in the *Cyp7b1*$^{-/-}$ mice, which might be explained by an induction of its negative regulator *Nr0b2* (Figure 25A). No major effects on gene expression were detected for *Baat* and *Abcb11*, encoding for proteins that mediate conjugation and biliary secretion of bile acids, respectively. Interestingly, CYP7B1 deficiency did not have a major impact on bile acid levels in portal blood (Figure 26A).

In contrast to bile acids, a significant effect was observed for the substrates of CYP7B1 that are generated by CYP27A1 and cholesterol 25-hydroxylase (Ma and Nelson 2019) 27-HC and 25-HC, respectively (Figure 26B). These sterols were higher in the livers of *Cyp7b1*$^{-/-}$ mice while hydroxycholesterols that are not CYP7B1 substrates (22-HC, 24s-HC) were unaltered (Figure 26B). Overall, these data indicate that CYP7B1 primarily influences hydroxycholesterol levels but has little effect on bile acid metabolism in the dietary MAFLD model.

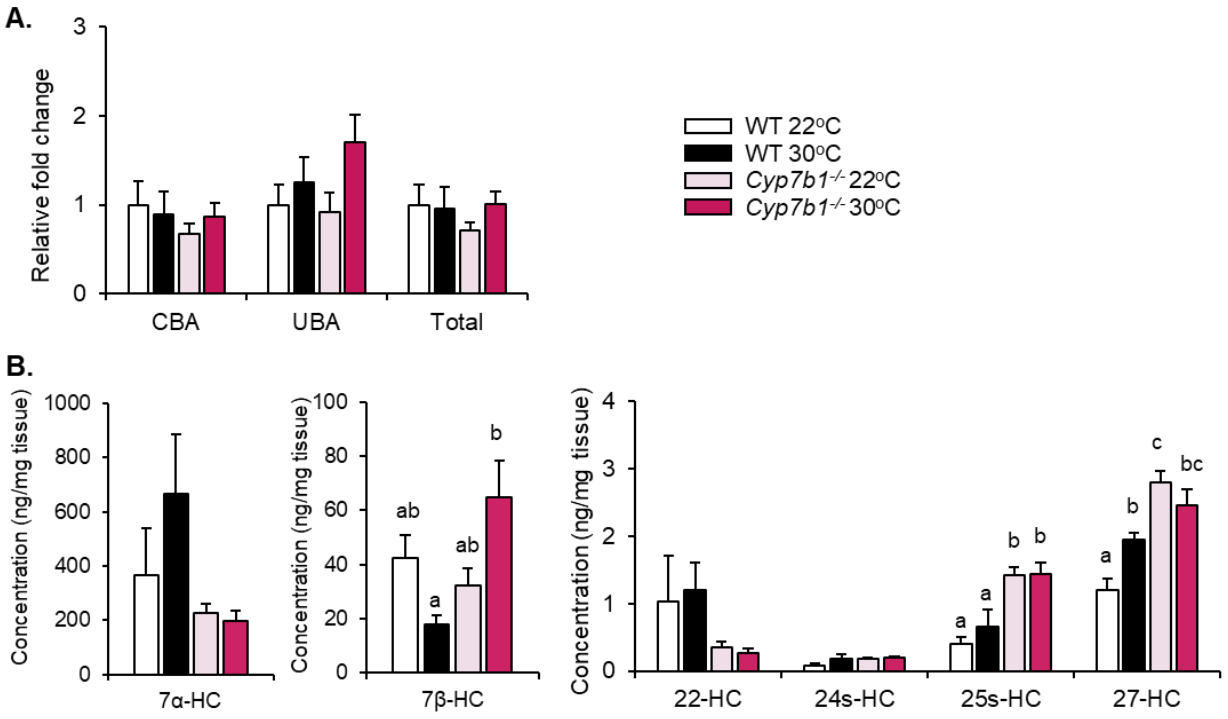

Figure 26. Changes in bile acids and oxysterols after 8 months of CD-HFD. A) Relative change of portal bile acid levels in comparison to WT 22°C mice (N=9-16) and (B) Levels of hepatic hydroxycholesterol species (hydroxycholesterol metabolites were measured by Niklas Roeder) (N=8) of *Cyp7b1*$^{-/-}$ and WT littermates housed under 22°C or 30°C. Data are shown as mean values ± SEM. Different letters indicate significant differences between groups ($p<0.05$) determined by two-way ANOVA.

To investigate whether these pathological alterations were accompanied by specific inflammatory responses, immune cell profiling by flow cytometry analysis of liver and spleen was performed. In liver, isolation of a sufficient number of viable non-parenchymal liver cells was inadequate, which probably could be explained by excess hepatic lipid deposition and fibrosis after 8-month feeding. In spleen, flow cytometry analysis revealed that *Cyp7b1*$^{-/-}$ mice had significantly increased numbers of total CD3+ T cells as well as the CD8+, CD4+ and CD4+CD25+ subpopulations (Figure 27). A similar trend was observed for Ly6G^{-} monocytes and Ly6C^{high} inflammatory monocytes but not for NK, NKT cells and neutrophils. Together these results showed that CYP7B1-deficiency modulates immune cell subpopulations in spleen, suggesting systemic effects on inflammation.

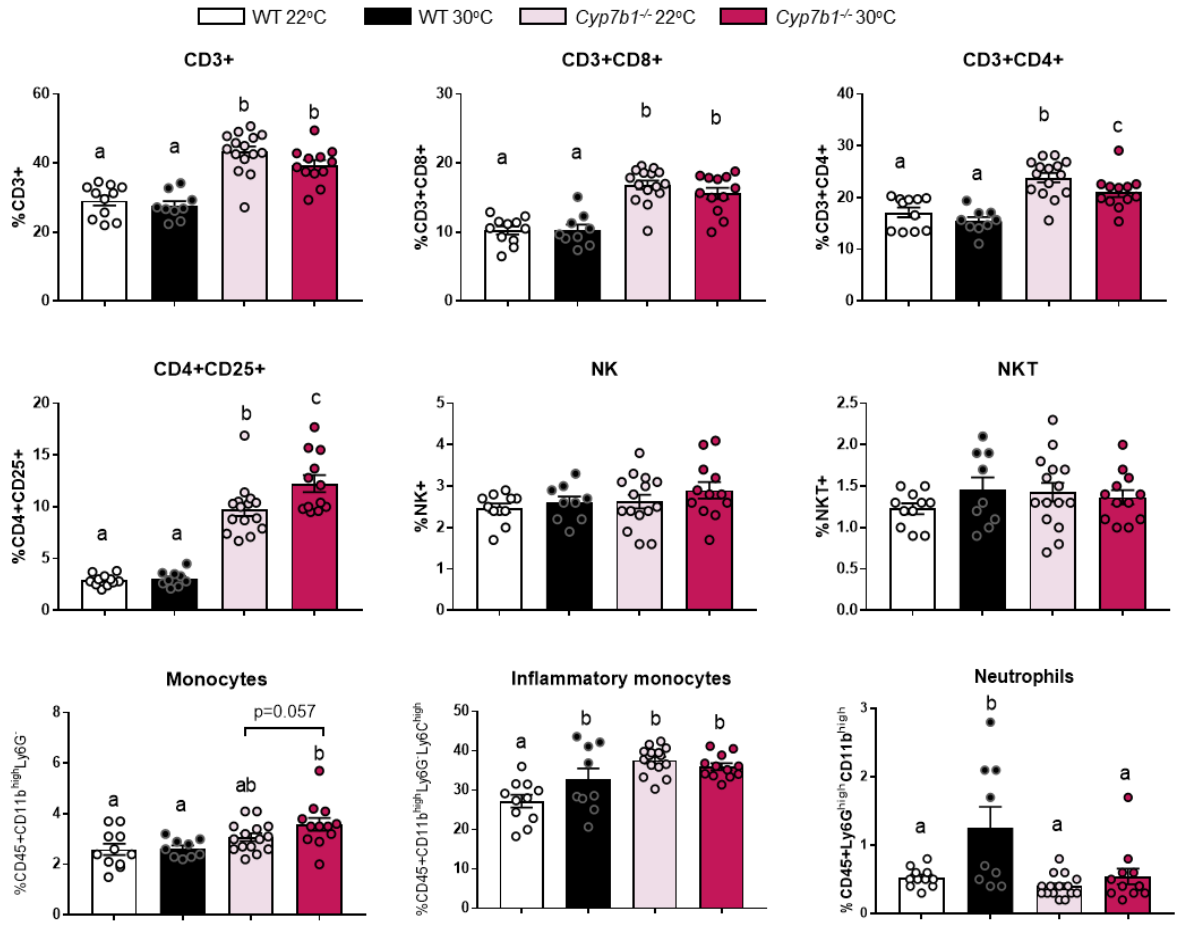

Figure 27. **Immune cell profiling of spleen after 8 months of CD-HFD.** Flow cytometry was performed to determine CD3+, CD3+CD8+, CD3+CD4+ and CD4+CD25+ lymphocytes as well as NK, NKT, monocytes, inflammatory monocytes and neutrophils in *Cyp7b1*$^{-/-}$ and wild littermates type housed under 22˚C or 30˚C, all fed a CD-HFD for 8 months. Data are shown as mean values ± SEM. N=9-16 mice/group. Different letters indicate significant differences between groups ($p<0.05$) determined by two-way ANOVA.

To study the impact of CYP7B1 deficiency on immune cell infiltration into the liver, hepatic immune cell profiling was performed in *Cyp7b1*$^{-/-}$ and WT mice housed at 22°C or 30°C after a CD-HFD feeding for only three weeks. This time point represented an earlier stage of diet-induced MAFLD, enabling efficient organ disintegration and thus flow cytometry. As in spleen the most prominent differences were observed in T lymphocytes, hepatic T cell sub-populations were specifically studied (Figure 28). Characterization of liver-infiltrating T cells by flow cytometry did not show significant differences as depicted by the comparable CD3+, CD3+CD8+ and CD3+CD4+ subpopulations (Figure 28A). However, specific analysis of isolated T cells re-stimulated with PMA/ionomycin showed

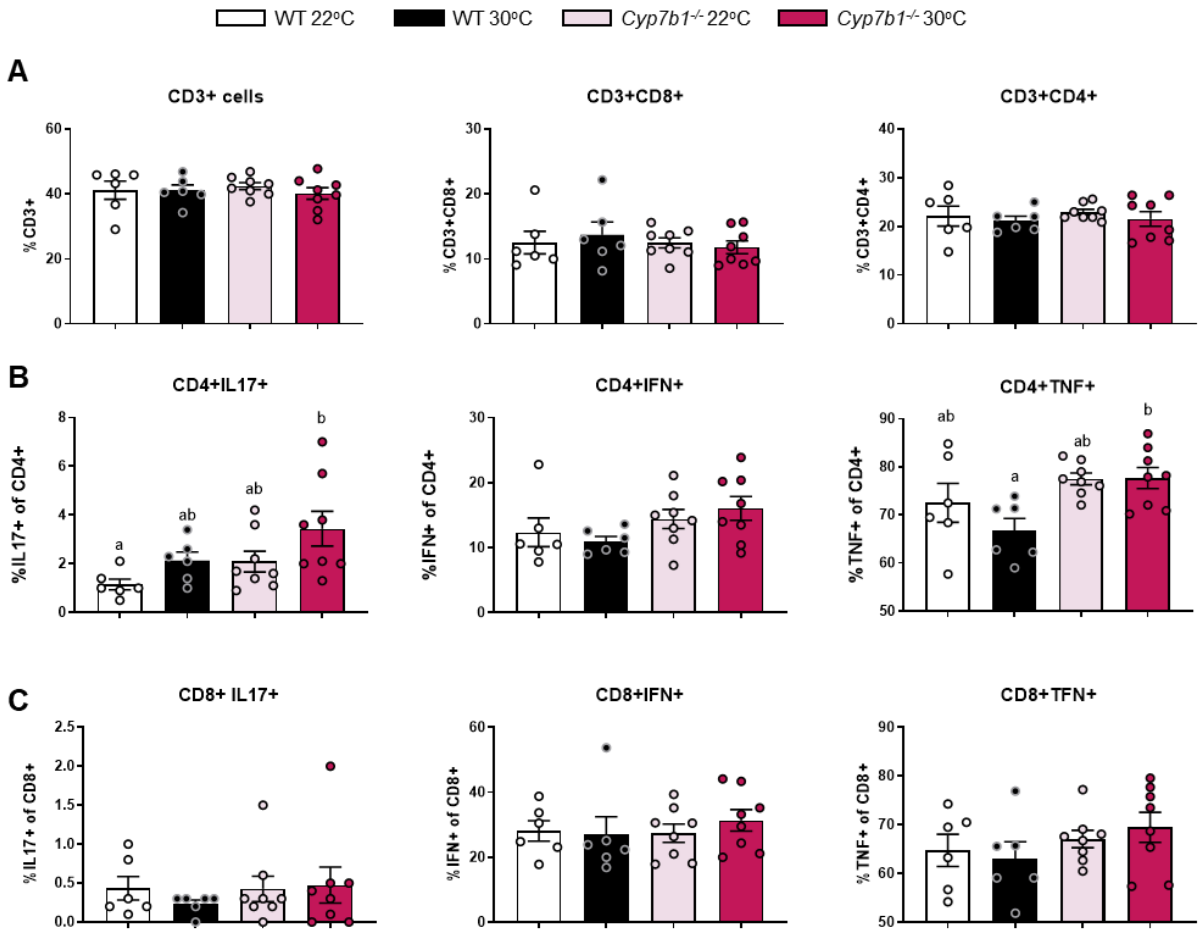

Figure 28. Immune cells profiling of liver after 3 weeks of CD-HFD. FACS analysis of (A) all CD3+ lymphocytes, as well as IL17-, IFN-, TNF-producing (B) CD3+CD8+ and (C) CD3+CD4+ cells in livers of *Cyp7b1*$^{-/-}$ and wild type littermates housed under 22°C or 30°C. Data are shown as mean values ± SEM of N=6-8 mice/group. Different letters indicate significant differences between groups ($p<0.05$) determined by two-way ANOVA

that IL17- and IFN-producing CD4+ cells from *Cyp7b1*$^{-/-}$ mice trended to be higher (Figure 28B). Moreover, at thermoneutrality TNF-producing CD4+ cells were significantly elevated in CYP7B1-deficient mice in comparison to their WT littermates (Figure 28B). The respective CD8+ cytokine producing cells were unaltered (Figure 28C). These data indicate that already short-term CD-HFD feeding causes subtle changes in T cell subpopulations in livers of CYP7B1-deficient mice.

To study whether CYP7B1 deficiency has effects on liver inflammation in the chronically fed mice, hepatic expression of inflammation-related genes including cytokines and chemokines was analyzed in WT and *Cyp7b1*$^{-/-}$ mice housed either at 22°C or 30°C. Most of the genes investigated exhibited higher expression in mice housed at

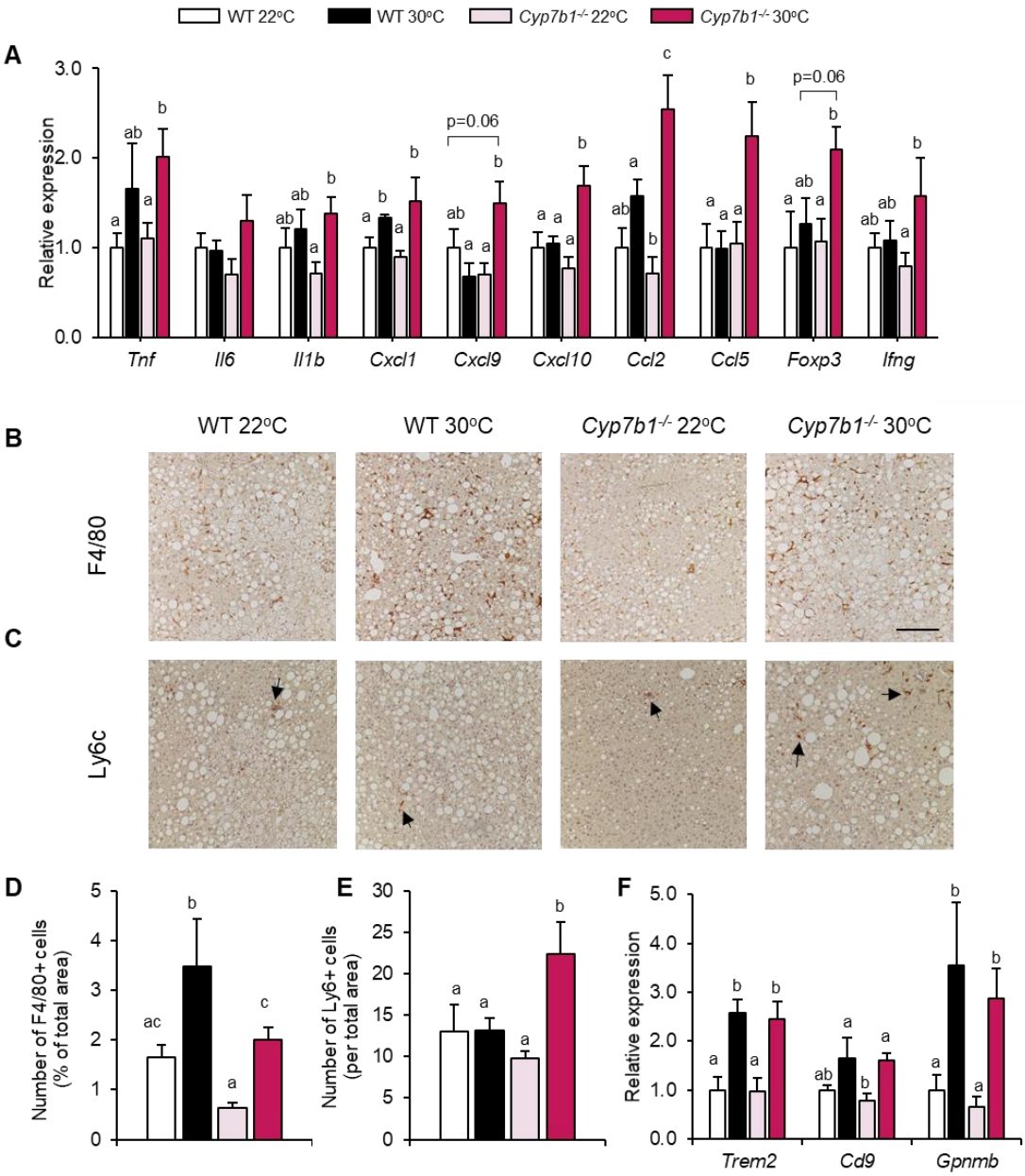

Figure 29. Hepatic histology and analysis of inflammatory markers after 8 months of CD-HFD. (A) Relative hepatic expression of inflammation-related genes (N=8 mice/group). (B, C) reepresentative images of (B) F4/80+ cells and (C) Ly6c+ cells (scale bar 100 µm) and (D, E) quantifications of (D) F4/80+ and (E) Ly6c+ images shown in B and C, respectively and (F) relative hepatic expression of Kupffer cell-related genes (N=9-16 mice/group) of *Cyp7b1*$^{-/-}$ and wild type littermates housed under 22°C or 30°C. Data are shown as mean values ± SEM. Different letters indicate significant differences between groups ($p<0.05$) determined by two-way ANOVA

30°C compared to those housed at 22°C, an effect that was more pronounced in the *Cyp7b1*$^{-/-}$ mice than in the WT mice for *Cxcl10*, *Ccl2* and *Ccl5* (Figure 29A). Staining for the tissue-resident F4/80-positive macrophages showed that thermoneutrality favors indeed their activation but higher in the WT albeit the large deviation (Figures 29B, 29D).

Analysis of the Kupffer cell-related gene markers including *Trem2*, *Cd9* and *Gpnmb* followed a similar pattern (Figure 29F). As CCL2 is a critical monocyte chemoattractant, infiltration of proinflammatory monocytes was determined by immunohistology. Increased numbers of infiltrating Ly6c-positive monocytes were measured specifically in livers of *Cyp7b1*$^{-/-}$ mice housed at thermoneutrality (Figure 29C, 29E). Together, these results indicate that proinflammatory immune responses are exaggerated in livers of mice lacking CYP7B1 that are housed at thermoneutrality.

As observed, CYP7B1-deficiency leads to lipid accumulation, proinflammatory and profibrotic responses only under thermoneutral housing conditions. Given the known role of cholesterol for MAFLD development, the expression of cholesterol handling proteins was next studied (Figure 30). The liver X receptor (LXR) positively regulates the transcription of hepatic cholesterol export pumps including dimeric ABCG5/ABCG8,

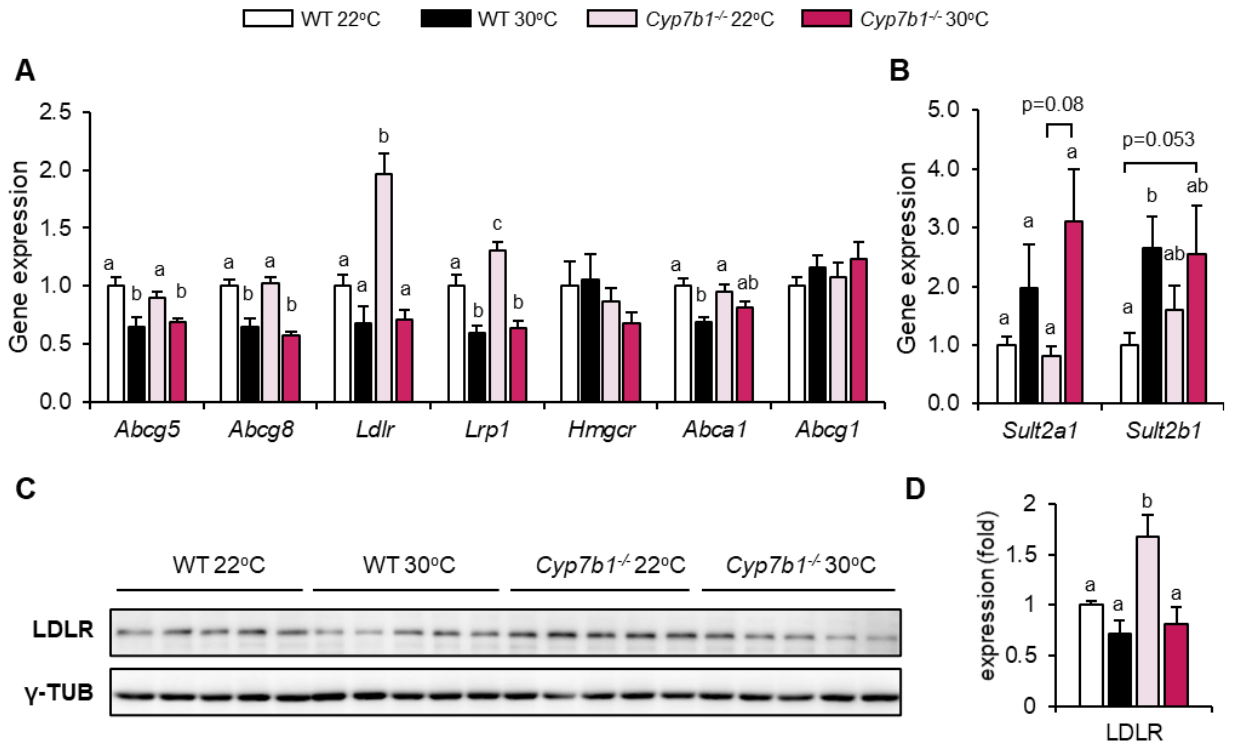

Figure 30. Expression of cholesterol handling proteins after 8 months of CD-HFD. (A) Relative hepatic expression of lipoprotein receptors and cholesterol metabolism-related genes and (B) hepatic sulfotranferases (N=8), (C) Western blot analysis and (D) quantification of hepatic LDLR gamma tubulin (γ-TUB) was used as loading control and for normalization. Data are shown as mean values ± SEM of *Cyp7b1*$^{-/-}$ and wild type littermates housed under 22°C or 30°C. Different letters indicate significant differences between groups ($p<0.05$) determined by two-way ANOVA.

ABCA1 and ABCG1 (Ma and Nelson 2019). Despite the elevation of the LXR agonists 25-HC and 27-HC (Figure 26), expression of these genes was not affected by CYP7B1 deficiency (Figure 30A), arguing against activation of LXR under this condition. Also, in all 30°C-housed mice slightly higher expression of the bile acid and oxysterol sulfotransferases *Sult2a1* and *Sult2b1*, respectively, was observed (Figure 30B). This could be indicative of elevated sulfated metabolites that however were not measured in this study. Notably, *Cyp7b1*$^{-/-}$ mice housed at 22°C but not at 30°C exhibited higher liver expression of the LDL receptor (LDLR) both at the mRNA (Figure 30A) and the protein (Figures 30C, 30D) level. Similarly, the LDLR-related protein-1 encoding gene (*Lrp1)* was expressed at higher levels in these mice. No regulation was observed for hydroxyl-methylglutaryl-CoA reductase (*Hmgcr*), suggesting that sterol-regulatory element-binding protein-2 that positively regulates both *Ldlr* and *Hmgcr* is not responsible for the LDLR upregulation in *Cyp7b1*$^{-/-}$ mice housed at 22°C. Taken together and in line with experiments performed in LDLR deficient mice (Bieghs et al. 2012), these data suggest that increased flux of lipoprotein-associated lipids into hepatocytes is protective in the context of MAFLD at 22°C. On the other hand, hepatic lipoprotein receptor expression is not induced in CYP7B1-deficient mice at thermoneutrality, favoring proinflammatory and fibrotic responses possibly due to lipid and oxysterol accumulation in non-parenchymal and immune cells.

In conclusion, these data showed that CYP7B1 protects against diet-induced MAFLD progression in mice housed at thermoneutrality.

Part G: Discussion

1. Regulation of *Cyp7b1* expression upon cold exposure

Given the temperature-dependent expression of hepatic *Cyp7b1* upon a WTD feeding, studying its regulation under various conditions, including the duration as well as the intensity of cold exposure that are required to promote this effect, was particularly intriguing. The animal experiments showed that a minimum of 3-day extreme cold exposure (6^{o}C) is necessary to trigger *Cyp7b1* upregulation, an effect that was largely absent at earlier time points. This could indicate that acute stimulation of BAT is not directly connected with the increased hepatic expression of *Cyp7b1* but prolonged conditions of energy expenditure and increased caloric consumption (e.g. after 3 days) are crucial for the induction of the alternative synthesis pathway of BAs. This might occur in response to elevated delivery of cholesterol remnants into the liver and in an effort of the organ to maintain cholesterol homeostasis via its enhanced catabolism. In line with previous observations, β3-adrenergic BAT stimulation via CL-316,243 administration for a week could still increase food consumption and at the same time *Cyp7b1* expression (data not shown), pointing towards a synergistic effect of BAT activation and caloric consumption. Additionally, a 4-day exposure at 6^{o}C and 16^{o}C promoted a similar effect, but housing at conventional temperature (22^{o}C) was not sufficient to induce hepatic *Cyp7b1* expression, at least for the given time period. That could support the notion that increased energy expenditure in combination with conditions of increased caloric consumption via food intake might be prerequisite to promote the alternative conversion of cholesterol to bile acids via CYP7B1. However, cholesterol itself was rather dispensable for the induction of *Cyp7b1* expression after cold exposure as double inhibition of its de novo biosynthesis and absorption did not diminish the enzyme's upregulation upon cold exposure.

Another point to be addressed during the first part of this thesis was the role of insulin signaling as several studies have reported its connection with *Cyp7b1* regulation (Biddinger et al. 2008) (Kakiyama et al. 2020). During fasting-refeeding studies, which were used to promote insulin secretion and signaling, no alterations were observed in the

expression of hepatic *Cyp7b1* upon cold exposure. However, this does not ultimately mean that insulin is not playing a significant role, as the approach employed in this thesis work was more indirect and largely depends on the preference of mice to eat after the fasting period. As an alternative approach, inhibition of insulin receptor, e.g. with the specific antagonist S961 (Vikram and Jena 2010) in cold-exposed mice could clarify whether insulin signaling is indeed important for the enzyme's transcription. Furthermore, the role of insulin for *Cyp7b1* induction could be also examined in insulin resistance mouse models like *db*/*db* mice (Hummel, Dickie, and Coleman 1966) that would be exposed to conditions of increased energy expenditure and BAT activation.

Digging deeper into identifying the potential transcription factors that are implicated in *Cyp7b1* regulation, it was found in the current work that RORα agonism at thermoneutrality can efficiently promote its expression. This was mirrored to elevated levels of alternatively produced bile acids such as CDCA and UDCA, as well as their taurine conjugates. In line with the literature (Wada et al. 2008) these data indicate that *Cyp7b1* can be transcriptionally activated by RORα, even under conditions of WTD. However, RORα antagonism in cold exposed mice, did not halt the gene's upregulation, which prompted us to conclude that RORα might not be the sole transcriptional activator, especially under conditions of high energy demand.

In order to identify the *Cyp7b1* transcription factor, untargeted approaches such as reverse ChIP followed by untargeted mass spectrometry analysis of the proteins which are bound to the gene promoter would be needed. In addition, it cannot be excluded that *Cyp7b1* under thermoneutral conditions is under the control of specific miRNA silencing, which can be altered by cold exposure and BAT stimulation. An intriguing hypothesis would be that BAT-derived molecules that are targeted to the liver could influence such responses. Interestingly, BAT-produced exosomes that can be released into the circulation have been reported to carry miRNAs (Y. Chen et al. 2016). In this particular study, exosomes from activated BAT showed that the enrichment of specific miRNAs which have *Cyp7b1* as a putative target, such as miR-144 and miR-155 (Cheng et al. 2020)(Brie et al. 2020) was significantly decreased. It would be thus reasonable to question whether BAT activation can influence the levels of exosome-circulating miRNAs that may in turn alter transcriptional responses in the liver. Therefore, investigation of

Cyp7b1 expression in cold exposed mice that will be administered with exosomes containing mimics for the respective miRNAs would be plausible to follow.

2. Implication of CYP7B1 and related metabolites in systemic metabolism and brown adipose tissue activation

Under conditions of cold exposure, the thermogenic brown and beige adipose tissues are activated to promote adaptive thermogenesis and heat production while bile acid signaling has been reported as a positive regulator of the thermogenic programs in mice as well as in humans (Watanabe et al. 2006) (Broeders et al. 2015). In previous studies, *Cyp7b1* deficiency attenuated the expression and the protein levels of UCP1 in BAT as well as WAT depots (Worthmann et al. 2017). To further investigate the interplay between BA and BAT under *Cyp7b1* deficiency, it was hypothesized that next to reduced fecal BA levels and lower energy expenditure in BAT, *Cyp7b1*$^{-/-}$ mice would have altered lipoprotein clearance when exposed to cold temperatures. In line with the previous report (Worthmann et al. 2017), *Cyp7b1*$^{-/-}$ mice not only exerted reduced fecal but also systemic BA levels. These translated into reduced BA-mediated BAT activation as assessed by the reduced levels of pPKA substrates. This is in accordance with reduced levels of phosphorylation of cAMP response element binding protein (pCREB) observed in mice lacking TGR5 specifically in adipocytes (Velazquez-Villegas et al. 2018). Therefore, it is reasonable to speculate that, in this model, reductions in pPKA substrate might stem from attenuated TGR5-signalling. In addition, lower levels of OXPHOS complex I detected in cold-housed *Cyp7b1*$^{-/-}$ mice may be a result of decreased PKA signaling (Papa et al. 2012) and thus also mediated by the impaired BA-TGR5-axis after loss of *Cyp7b1*. In line with the hypothesis that CYP7B1-derived bile acids could influence postprandial metabolism, it was observed that attenuated activation of BAT in *Cyp7b1*$^{-/-}$ affected the clearance of TRL particles. Specifically, BAT uptake of entire TRL (^{14}C-cholesterol tracer) and TRL-derived fatty acids (^{3}H-triolein tracer) was decreased in the absence of *Cyp7b1*, while WAT uptake of cold-housed WT and *Cyp7b1*$^{-/-}$ mice remained similar. This is line with the diminished thermogenic BAT markers and points towards an attenuated thermogenic response of the organ. This could be partly explained by a potential

reduction in CDCA production, the main product of CYP7B1 and the alternative synthesis pathway, which is a potent agonist for TGR5 and has been connected with increased BAT activity in mice as well as in humans (Broeders et al. 2015) (Teodoro et al. 2014).

Additionally, especially under cold exposure, cholesterol tracers were increased at distal parts of the intestinal track in *Cyp7b1*$^{-/-}$ mice. Given that BA are important mediators of lipid digestion processes (Kuipers, Bloks, and Groen 2014),this could be translated to either an accelerated cholesterol processing throughout the gastrointestinal lumen and/or a higher uptake from the enterocytes. Interestingly, it has been shown that bile acids with high hydrophilicity index, such as muricholic acids, inhibit the intestinal absorption of cholesterol (D. Q. H. Wang et al. 2003). Since CYP7B1 is effectively producing CDCA, that in mice can be further 6β-hydroxylated to muricholics via the action of CYP2C70 (Takahashi et al. 2016), inability of increasing *Cyp7b1* expression at cold and subsequently a reduced muricholic bile acid pool, could enhance cholesterol absorption in the intestinal tract. To delineate whether the intestinal lipid absorption and re-secretion is altered upon CYP7B1-deficiency in the context of different ambient temperatures, chylomicron production assay after inhibition of lipoprotein lipases was performed. Here, cholesterol and triolein tracers in the plasma were comparable in all groups, thus ruling out possible effects of *Cyp7b1* and CYP7B1-derived BA on intestinal lipid ingestion. In response to cold, BAT not only takes up TRL derived fatty acids but also entire TRL particles (Bartelt et al. 2011)(Fischer et al. 2021), a process which is dependent on insulin (Heine et al. 2018). LPL is an important mediator of TRL hydrolysis (Auwerx, Leroy, and Schoonjans 1992) and is transported to the capillary lumen by GPIHBP1 (Davies et al. 2010). In accordance with reduced uptake of fatty acids and entire TRL particles, also LPL as well as GPIHBP1 levels were reduced in cold-exposed *Cyp7b1*$^{-/-}$ mice. Moreover, ANGPTL4 has been described to be critical for BAT TRL uptake (Dijk et al. 2015)and *Angptl4* transcript levels were increased in cold-housed *Cyp7b1*$^{-/-}$ mice. Of note, as described before (Kakiyama et al. 2020), *Cyp7b1* is tightly associated with insulin resistance and cold exposed *Cyp7b1*$^{-/-}$ mice seem to be insulin resistant. This might be explained by the reduced thermogenic activity and subsequent lower energy expenditure observed in *Cyp7b1*$^{-/-}$ mice which ultimately results in the development of obesity. As LPL is activated by insulin (Sadur and Eckel 1982) also in BAT (Mitchell et al. 1992) and LPL

activation is compromised by insulin resistance (Panarotto et al. 2002), reduced LPL levels in cold-housed *Cyp7b1*$^{-/-}$ mice might result from their insulin resistance.

In summary, the above studies showed that CYP7B1-derived BA are important mediators of BAT function and influence BAT-dependent lipoprotein clearance in response to cold-temperatures. Mechanistically, the compromised lipoprotein clearance in *Cyp7b1*$^{-/-}$ mice was dependent on reduced LPL levels which were linked to global insulin resistance (Figure 31). All the above highlight the relevance of BA derived via the alternative route as modulators of BAT thermogenesis.

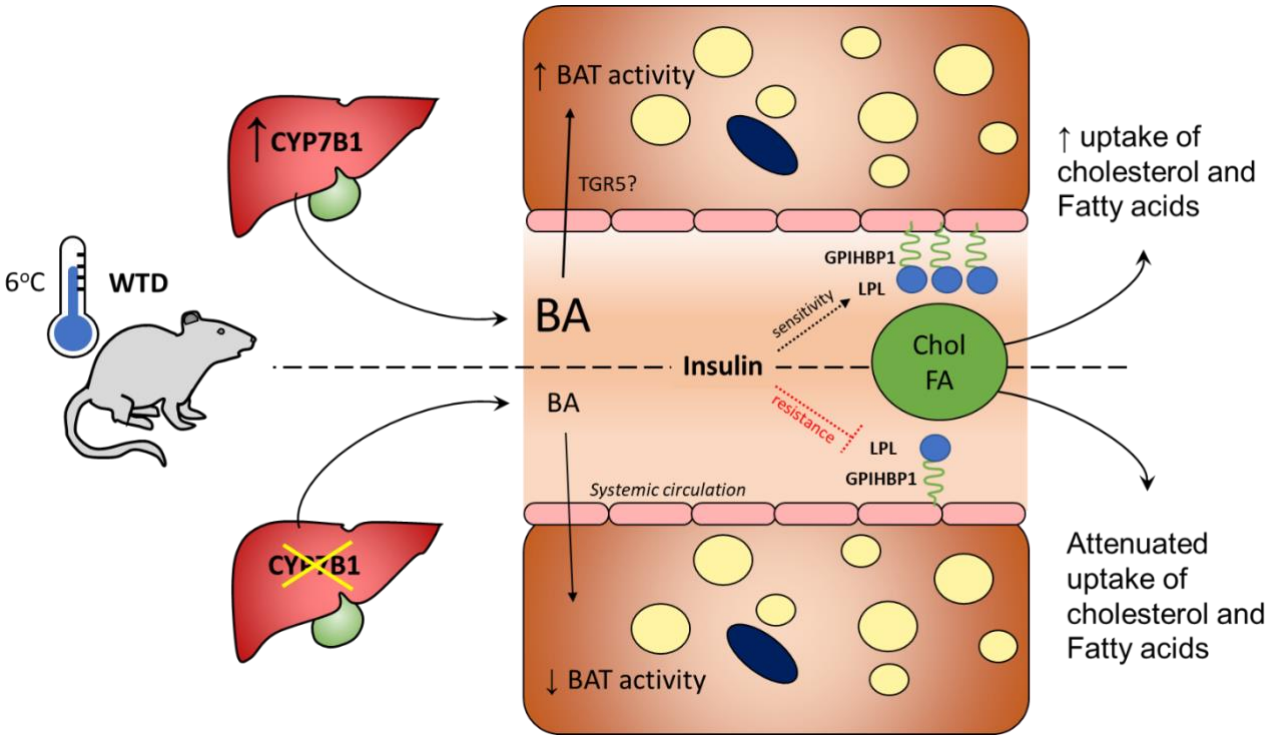

Figure 31. Graphical abstract summarizing the findings regarding the relevance of *Cyp7b1* for brown adipose tissue lipoprotein processing.

3. Implication of CYPB1 and related metabolites in MAFLD

As already discussed in the introduction, changes in bile acid and oxysterol levels contribute and/or occur during the establishment of metabolic abnormalities such as type 2 diabetes and MAFLD (Evangelakos et al. 2021, Ahmad and Haeusler 2019). Therefore,

unravelling the contribution of specific cytochrome P450 superfamily enzymes that mediate their biosynthetic pathways can shed light on their pathophysiological role. Interestingly, the alternative bile acid synthesis pathway seems to be differentially altered in metabolic-related disorders, since CYP7B1 has been described to be decreased in murine models as well as patients with type 2 diabetes (Worthmann et al. 2017)(C. Chen et al. 2016) (Biddinger et al. 2008) but was found elevated in patients with progressive MAFLD (Lake et al. 2013). Of note, the results of mechanistic studies investigating the role of CYP7B1 in MAFLD are quite inconsistent. In a recent study, Raselli et al. pointed towards a non-essential role of CYP7B1 in MAFLD progression, as both hepatic fibrosis and disease activity score were comparable between HFD-fed WT and *Cyp7b1*$^{-/-}$ mice (Raselli et al. 2019). On the contrary, Kakiyama et al. provided evidence that, especially under conditions of insulin resistance, CYP7B1 could mediate progression to steatohepatitis, owing to the accumulation of toxic oxysterols that could promote inflammation and liver damage (Kakiyama et al. 2020). Recently, it has been shown that thermoneutral housing, a condition of low brown adipose tissue activity and diminished energy expenditure (Heeren and Scheja 2021), provides a suitable model of exacerbated diet-induced MAFLD in mice (Giles et al. 2017). Both Raselli et al. and Kakiyama et al. studied mice housed only at conventional room temperature which exposes mice to a mild cold stress. However, those studies did not take into consideration the fact that CYP7B1 is regulated by ambient temperature. Therefore, this thesis aimed to investigate the role of the alternative synthesis pathway under optimal housing environments, in an effort to better mimic the human thermoneutral state.

By using the MCD feeding model of steatohepatitis, it was observed that mild cold exposure reduces hepatic triglyceride deposition - with the effect being more prominent in the *Cyp7b1*$^{-/-}$ mice - while hepatic cholesterol accumulation as well as plasma lipids were unaffected by this treatment. The reduced hepatic steatosis after housing at 22^{o}C is in line with previous studies showing that mild cold exposure can alleviate the symptoms of MAFLD. Despite that thermoneutral temperatures slightly exacerbated fibrosis and mild cold exposure had a protective effect against hepatic fibrosis the liver injury-related ALT levels showed an opposite trend in the plasma, as they were elevated in all groups kept at 22^{o}C. However, even though these results are quite contradictory, no differences were

attributed to the presence or absence CYP7B1. Therefore, deletion of CYP7B1 did not show to affect the progression of the disease in comparison to the wild type and in either temperature. Additionally, in contrast to the well described induction of *Cyp7b1* upon cold stimulation, mild cold exposure for a total of 2 weeks didn't increase its expression as expected. This could suggest that the temperature of 22ºC is not sufficient for the induction of its expression and/or the experimental conditions (MCD diet, time of intervention) result in altered responses in the liver.

Nevertheless, a potential role for CYP7B1 and its metabolites in metabolic associated diseases cannot be deduced owing to the controversial effects of the MCD diet and at the same time the limited duration of the study due to ethical reason (see below). Notably, the MCD feeding model, despite promoting a rapid hepatic damage as already reported (Anstee and Goldin 2006), does not correlate with features of the human metabolic liver disease, such as obesity and insulin resistance (Rinella and Green 2004). During the study, the MCD-fed mice, regardless of genotype and housing temperature, lost significant percentage of body weight (~20%) and became cachectic, which resulted in early termination of the feeding. In addition, all mice showed macroscopically minor hepatic steatosis. However, excessive fat deposition is considered a crucial step for the establishment of the disease in humans. Failure to reproduce this hepatic phenotype can be attributed to the fact that methionine and choline deficiency primarily mediate liver damage as a result of increased oxidative stress. The latter is caused due to the accumulation of reactive oxygen species (ROS) which are produced during CYP2E1-mediated ω-oxidation (Gao et al. 2004). Perhaps this rapid progression towards hepatic damage accompanied by the relatively low fat-content of the diet cannot recapitulate the chronic establishment of MAFLD in humans.

High fat diet in combination with choline deficiency have been established in an effort to mimic the establishment of MAFLD as it is observed in humans (Wolf et al. 2014a). Here, hepatic *Cyp7b1* expression was significantly higher in WT mice housed under sustained mild-cold exposure (22°C) for 8 months in comparison to thermoneutrality. This indicated that the alternative route of BA synthesis is triggered at prolonged low ambient temperatures, which are associated with enhanced hepatic cholesterol metabolism and accelerated lipoprotein clearance (Bartelt et al. 2011)(Bartelt et al. 2017)(Berbeé et al.

2015). Together, these processes could explain the milder MAFLD phenotype of conventionally housed mice when compared to mice housed at thermoneutrality (Giles et al. 2017). In line with Raselli et al. (Raselli et al. 2019), CYP7B1 deficient mice housed at 22°C have a disease phenotype upon CD-HFD feeding largely indistinguishable from their WT littermates housed at the same temperature. In contrast, *Cyp7b1*$^{-/-}$ mice housed at 30°C are characterized by exacerbated MAFLD (summarized in Figure 32). These data indicate that CYP7B1 activity counteracts disease progression specifically under conditions of low thermogenic stress that actually represent typical human living conditions (Fischer, Cannon, and Nedergaard 2018b)(Ganeshan and Chawla 2017). In order to delineate how CYP7B1-dependent hydroxycholesterols and/or bile acids influence diet-induced energy homeostasis in the context of MAFLD progression, future studies that will focus on parameters such as core body temperature, energy expenditure, and heat loss are warranted.

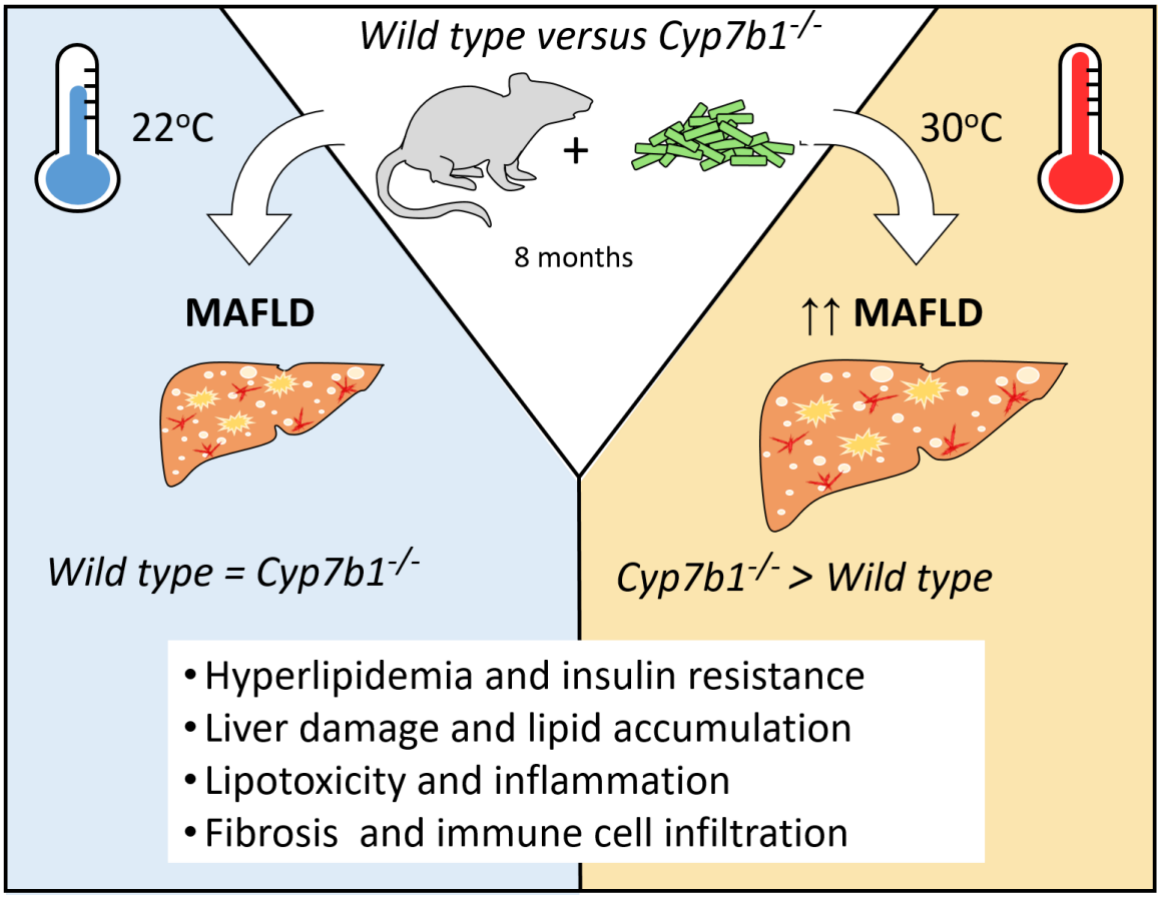

Figure 32. Graphical abstract of the CD-HFD intervention in WT and *Cyp7b1*$^{-/-}$ mice housed at different ambient temperatures (adapted from Evangelakos et al., 2021)

The alternative pathway is described as a minor contributor in the biosynthesis of bile acids compared to the classical one. Previously, it was shown that hepatic CYP7B1 mRNA was moderately reduced in human liver samples of obese diabetic compared to non-obese subjects (Worthmann et al. 2017). Recent publications aiming at the identification of hepatic transcriptomic signatures, distinguishing simple steatosis from steatohepatitis, did not report differential mRNA expression of CYP7B1 when comparing these groups (Suppli et al. 2019)(Vandel et al. 2021). However, the comparable expression data do not necessarily mean that alterations in CYP7B1 activity may have an impact during MAFLD in humans. Supporting this possibility, newborns with loss of function CYP7B1 mutations develop severe liver phenotypes (Setchell et al. 1998)(Ueki et al. 2008). These patients lacking CYP7B1 activity are characterized by elevated levels of 24-HC, 25-HC, 27-HC, 3β-hydroxy-5-cholenoic and 3β-hydroxy-5-cholestenoic acids, aggressive hepatic fibrosis and inflammation that eventually lead to liver failure and premature death. Similarly, the CD-HFD study showed that CYP7B1 deficiency in rodents leads to hepatic accumulation of the enzyme's specific hydroxycholesterol substrates 25-HC and 27-HC. All in all, the 30°C-housed *Cyp7b1*$^{-/-}$ mice presented a hepatic milieu characterized by accumulation of specific hydroxycholesterols. On the other hand, in the current thesis work it is shown that the 22°C-housed *Cyp7b1*$^{-/-}$ mice display upregulation of *Cyp27a1* that may explain the slightly higher levels of its respective hydroxycholesterol product 27-HC. Interestingly, Bieghs et al. described that administration of 27-HC in high-fat- high cholesterol diet-fed mice can lower cholesterol-induced inflammation and attenuate steatohepatitis over time (Bieghs et al. 2013). This feature of 27-HC could, at least in part, contribute to the milder MAFLD-related phenotype in the conventional housed *Cyp7b1*$^{-/-}$ mice. However, despite the slight increase of 27-HC which is a potent LXRα agonist, no alteration in LXRα-target genes was observed in these mice. This could imply that LXRα cannot be activated under these conditions e.g. due to increased sulfated hydroxycholesterols that exert antagonistic effects on this receptor (W. Chen et al. 2007). In fact, we found that hepatic expression of *Sult2b1* was increased by thermoneutral housing and trended to be higher in *Cyp7b1*$^{-/-}$ mice, that also present hepatic accumulation of 27-HC. Even though sulfated hydroxycholesterol levels were not directly determined, these data could argue towards their rapid reduction via relevant sulfotransferases, explaining why LXRα regulated markers could not be induced.

An additional explanation for the alleviated phenotype of the 22°C-housed *Cyp7b1*$^{-/-}$ mice in comparison to their 30°C-housed littermates could be the specific upregulation of both *Ldlr* and *Lrp1* genes. Interestingly, deficiency in either *Ldlr* or *Lrp1* has been connected to increased susceptibility for hepatic steatosis and inflammation in mice (Bieghs et al. 2012) (Hamlin et al. 2018). Therefore, upregulation of these genes and their encoded lipoprotein receptors, LDLR and LRP1 respectively, at 22ºC could protect *Cyp7b1*$^{-/-}$ mice against diet-induced MAFLD progression. On the other hand, their low expression at thermoneutrality may favor lipotoxic responses mediated by accumulating lipoproteins and oxysterols. It is known that clearance of LDL-cholesterol particles leads to hyperlipidemia, a feature which was also present in the *Cyp7b1*$^{-/-}$ mice housed at 30°C. The subsequent prolonged half-life of LDL in the circulation renders the particles prone to oxidation that can ultimately be taken up by various other receptors and trigger inflammatory responses in the liver (Kunjathoor et al. 2002). Despite its protective effect, it is still unclear how LDLR could be upregulated in 22ºC-housed *Cyp7b1*$^{-/-}$ mice, especially because its master transcription factor SREBP2 did not have a positive regulation on other target genes. Nevertheless, the relevance of LDLR in the MAFLD-associated phenotype in CYP7B1-deficient mice could be further investigated in double knockout mice (*Ldlr*$^{-/-}$ *Cyp7b1*$^{-/-}$) fed with a CD-HFD and housed under the different environmental temperatures.

Hepatic accumulation of specific lipid classes such as diacylglycerols has been connected to hepatic insulin resistance and also with the progression of MAFLD in mice and humans (Gorden et al. 2011) (Petersen and Shulman 2017) (Vvedenskaya et al. 2021). Diacylglycerols can specifically activate isoforms of the protein kinase C family (particularly PKCε), that in turn destabilize the tyrosine kinase activity of the insulin receptor (IR) and inhibit insulin signaling (Petersen et al. 2016). As anticipated, inhibition of PKCε was shown to prevent high fat diet-induced insulin resistance in rats (Samuel et al. 2007). Therefore, increased levels of hepatic diacylglycerols in CD-HFD-fed *Cyp7b1*$^{-/-}$ mice housed at thermoneutrality could be correlated with insulin resistance, an observation supported by their hyperinsulinemia, and subsequently with the aggravated MAFLD phenotype that they exert. However, whether diacylglycerol accumulation is a result of induced hepatic triglyceride hydrolysis, attenuated degradation via diacylglycerol

acyltransferases (DGATs), increased synthesis via monoacylglycerol acyltransferases (MGATs) or how these processes are influenced by loss of the *Cyp7b1*-derived metabolites remains elusive. On that note, MGAT expression and actively was positively associated with MAFLD progression as analyzed in human liver biopsies (Hall et al. 2012). An interesting finding was that cholesterol esters were also specifically elevated in the livers of *Cyp7b1*$^{-/-}$ mice housed at 30^{o}C. Hepatic accumulation of this lipid class could argue against aggravated lipotoxicity and hence MAFLD, once cholesterol esterification is one the major mechanisms to prevent intracellular levels of free cholesterol that is very toxic for the cells (Arguello et al. 2015). However, determination of hepatic free cholesterol revealed that *Cyp7b1*$^{-/-}$ mice housed at 30^{o}C had lower levels than their WT littermates (data not shown). Altogether, these observations could suggest that accumulation of cholesterol in the 30^{o}C-housed *Cyp7b1*$^{-/-}$ mice is not detected owing to counteracting mechanisms that are triggered in order to eliminate this hepatotoxic molecule. For example, the activity of hepatic acyl-CoA cholesterol acyltransferase (ACAT), the responsible enzyme for the above esterification, might be triggered in these mice and in combination with inadequate loading of cholesterol esters to ApoB100-containing particles could result in accumulation of this lipid species in the liver. However, whether ACAT activity or expression are increased in these mice was not investigated.

Oxysterols have potent immunomodulatory functions as they can activate several nuclear receptors such as liver X receptors (LXRs) and retinoic acid orphan receptors (RORs). Next to their role in regulating cholesterol and energy metabolism, these transcription factors are known to influence immune functions including macrophage phagocytosis, T- and B-lymphocyte activation, immune cell migration and polarization (Spann and Glass 2013). Cell types of both the innate and the adaptive immune systems are important mediators of MAFLD progression. Here, we observed a trend for increased numbers of hepatic IL17-, TNF- and INF-producing CD4+ lymphocytes in CYP7B1 deficient mice in the early stages of MAFLD progression under thermoneutral conditions. That means that hepatic milieu caused by CYP7B1 deficiency can drive the expansion of specific T cell populations, particularly under thermoneutrality. According to recent literature (Willinger 2019)(Reinmuth et al. 2021), specific oxysterols can bind to receptors present in T cells, thus influencing their activation. Interestingly, T cell activation has been

shown to trigger the activity of SULT2B1, which produces the sulfated antagonists of LXR (Glass and Saijo 2008), and eventually suppresses pathways related to cholesterol excretion (Bensinger et al. 2008). Intrahepatic cholesterol retention from early stages could also lead to the production of cholesterols esters, which we observed increased after 8 months of CD-HFD in the 30ºC-housed *Cyp7b1*$^{-/-}$ mice. All the above stress the interplay of LXR signaling during metabolic homeostasis that could, at least in part, explain modulations observed in immune cell phenotyping in the context of CYP7B1 deficiency and housing temperature.

After 8 months of CD-HFD feeding, that represents the later stages of MAFLD progression, liver stiffness and hepatic lipid accumulation prevented immune cell profiling by flow cytometry. However, immunohistology and expression analysis of inflammatory genes provided evidence that the release of specific cytokines and chemokines such as CCL2 and CCL5 by liver cells promoted the recruitment of T cells and inflammatory LyC6^{+} monocytes in thermoneutral housed CYP7B1-deficient mice. Importantly, these chemokines have been described to be elevated in MAFLD patients and to be important for the progression MAFLD in murine models (Berres et al. 2010) (Baeck et al. 2012). Definitely future studies are warranted to delineate the detailed mechanisms and the relevance of specific oxysterols for the regulation of immune cell subtypes in murine as well as human MAFLD. As a result, our study demonstrates the relevance of CYP7B1 for the prevention of MAFLD and associated immunometabolic disturbances in the context of thermoneutrality.

It is of note that the phenotype of CYP7B1 deficiency is different between species (Li-Hawkins et al. 2000). Murine knockout mice are largely indistinguishable from the WT littermates while mutations in humans have been reported deleterious (Setchell et al. 1998) (Dai et al. 2014). Here, as discussed in the introduction, the fundamentally dissimilar bile acid pool between mice and humans might also play a significant role. Given the trials to mimic the human thermoneutral zone in this study by acclimating the animals at 30ºC, further investigation regarding the role of CYP7B1 should be conducted in mice that lack CYP2C70 and exert thus a humanized bile acid pool (Takahashi et al. 2016) (De Boer et al. 2020). Based on the data generated in my thesis work, employing the *Cyp2c70*$^{-/-}$ *Cyp7b1*$^{-/-}$ double knockout model in diet induced MAFLD studies could

shed light in previous unappreciated features that are potentially implicated in the human disease state and help towards understanding the species-divergent phenotypes of CYP7B1 deficiency.

Part H: References

Acton, Susan, Attilio Rigotti, Katherine T. Landschulz, Shangzhe Xu, Helen H. Hobbs, and Monty Kriegert. 1996. “Identification of Scavenger Receptor SR-BI as a High Density Lipoprotein Receptor.” *Science*. https://doi.org/10.1126/science.271.5248.518.

Agouni, Abdelali, Carl Owen, Alicja Czopek, Nimesh Mody, and M. Delibegovic Mirela. 2010. “In Vivo Differential Effects of Fasting, Re-Feeding, Insulin and Insulin Stimulation Time Course on Insulin Signaling Pathway Components in Peripheral Tissues.” *Biochemical and Biophysical Research Communications*. https://doi.org/10.1016/j.bbrc.2010.09.018.

Ahmad, Tiara R., and Rebecca A. Haeusler. 2019. “Bile Acids in Glucose Metabolism and Insulin Signalling — Mechanisms and Research Needs.” *Nature Reviews Endocrinology*. https://doi.org/10.1038/s41574-019-0266-7.

Ahn, Sang Bong, Kiseok Jang, Dae Won Jun, Byung Hoon Lee, and Kye Jung Shin. 2014. “Expression of Liver X Receptor Correlates with Intrahepatic Inflammation and Fibrosis in Patients with Nonalcoholic Fatty Liver Disease.” *Digestive Diseases and Sciences*. https://doi.org/10.1007/s10620-014-3289-x.

Ananthanarayanan, M., N. Balasubramanian, Makoto Makishima, David J. Mangelsdorf, and Frederick J. Suchy. 2001. “Human Bile Salt Export Pump Promoter Is Transactivated by the Farnesoid X Receptor/Bile Acid Receptor.” *Journal of Biological Chemistry*. https://doi.org/10.1074/jbc.M011610200.

Ananthanarayanan, M., Oi Cheng Ng, J. L. Boyer, and F. J. Suchy. 1994. “Characterization of Cloned Rat Liver Na+-Bile Acid Cotransporter Using Peptide and Fusion Protein Antibodies.” *American Journal of Physiology - Gastrointestinal and Liver Physiology*. https://doi.org/10.1152/ajpgi.1994.267.4.g637.

Anstee, Quentin M., and Robert D. Goldin. 2006. “Mouse Models in Non-Alcoholic Fatty Liver Disease and Steatohepatitis Research.” *International Journal of Experimental Pathology*. https://doi.org/10.1111/j.0959-9673.2006.00465.x.

Anstee, Quentin M., Giovanni Targher, and Christopher P. Day. 2013. “Progression of NAFLD to Diabetes Mellitus, Cardiovascular Disease or Cirrhosis.” *Nature Reviews Gastroenterology and Hepatology*. https://doi.org/10.1038/nrgastro.2013.41.

Arab, Juan P., Saul J. Karpen, Paul A. Dawson, Marco Arrese, and Michael Trauner. 2017. “Bile

Acids and Nonalcoholic Fatty Liver Disease: Molecular Insights and Therapeutic Perspectives." *Hepatology* 65 (1): 350–62. https://doi.org/10.1002/hep.28709.

Aranha, Márcia M., Helena Cortez-Pinto, Adília Costa, Isabel B.Moreira Da Silva, Maria E. Camilo, Miguel Carneiro De Moura, and Cecília M.P. Rodrigues. 2008. "Bile Acid Levels Are Increased in the Liver of Patients with Steatohepatitis." *European Journal of Gastroenterology and Hepatology* 20 (6): 519–25. https://doi.org/10.1097/MEG.0b013e3282f4710a.

Arguello, Graciela, Elisa Balboa, Marco Arrese, and Silvana Zanlungo. 2015. "Recent Insights on the Role of Cholesterol in Non-Alcoholic Fatty Liver Disease." *Biochimica et Biophysica Acta - Molecular Basis of Disease*. https://doi.org/10.1016/j.bbadis.2015.05.015.

Auwerx, Johan, Pascale Leroy, and Kristina Schoonjans. 1992. "Lipoprotein Lipase: Recent Contributions from Molecular Biology." *Critical Reviews in Clinical Laboratory Sciences*. https://doi.org/10.3109/10408369209114602.

Baeck, Christer, Alexander Wehr, Karlin Raja Karlmark, Felix Heymann, Mihael Vucur, Nikolaus Gassler, Sebastian Huss, et al. 2012. "Pharmacological Inhibition of the Chemokine CCL2 (MCP-1) Diminishes Liver Macrophage Infiltration and Steatohepatitis in Chronic Hepatic Injury." *Gut* 61 (3): 416–26. https://doi.org/10.1136/gutjnl-2011-300304.

Bartelt, Alexander, Oliver T. Bruns, Rudolph Reimer, Heinz Hohenberg, Harald Ittrich, Kersten Peldschus, Michael G. Kaul, et al. 2011. "Brown Adipose Tissue Activity Controls Triglyceride Clearance." *Nature Medicine*. https://doi.org/10.1038/nm.2297.

Bartelt, Alexander, and Joerg Heeren. 2014. "Adipose Tissue Browning and Metabolic Health." *Nature Reviews Endocrinology*. https://doi.org/10.1038/nrendo.2013.204.

Bartelt, Alexander, Clara John, Nicola Schaltenberg, Jimmy F.P. Berbée, Anna Worthmann, M. Lisa Cherradi, Christian Schlein, et al. 2017. "Thermogenic Adipocytes Promote HDL Turnover and Reverse Cholesterol Transport." *Nature Communications* 8. https://doi.org/10.1038/ncomms15010.

Bechmann, Lars P., Rebekka A. Hannivoort, Guido Gerken, Gökhan S. Hotamisligil, Michael Trauner, and Ali Canbay. 2012. "The Interaction of Hepatic Lipid and Glucose Metabolism in Liver Diseases." *Journal of Hepatology* 56 (4): 952–64. https://doi.org/10.1016/j.jhep.2011.08.025.

Bensinger, Steven J., Michelle N. Bradley, Sean B. Joseph, Noam Zelcer, Edith M. Janssen, Mary Ann Hausner, Roger Shih, et al. 2008. "LXR Signaling Couples Sterol Metabolism to

Proliferation in the Acquired Immune Response." *Cell*. https://doi.org/10.1016/j.cell.2008.04.052.

Berbeé, Jimmy F.P., Mariëtte R. Boon, P. Padmini S.J. Khedoe, Alexander Bartelt, Christian Schlein, Anna Worthmann, Sander Kooijman, et al. 2015. "Brown Fat Activation Reduces Hypercholesterolaemia and Protects from Atherosclerosis Development." *Nature Communications* 6. https://doi.org/10.1038/ncomms7356.

Berkel, Theo J.C. van, Kees Fluiter, Agnes G. van Velzen, Carla J.M. Vogelezang, and Gijsbertus J. Ziere. 1995. "LDL Receptor-Independent and -Dependent Uptake of Lipoproteins." *Atherosclerosis*. https://doi.org/10.1016/0021-9150(95)90072-1.

Berlanga, Alba, Esther Guiu-Jurado, José Antonio Porras, and Teresa Auguet. 2014. "Molecular Pathways in Non-Alcoholic Fatty Liver Disease." *Clinical and Experimental Gastroenterology*. https://doi.org/10.2147/CEG.S62831.

Berres, Marie Luise, Rory R. Koenen, Anna Rueland, Mirko Moreno Zaldivar, Daniel Heinrichs, Hacer Sahin, Petra Schmitz, et al. 2010. "Antagonism of the Chemokine Ccl5 Ameliorates Experimental Liver Fibrosis in Mice." *Journal of Clinical Investigation* 120 (11): 4129–40. https://doi.org/10.1172/JCI41732.

Bhattacharjee, Jashdeep, Michelle Kirby, Samir Softic, Lili Miles, Rosa-Maria Salazar-Gonzalez, Pranav Shivakumar, and Rohit Kohli. 2017. "Hepatic Natural Killer T-Cell and CD8+ T-Cell Signatures in Mice with Nonalcoholic Steatohepatitis." *Hepatology Communications*. https://doi.org/10.1002/hep4.1041.

Biddinger, Sudha B., Joel T. Haas, Bian B. Yu, Olivier Bezy, Enxuan Jing, Wenwei Zhang, Terry G. Unterman, Martin C. Carey, and C. Ronald Kahn. 2008. "Hepatic Insulin Resistance Directly Promotes Formation of Cholesterol Gallstones." *Nature Medicine* 14 (7): 778–82. https://doi.org/10.1038/nm1785.

Bieghs, Veerle, Patrick J. Van Gorp, Kristiaan Wouters, Tim Hendrikx, Marion J. Gijbels, Marc van Bilsen, Jaap Bakker, et al. 2012. "Ldl Receptor Knock-out Mice Are a Physiological Model Particularly Vulnerable to Study the Onset of Inflammation in Non-Alcoholic Fatty Liver Disease." *PLoS ONE*. https://doi.org/10.1371/journal.pone.0030668.

Bieghs, Veerle, Tim Hendrikx, Patrick J. Van Gorp, Fons Verheyen, Yasmin Dias Guichot, Sofie M.A. Walenbergh, Mike L.J. Jeurissen, et al. 2013. "The Cholesterol Derivative 27-Hydroxycholesterol Reduces Steatohepatitis in Mice." *Gastroenterology* 144 (1): 167-178.e1. https://doi.org/10.1053/j.gastro.2012.09.062.

Bjursell, Mikael, Marianne Wedin, Therése Admyre, Majlis Hermansson, Gerhard Böttcher, Melker Göransson, Daniel Lindén, Krister Bamberg, Jan Oscarsson, and Mohammad Bohlooly-Y. 2013. “Ageing Fxr Deficient Mice Develop Increased Energy Expenditure, Improved Glucose Control and Liver Damage Resembling NASH.” *PLoS ONE* 8 (5). https://doi.org/10.1371/journal.pone.0064721.

Boer, Jan Freark De, Vincent W. Bloks, Esther Verkade, M. Rebecca Heiner-Fokkema, and Folkert Kuipers. 2018. “New Insights in the Multiple Roles of Bile Acids and Their Signaling Pathways in Metabolic Control.” *Current Opinion in Lipidology*. https://doi.org/10.1097/MOL.0000000000000508.

Boer, Jan Freark De, Esther Verkade, Niels L. Mulder, Hilde D. De Vries, Nicolette Huijkman, Martijn Koehorst, Theo Boer, et al. 2020. “A Human-like Bile Acid Pool Induced by Deletion of Hepatic Cyp2c70 Modulates Effects of FXR Activation in Mice.” *Journal of Lipid Research*. https://doi.org/10.1194/jlr.RA119000243.

Brie, Belen, Ana Ornstein, Maria Cecilia Ramirez, Isabel Lacau-Mengido, and Damasia Becu-Villalobos. 2020. “Epigenetic Modifications in the Gh-Dependent Prlr, Hnf6, Cyp7b1, Adh1 and Cyp2a4 Genes.” *Journal of Molecular Endocrinology*. https://doi.org/10.1530/JME-19-0205.

Broeders, Evie P.M., Emmani B.M. Nascimento, Bas Havekes, Boudewijn Brans, Kay H.M. Roumans, Anne Tailleux, Gert Schaart, et al. 2015. “The Bile Acid Chenodeoxycholic Acid Increases Human Brown Adipose Tissue Activity.” *Cell Metabolism* 22 (3): 418–26. https://doi.org/10.1016/j.cmet.2015.07.002.

Brown, Andrew J., Laura J. Sharpe, and Michael J. Rogers. 2021. “Oxysterols: From Physiological Tuners to Pharmacological Opportunities.” *British Journal of Pharmacology*. https://doi.org/10.1111/bph.15073.

Calkin, Anna C., and Peter Tontonoz. 2012. “Transcriptional Integration of Metabolism by the Nuclear Sterol-Activated Receptors LXR and FXR.” *Nature Reviews Molecular Cell Biology*. https://doi.org/10.1038/nrm3312.

Cannon, Barbara, and Jan Nedergaard. 2004. “Brown Adipose Tissue: Function and Physiological Significance.” *Physiological Reviews*. https://doi.org/10.1152/physrev.00015.2003.

Caron, Sandrine, Carolina Huaman Samanez, Hélène Dehondt, Maheul Ploton, Olivier Briand, Fleur Lien, Emilie Dorchies, et al. 2013. “Farnesoid X Receptor Inhibits the Transcriptional

Activity of Carbohydrate Response Element Binding Protein in Human Hepatocytes." *Molecular and Cellular Biology*. https://doi.org/10.1128/mcb.01004-12.

Cavelier, Clara, Iris Lorenzi, Lucia Rohrer, and Arnold von Eckardstein. 2006. "Lipid Efflux by the ATP-Binding Cassette Transporters ABCA1 and ABCG1." *Biochimica et Biophysica Acta - Molecular and Cell Biology of Lipids*. https://doi.org/10.1016/j.bbalip.2006.04.012.

Cha, Ji Young, and Joyce J. Repa. 2007. "The Liver X Receptor (LXR) and Hepatic Lipogenesis: The Carbohydrate-Response Element-Binding Protein Is a Target Gene of LXR." *Journal of Biological Chemistry*. https://doi.org/10.1074/jbc.M605023200.

Chen, Chang, Bingying Hu, Tongzhi Wu, Yang Zhang, Yong Xu, Yulin Feng, and Hongliang Jiang. 2016. "Bile Acid Profiles in Diabetic (Db/Db) Mice and Their Wild Type Littermates." *Journal of Pharmaceutical and Biomedical Analysis* 131: 473–81. https://doi.org/10.1016/j.jpba.2016.09.023.

Chen, Wenling, Guoxen Chen, Daphne L. Head, David J. Mangelsdorf, and David W. Russell. 2007. "Enzymatic Reduction of Oxysterols Impairs LXR Signaling in Cultured Cells and the Livers of Mice." *Cell Metabolism*. https://doi.org/10.1016/j.cmet.2006.11.012.

Chen, Yong, Joschka J. Buyel, Mark J.W. Hanssen, Franziska Siegel, Ruping Pan, Jennifer Naumann, Michael Schell, et al. 2016. "Exosomal MicroRNA MiR-92a Concentration in Serum Reflects Human Brown Fat Activity." *Nature Communications*. https://doi.org/10.1038/ncomms11420.

Cheng, Joan, Angela Cheng, Bethan L. Clifford, Xiaohui Wu, Ulf Hedin, Lars Maegdefessel, Nathalie Pamir, Tamer Sallam, Elizabeth J. Tarling, and Thomas Q. De Aguiar Vallim. 2020. "MicroRNA-144 Silencing Protects against Atherosclerosis in Male, but Not Female Mice." *Arteriosclerosis, Thrombosis, and Vascular Biology*. https://doi.org/10.1161/ATVBAHA.119.313633.

Chevre, Raphael, Laia Trigueros-Motos, David Castaño, Tricia Chua, Maria Corliano, Jay V. Patankar, Lareina Sng, et al. 2018. "Therapeutic Modulation of the Bile Acid Pool by Cyp8b1 Knockdown Protects against Nonalcoholic Fatty Liver Disease in Mice." *FASEB Journal*. https://doi.org/10.1096/fj.201701084RR.

Chiang, John Y.L., and Jessica M. Ferrell. 2019. "Bile Acids as Metabolic Regulators and Nutrient Sensors." *Annual Review of Nutrition*. https://doi.org/10.1146/annurev-nutr-082018-124344.

Chiang, John Y.L., Rhonda Kimmel, and Diane Stroup. 2001. "Regulation of Cholesterol 7α-

Hydroxylase Gene (CYP7A1) Transcription by the Liver Orphan Receptor (LXRα).” *Gene*. https://doi.org/10.1016/S0378-1119(00)00518-7.

Cohen, Jonathan C., Jay D. Horton, and Helen H. Hobbs. 2011. “Human Fatty Liver Disease: Old Questions and New Insights.” *Science* 332 (6037): 1519–23. https://doi.org/10.1126/science.1204265.

Cypess, Aaron M., Sanaz Lehman, Gethin Williams, Ilan Tal, Dean Rodman, Allison B. Goldfine, Frank C. Kuo, et al. 2009. “Identification and Importance of Brown Adipose Tissue in Adult Humans.” *New England Journal of Medicine*. https://doi.org/10.1056/nejmoa0810780.

Dai, Dongling, Philippa B. Mills, Emma Footitt, Paul Gissen, Patricia McClean, Jens Stahlschmidt, Isabelle Coupry, et al. 2014. “Liver Disease in Infancy Caused by Oxysterol 7α-Hydroxylase Deficiency: Successful Treatment with Chenodeoxycholic Acid.” *Journal of Inherited Metabolic Disease*. https://doi.org/10.1007/s10545-014-9695-6.

Dasarathy, Srinivasan, Yu Yang, Arthur J. McCullough, Susan Marczewski, Carole Bennett, and Satish C. Kalhan. 2011. “Elevated Hepatic Fatty Acid Oxidation, High Plasma Fibroblast Growth Factor 21, and Fasting Bile Acids in Nonalcoholic Steatohepatitis.” *European Journal of Gastroenterology and Hepatology* 23 (5): 382–88. https://doi.org/10.1097/MEG.0b013e328345c8c7.

Davies, Brandon S.J., Anne P. Beigneux, Richard H. Barnes, Yiping Tu, Peter Gin, Michael M. Weinstein, Chika Nobumori, et al. 2010. “GPIHBP1 Is Responsible for the Entry of Lipoprotein Lipase into Capillaries.” *Cell Metabolism*. https://doi.org/10.1016/j.cmet.2010.04.016.

Dawson, Paul A., Melissa Hubbert, Jamie Haywood, Ann L. Craddock, Noa Zerangue, Whitney V. Christian, and Nazzareno Ballatori. 2005. “The Heteromeric Organic Solute Transporter α-β, Ostα-Ostβ, Is an Ileal Basolateral Bile Acid Transporter.” *Journal of Biological Chemistry*. https://doi.org/10.1074/jbc.M412752200.

Dawson, Paul A., Tian Lan, and Anuradha Rao. 2009. “Bile Acid Transporters.” *Journal of Lipid Research*. https://doi.org/10.1194/jlr.r900012-jlr200.

Day, C. P., and O. F.W. James. 1998. “Steatohepatitis: A Tale of Two ‘Hits’?” *Gastroenterology*. https://doi.org/10.1016/S0016-5085(98)70599-2.

Dijk, Wieneke, Markus Heine, Laurent Vergnes, Mariëtte R. Boon, Gert Schaart, Matthijs K.C. Hesselink, Karen Reue, et al. 2015. “ANGPTL4 Mediates Shuttling of Lipid Fuel to Brown

Adipose Tissue during Sustained Cold Exposure." *ELife*. https://doi.org/10.7554/eLife.08428.

Doege, Holger, Dirk Grimm, Alaric Falcon, Bernice Tsang, Theresa A. Storm, Hui Xu, Angelica M. Ortegon, Melissa Kazantzis, Mark A. Kay, and Andreas Stahl. 2008. "Silencing of Hepatic Fatty Acid Transporter Protein 5 in Vivo Reverses Diet-Induced Non-Alcoholic Fatty Liver Disease and Improves Hyperglycemia." *Journal of Biological Chemistry*. https://doi.org/10.1074/jbc.M803510200.

Edwards, Peter A., Matthew A. Kennedy, and Puiying A. Mak. 2002. "LXRs; Oxysterol-Activated Nuclear Receptors That Regulate Genes Controlling Lipid Homeostasis." *Vascular Pharmacology*. https://doi.org/10.1016/S1537-1891(02)00175-1.

Eissing, Leah, Thomas Scherer, Klaus Tödter, Uwe Knippschild, Jan Willem Greve, Wim A. Buurman, Hans O. Pinnschmidt, et al. 2013. "De Novo Lipogenesis in Human Fat and Liver Is Linked to ChREBP-β and Metabolic Health." *Nature Communications*. https://doi.org/10.1038/ncomms2537.

Ekstedt, Mattias, Lennart E. Franzén, Ulrik L. Mathiesen, Lars Thorelius, Marika Holmqvist, Göran Bodemar, and Stergios Kechagias. 2006. "Long-Term Follow-up of Patients with NAFLD and Elevated Liver Enzymes." *Hepatology*. https://doi.org/10.1002/hep.21327.

Eslam, Mohammed, Arun J. Sanyal, Jacob George, Arun Sanyal, Brent Neuschwander-Tetri, Claudio Tiribelli, David E. Kleiner, et al. 2020. "MAFLD: A Consensus-Driven Proposed Nomenclature for Metabolic Associated Fatty Liver Disease." *Gastroenterology* 158 (7): 1999-2014.e1. https://doi.org/10.1053/j.gastro.2019.11.312.

Evangelakos, Ioannis, Joerg Heeren, Esther Verkade, and Folkert Kuipers. 2021. "Role of Bile Acids in Inflammatory Liver Diseases." *Seminars in Immunopathology*. https://doi.org/10.1007/s00281-021-00869-6.

Feldstein, Ariel E., Nathan W. Werneburg, Ali Canbay, Maria Eugenia Guicciardi, Steven F. Bronk, Robert Rydzewski, Laurence J. Burgart, and Gregory J. Gores. 2004. "Free Fatty Acids Promote Hepatic Lipotoxicity by Stimulating TNF-α Expression via a Lysosomal Pathway." *Hepatology*. https://doi.org/10.1002/hep.20283.

Ferrell, Jessica M., Preeti Pathak, Shannon Boehme, Tricia Gilliland, and John Y.L. Chiang. 2019. "Deficiency of Both Farnesoid X Receptor and Takeda G Protein–Coupled Receptor 5 Exacerbated Liver Fibrosis in Mice." *Hepatology* 70 (3): 955–70. https://doi.org/10.1002/hep.30513.

Ferslew, Brian C., Guoxiang Xie, Curtis K. Johnston, Mingming Su, Paul W. Stewart, Wei Jia, Kim L.R. Brouwer, and A. Sidney Barritt. 2015. “Altered Bile Acid Metabolome in Patients with Nonalcoholic Steatohepatitis.” *Digestive Diseases and Sciences* 60 (11): 3318–28. https://doi.org/10.1007/s10620-015-3776-8.

Fessler, Michael B. 2018. “The Challenges and Promise of Targeting the Liver X Receptors for Treatment of Inflammatory Disease.” *Pharmacology and Therapeutics*. https://doi.org/10.1016/j.pharmthera.2017.07.010.

Fessler, Michael B., Lawrence L. Rudel, and J. Mark Brown. 2009. “Toll-like Receptor Signaling Links Dietary Fatty Acids to the Metabolic Syndrome.” *Current Opinion in Lipidology*. https://doi.org/10.1097/MOL.0b013e32832fa5c4.

Fischer, Alexander W., Barbara Cannon, and Jan Nedergaard. 2018a. “Optimal Housing Temperatures for Mice to Mimic the Thermal Environment of Humans: An Experimental Study.” *Molecular Metabolism* 7 (October 2017): 161–70. https://doi.org/10.1016/j.molmet.2017.10.009.

———. 2018b. “Optimal Housing Temperatures for Mice to Mimic the Thermal Environment of Humans: An Experimental Study.” *Molecular Metabolism* 7 (October 2017): 161–70. https://doi.org/10.1016/j.molmet.2017.10.009.

Fischer, Alexander W., Michelle Y. Jaeckstein, Kristina Gottschling, Markus Heine, Frederike Sass, Nils Mangels, Christian Schlein, et al. 2021. “Lysosomal Lipoprotein Processing in Endothelial Cells Stimulates Adipose Tissue Thermogenic Adaptation.” *Cell Metabolism*. https://doi.org/10.1016/j.cmet.2020.12.001.

Foretz, Marc, Corinne Pacot, Isabelle Dugail, Patricia Lemarchand, Colette Guichard, Xavier le Lièpvre, Cécile Berthelier-Lubrano, et al. 1999. “ADD1/SREBP-1c Is Required in the Activation of Hepatic Lipogenic Gene Expression by Glucose.” *Molecular and Cellular Biology*. https://doi.org/10.1128/mcb.19.5.3760.

Gälman, Cecilia, Ingela Arvidsson, Bo Angelin, and Mats Rudling. 2003. “Monitoring Hepatic Cholesterol 7α-Hydroxylase Activity by Assay of the Stable Bile Acid Intermediate 7α-Hydroxy-4-Cholesten-3-One in Peripheral Blood.” *Journal of Lipid Research*. https://doi.org/10.1194/jlr.D200043-JLR200.

Ganeshan, Kirthana, and Ajay Chawla. 2017. “Warming the Mouse to Model Human Diseases.” *Nature Reviews Endocrinology*. https://doi.org/10.1038/nrendo.2017.48.

Gao, Daqing, Chiming Wei, Lei Chen, Jiawen Huang, Shiqi Yang, and Anna Mae Diehl. 2004.

"Oxidative DNA Damage and DNA Repair Enzyme Expression Are Inversely Related in Murine Models of Fatty Liver Disease." *American Journal of Physiology - Gastrointestinal and Liver Physiology*. https://doi.org/10.1152/ajpgi.00228.2004.

Ge, Liang, Jing Wang, Wei Qi, Hong Hua Miao, Jian Cao, Yu Xiu Qu, Bo Liang Li, and Bao Liang Song. 2008. "The Cholesterol Absorption Inhibitor Ezetimibe Acts by Blocking the Sterol-Induced Internalization of NPC1L1." *Cell Metabolism*. https://doi.org/10.1016/j.cmet.2008.04.001.

Ghazarian, Magar, Xavier S. Revelo, Mark K. Nøhr, Helen Luck, Kejing Zeng, Helena Lei, Sue Tsai, et al. 2017. "Type I Interferon Responses Drive Intrahepatic T Cells to Promote Metabolic Syndrome." *Science Immunology*. https://doi.org/10.1126/sciimmunol.aai7616.

Giles, Daniel A., Maria E. Moreno-Fernandez, Traci E. Stankiewicz, Simon Graspeuntner, Monica Cappelletti, David Wu, Rajib Mukherjee, et al. 2017. "Thermoneutral Housing Exacerbates Nonalcoholic Fatty Liver Disease in Mice and Allows for Sex-Independent Disease Modeling." *Nature Medicine* 23 (7): 829–38. https://doi.org/10.1038/nm.4346.

Giles, Daniel A., Bhama Ramkhelawon, Elizabeth M. Donelan, Traci E. Stankiewicz, Susan B. Hutchison, Rajib Mukherjee, Monica Cappelletti, et al. 2016. "Modulation of Ambient Temperature Promotes Inflammation and Initiates Atherosclerosis in Wild Type C57BL/6 Mice." *Molecular Metabolism*. https://doi.org/10.1016/j.molmet.2016.09.008.

Glass, Christopher K., and Kaoru Saijo. 2008. "Immunology: Oxysterols Hold T Cells in Check." *Nature*. https://doi.org/10.1038/455040a.

Goodwin, Bryan, Stacey A. Jones, Roger R. Price, Michael A. Watson, David D. McKee, Linda B. Moore, Cristin Galardi, et al. 2000. "A Regulatory Cascade of the Nuclear Receptors FXR, SHP-1, and LRH-1 Represses Bile Acid Biosynthesis." *Molecular Cell*. https://doi.org/10.1016/S1097-2765(00)00051-4.

Gorden, D. Lee, Pavlina T. Ivanova, David S. Myers, J. Oliver McIntyre, Michael N. VanSaun, J. Kelly Wright, Lynn M. Matrisian, and H. Alex Brown. 2011. "Increased Diacylglycerols Characterize Hepatic Lipid Changes in Progression of Human Nonalcoholic Fatty Liver Disease; Comparison to a Murine Model." *PLoS ONE*. https://doi.org/10.1371/journal.pone.0022775.

Govaere O, Cockell S, Tiniakos D, Queen R, Younes R, and Vacca M. 2020. "Transcriptomic Profiling Across the Non-Alcoholic Fatty Liver Disease Spectrum Reveals Gene Signatures for Steatohepatitis and Fibrosis." *Science Translational Medicine*, 1–18.

Griffett, Kristine, Laura A. Solt, Bahaa El Dien M. El-Gendy, Theodore M. Kamenecka, and Thomas P. Burris. 2013. “A Liver-Selective LXR Inverse Agonist That Suppresses Hepatic Steatosis.” *ACS Chemical Biology*. https://doi.org/10.1021/cb300541g.

Griffett, Kristine, Ryan D. Welch, Colin A. Flaveny, Grant R. Kolar, Brent A. Neuschwander-Tetri, and Thomas P. Burris. 2015. “The LXR Inverse Agonist SR9238 Suppresses Fibrosis in a Model of Non-Alcoholic Steatohepatitis.” *Molecular Metabolism*. https://doi.org/10.1016/j.molmet.2015.01.009.

Grzych, Guillaume, Oscar Chávez-Talavera, Amandine Descat, Dorothée Thuillier, An Verrijken, Mostafa Kouach, Vanessa Legry, et al. 2021. “NASH-Related Increases in Plasma Bile Acid Levels Depend on Insulin Resistance.” *JHEP Reports*. https://doi.org/10.1016/j.jhepr.2020.100222.

Guillemot-Legris, Owein, Valentin Mutemberezi, Patrice D. Cani, and Giulio G. Muccioli. 2016. “Obesity Is Associated with Changes in Oxysterol Metabolism and Levels in Mice Liver, Hypothalamus, Adipose Tissue and Plasma.” *Scientific Reports*. https://doi.org/10.1038/srep19694.

Halilbasic, Emina, Thierry Claudel, and Michael Trauner. 2013. “Bile Acid Transporters and Regulatory Nuclear Receptors in the Liver and Beyond.” *Journal of Hepatology*. https://doi.org/10.1016/j.jhep.2012.08.002.

Hall, Angela M., Kou Kou, Zhouji Chen, Terri A. Pietka, Mrudula Kumar, Kevin M. Korenblat, Kyuha Lee, et al. 2012. “Evidence for Regulated Monoacylglycerol Acyltransferase Expression and Activity in Human Liver.” *Journal of Lipid Research*. https://doi.org/10.1194/jlr.P025536.

Hamlin, Allyson N., Sivaprakasam Chinnarasu, Yinyuan Ding, Xunde Xian, Joachim Herz, Anja Jaeschke, and David Y. Hui. 2018. “Low-Density Lipoprotein Receptor–Related Protein-1 Dysfunction Synergizes with Dietary Cholesterol to Accelerate Steatohepatitis Progression.” *Journal of Biological Chemistry*. https://doi.org/10.1074/jbc.RA118.001952.

Harley, Isaac T.W., Traci E. Stankiewicz, Daniel A. Giles, Samir Softic, Leah M. Flick, Monica Cappelletti, Rachel Sheridan, et al. 2014. “IL-17 Signaling Accelerates the Progression of Nonalcoholic Fatty Liver Disease in Mice.” *Hepatology*. https://doi.org/10.1002/hep.26746.

Heeren, Joerg, and Ludger Scheja. 2021. “Metabolic-Associated Fatty Liver Disease and Lipoprotein Metabolism.” *Molecular Metabolism*. https://doi.org/10.1016/j.molmet.2021.101238.

Heine, Markus, Alexander W. Fischer, Christian Schlein, Caroline Jung, Leon G. Straub, Kristina Gottschling, Nils Mangels, et al. 2018. “Lipolysis Triggers a Systemic Insulin Response Essential for Efficient Energy Replenishment of Activated Brown Adipose Tissue in Mice.” *Cell Metabolism*. https://doi.org/10.1016/j.cmet.2018.06.020.

Horton, Jay D., Joseph L. Goldstein, and Michael S. Brown. 2002. “SREBPs: Activators of the Complete Program of Cholesterol and Fatty Acid Synthesis in the Liver.” *Journal of Clinical Investigation*. https://doi.org/10.1172/jci15593.

Hummel, Katharine P., Margaret M. Dickie, and Douglas L. Coleman. 1966. “Diabetes, a New Mutation in the Mouse.” *Science*. https://doi.org/10.1126/science.153.3740.1127.

Ikegami, Tadashi, Hideyuki Hyogo, Akira Honda, Teruo Miyazaki, Katsutoshi Tokushige, Etsuko Hashimoto, Kazuo Inui, Yasushi Matsuzaki, and Susumu Tazuma. 2012. “Increased Serum Liver X Receptor Ligand Oxysterols in Patients with Non-Alcoholic Fatty Liver Disease.” *Journal of Gastroenterology* 47 (11): 1257–66. https://doi.org/10.1007/s00535-012-0585-0.

Inagaki, Takeshi, Mihwa Choi, Antonio Moschetta, Li Peng, Carolyn L. Cummins, Jeffrey G. McDonald, Guizhen Luo, et al. 2005. “Fibroblast Growth Factor 15 Functions as an Enterohepatic Signal to Regulate Bile Acid Homeostasis.” *Cell Metabolism* 2 (4): 217–25. https://doi.org/10.1016/j.cmet.2005.09.001.

Inoue, Mitsutaka, Takaaki Ohtake, Wataru Motomura, Nobuhiko Takahashi, Yayoi Hosoki, Shigeki Miyoshi, Yasuaki Suzuki, Hiroyuki Saito, Yutaka Kohgo, and Toshikatsu Okumura. 2005. “Increased Expression of PPARγ in High Fat Diet-Induced Liver Steatosis in Mice.” *Biochemical and Biophysical Research Communications*. https://doi.org/10.1016/j.bbrc.2005.08.070.

Inzaugarat, María Eugenia, Nazarena Eugenia Ferreyra Solari, Luis Ariel Billordo, Raquel Abecasis, Adrian C. Gadano, and Alejandra Claudia Cherñavsky. 2011. “Altered Phenotype and Functionality of Circulating Immune Cells Characterize Adult Patients with Nonalcoholic Steatohepatitis.” *Journal of Clinical Immunology*. https://doi.org/10.1007/s10875-011-9571-1.

Ishibashi, Hiromi, Minoru Nakamura, Atsumasa Komori, Kiyoshi Migita, and Shinji Shimoda. 2009. “Liver Architecture, Cell Function, and Disease.” *Seminars in Immunopathology*. https://doi.org/10.1007/s00281-009-0155-6.

Ishimoto, Kenji, Keisuke Tachibana, Mikako Sumitomo, Shiho Omote, Ikuko Hanano, Daisuke Yamasaki, Yuichiro Watanabe, et al. 2006. “Identification of Human Low-Density

Lipoprotein Receptor as a Novel Target Gene Regulated by Liver X Receptor Alpha." *FEBS Letters*. https://doi.org/10.1016/j.febslet.2006.08.010.

Iuliano, Luigi. 2011. "Pathways of Cholesterol Oxidation via Non-Enzymatic Mechanisms." *Chemistry and Physics of Lipids*. https://doi.org/10.1016/j.chemphyslip.2011.06.006.

Jacquemin, Emmanuel, Bruno Hagenbuch, Bruno Stieger, Allan W. Wolkoff, and Peter J. Meier. 1994. "Expression Cloning of a Rat Liver Na+-Independent Organic Anion Transporter." *Proceedings of the National Academy of Sciences of the United States of America*. https://doi.org/10.1073/pnas.91.1.133.

Janowski, Bethany A., Bei Shan, and David W. Russell. 2001. "The Hypocholesterolemic Agent LY295427 Reverses Suppression of Sterol Regulatory Element-Binding Protein Processing Mediated by Oxysterols." *Journal of Biological Chemistry*. https://doi.org/10.1074/jbc.M108348200.

Jiao, Na, Susan S. Baker, Adrian Chapa-Rodriguez, Wensheng Liu, Colleen A. Nugent, Maria Tsompana, Lucy Mastrandrea, et al. 2018. "Suppressed Hepatic Bile Acid Signalling despite Elevated Production of Primary and Secondary Bile Acids in NAFLD." *Gut* 67 (10): 1–11. https://doi.org/10.1136/gutjnl-2017-314307.

John, Clara, Philipp Werner, Anna Worthmann, Katrin Wegner, Klaus Tödter, Ludger Scheja, Sascha Rohn, Joerg Heeren, and Markus Fischer. 2014. "A Liquid Chromatography-Tandem Mass Spectrometry-Based Method for the Simultaneous Determination of Hydroxy Sterols and Bile Acids." *Journal of Chromatography A* 1371: 184–95. https://doi.org/10.1016/j.chroma.2014.10.064.

Joseph, Sean B., Antonio Castrillo, Bryan A. Laffitte, David J. Mangelsdorf, and Peter Tontonoz. 2003. "Reciprocal Regulation of Inflammation and Lipid Metabolism by Liver X Receptors." *Nature Medicine*. https://doi.org/10.1038/nm820.

Kakiyama, Genta, Dalila Marques, Rebecca Martin, Hajime Takei, Daniel Rodriguez-agudo, Sandra A Lasalle, Taishi Hashiguchi, et al. 2020. "Insulin Resistance Dysregulates CYP7B1 Leading to Oxysterol Accumulation : A Pathway for NAFL to NASH Transition." *Journal Lipid Research* 61 (12): 1629–44. https://doi.org/10.1194/jlr.RA120000924.

Kalhan, Satish C., Lining Guo, John Edmison, Srinivasan Dasarathy, Arthur J. McCullough, Richard W. Hanson, and Mike Milburn. 2011. "Plasma Metabolomic Profile in Nonalcoholic Fatty Liver Disease." *Metabolism: Clinical and Experimental* 60 (3): 404–13. https://doi.org/10.1016/j.metabol.2010.03.006.

Kandutsch, A. A., and H. W. Chen. 1973. “Inhibition of Sterol Synthesis in Cultured Mouse Cells by 7α Hydroxycholesterol, 7β Hydroxycholesterol, and 7 Ketocholesterol.” *Journal of Biological Chemistry*. https://doi.org/10.1016/s0021-9258(19)43148-7.

Kohjima, Motoyuki, Munechika Enjoji, Nobito Higuchi, Masaki Kato, Kazuhiro Kotoh, Tsuyoshi Yoshimoto, Tatsuya Fujino, et al. 2007. “Re-Evaluation of Fatty Acid Metabolism-Related Gene Expression in Nonalcoholic Fatty Liver Disease.” *International Journal of Molecular Medicine*. https://doi.org/10.3892/ijmm.20.3.351.

Krenkel, Oliver, Tobias Puengel, Olivier Govaere, Ali T. Abdallah, Jana C. Mossanen, Marlene Kohlhepp, Anke Liepelt, et al. 2018. “Therapeutic Inhibition of Inflammatory Monocyte Recruitment Reduces Steatohepatitis and Liver Fibrosis.” *Hepatology*. https://doi.org/10.1002/hep.29544.

Krenkel, Oliver, and Frank Tacke. 2017. “Liver Macrophages in Tissue Homeostasis and Disease.” *Nature Reviews Immunology*. https://doi.org/10.1038/nri.2017.11.

Kuipers, Folkert, Vincent W. Bloks, and Albert K. Groen. 2014. “Beyond Intestinal Soap - Bile Acids in Metabolic Control.” *Nature Reviews Endocrinology*. https://doi.org/10.1038/nrendo.2014.60.

Kuipers, Folkert, and Albert K. Groen. 2017. “An Unexpected Role for Bile Acid Synthesis in Adaptation to Low Temperature.” *Nature Medicine* 23 (7): 800–802. https://doi.org/10.1038/nm.4365.

Kumar, Naresh, Douglas J. Kojetin, Laura A. Solt, K. Ganesh Kumar, Philippe Nuhant, Derek R. Duckett, Michael D. Cameron, et al. 2011. “Identification of SR3335 (ML-176): A Synthetic RORα Selective Inverse Agonist.” *ACS Chemical Biology*. https://doi.org/10.1021/cb1002762.

Kunjathoor, Vidya V., Maria Febbraio, Eugene A. Podrez, Kathryn J. Moore, Lorna Andersson, Stephanie Koehn, Jeongmi S. Rhee, Roy Silverstein, Henry F. Hoff, and Mason W. Freeman. 2002. “Scavenger Receptors Class A-I/II and CD36 Are the Principal Receptors Responsible for the Uptake of Modified Low Density Lipoprotein Leading to Lipid Loading in Macrophages.” *Journal of Biological Chemistry*. https://doi.org/10.1074/jbc.M209649200.

Lade, Abigale, Luke A. Noon, and Scott L. Friedman. 2014. “Contributions of Metabolic Dysregulation and Inflammation to Nonalcoholic Steatohepatitis, Hepatic Fibrosis, and Cancer.” *Current Opinion in Oncology* 26 (1): 100–107. https://doi.org/10.1097/CCO.0000000000000042.

Lake, April D., Petr Novak, Petia Shipkova, Nelly Aranibar, Donald Robertson, Michael D. Reily, Zhenqiang Lu, Lois D. Lehman-McKeeman, and Nathan J. Cherrington. 2013. “Decreased Hepatotoxic Bile Acid Composition and Altered Synthesis in Progressive Human Nonalcoholic Fatty Liver Disease.” *Toxicology and Applied Pharmacology* 268 (2): 132–40. https://doi.org/10.1016/j.taap.2013.01.022.

Lambert, Jennifer E., Maria A. Ramos-Roman, Jeffrey D. Browning, and Elizabeth J. Parks. 2014. “Increased de Novo Lipogenesis Is a Distinct Characteristic of Individuals with Nonalcoholic Fatty Liver Disease.” *Gastroenterology*. https://doi.org/10.1053/j.gastro.2013.11.049.

Lee, Giljae, Hyun Ju You, Jasmohan S. Bajaj, Sae Kyung Joo, Junsun Yu, Seoyeon Park, Hyena Kang, et al. 2020. “Distinct Signatures of Gut Microbiome and Metabolites Associated with Significant Fibrosis in Non-Obese NAFLD.” *Nature Communications* 11 (1): 1–13. https://doi.org/10.1038/s41467-020-18754-5.

Lefebvre, Philippe, Bertrand Cariou, Fleur Lien, Folkert Kuipers, and Bart Staels. 2009. “Role of Bile Acids and Bile Acid Receptors in Metabolic Regulation.” *Physiological Reviews*. https://doi.org/10.1152/physrev.00010.2008.

Legry, Vanessa, Sven Francque, Joel T. Haas, An Verrijken, Sandrine Caron, Oscar Chávez-Talavera, Emmanuelle Vallez, et al. 2017. “Bile Acid Alterations Are Associated with Insulin Resistance, but Not with NASH, in Obese Subjects.” *Journal of Clinical Endocrinology and Metabolism* 102 (10): 3783–94. https://doi.org/10.1210/jc.2017-01397.

Li-Hawkins, Jia, Erik G. Lund, Stephen D. Turley, and David W. Russell. 2000. “Disruption of the Oxysterol 7α-Hydroxylase Gene in Mice.” *Journal of Biological Chemistry*. https://doi.org/10.1074/jbc.M001811200.

Li, Tiangang, and John Y.L. Chiang. 2014. “Bile Acid Signaling in Metabolic Disease and Drug Therapy.” *Pharmacological Reviews*. https://doi.org/10.1124/pr.113.008201.

Liu, Hailiang, Preeti Pathak, Shannon Boehme, and John Y. L. Chiang. 2016. “Cholesterol 7α-Hydroxylase Protects the Liver from Inflammation and Fibrosis by Maintaining Cholesterol Homeostasis.” *Journal of Lipid Research* 57 (10): 1831–44. https://doi.org/10.1194/jlr.M069807.

Livak, Kenneth J., and Thomas D. Schmittgen. 2001. “Analysis of Relative Gene Expression Data Using Real-Time Quantitative PCR and the 2-ΔΔCT Method.” *Methods*. https://doi.org/10.1006/meth.2001.1262.

Loomba, Rohit, and Arun J. Sanyal. 2013. “The Global NAFLD Epidemic.” *Nature Reviews Gastroenterology and Hepatology* 10 (11): 686–90. https://doi.org/10.1038/nrgastro.2013.171.

Lund, Erik G., Joseph M. Guileyardo, and David W. Russell. 1999. “CDNA Cloning of Cholesterol 24-Hydroxylase, a Mediator of Cholesterol Homeostasis in the Brain.” *Proceedings of the National Academy of Sciences of the United States of America*. https://doi.org/10.1073/pnas.96.13.7238.

Ma, Liqian, and Erik R. Nelson. 2019. “Oxysterols and Nuclear Receptors.” *Molecular and Cellular Endocrinology*. https://doi.org/10.1016/j.mce.2019.01.016.

Marí, Montserrat, Francisco Caballero, Anna Colell, Albert Morales, Juan Caballeria, Anna Fernandez, Carlos Enrich, José C. Fernandez-Checa, and Carmen García-Ruiz. 2006. “Mitochondrial Free Cholesterol Loading Sensitizes to TNF- and Fas-Mediated Steatohepatitis.” *Cell Metabolism*. https://doi.org/10.1016/j.cmet.2006.07.006.

Mastrodonato, Maria, Giuseppe Calamita, Roberta Rossi, Donatella Mentino, Leonilde Bonfrate, Piero Portincasa, Domenico Ferri, and Giuseppa E. Liquori. 2011. “Altered Distribution of Caveolin-1 in Early Liver Steatosis.” *European Journal of Clinical Investigation*. https://doi.org/10.1111/j.1365-2362.2010.02459.x.

Meljon, Anna, Spyridon Theofilopoulos, Cedric H.L. Shackleton, Gordon L. Watson, Norman B. Javitt, Hans Joachim Knölker, Ratni Saini, Ernest Arenas, Yuqin Wang, and William J. Griffiths. 2012. “Analysis of Bioactive Oxysterols in Newborn Mouse Brain by LC/MS.” *Journal of Lipid Research* 53 (11): 2469–83. https://doi.org/10.1194/jlr.D028233.

Michael, M. Dodson, Rohit N. Kulkarni, Catherine Postic, Steven F. Previs, Gerald I. Shulman, Mark A. Magnuson, and C. Ronald Kahn. 2000. “Loss of Insulin Signaling in Hepatocytes Leads to Severe Insulin Resistance and Progressive Hepatic Dysfunction.” *Molecular Cell*. https://doi.org/10.1016/S1097-2765(05)00015-8.

Mitchell, J. R.D., A. Jacobsson, T. G. Kirchgessner, M. C. Schotz, B. Cannon, and J. Nedergaard. 1992. “Regulation of Expression of the Lipoprotein Lipase Gene in Brown Adipose Tissue.” *American Journal of Physiology - Endocrinology and Metabolism*. https://doi.org/10.1152/ajpendo.1992.263.3.e500.

Molinaro, Antonio, Annika Wahlström, and Hanns Ulrich Marschall. 2018. “Role of Bile Acids in Metabolic Control.” *Trends in Endocrinology and Metabolism* 29 (1): 31–41. https://doi.org/10.1016/j.tem.2017.11.002.

Moore, J. Bernadette, Pippa J. Gunn, and Barbara A. Fielding. 2014. “The Role of Dietary Sugars and de Novo Lipogenesis in Non-Alcoholic Fatty Liver Disease.” *Nutrients*. https://doi.org/10.3390/nu6125679.

Morgan, Kengathevy, Adhemar Uyuni, Ganesh Nandgiri, Lin Mao, Luciano Castaneda, Elango Kathirvel, Samuel W. French, and Timothy R. Morgan. 2008. “Altered Expression of Transcription Factors and Genes Regulating Lipogenesis in Liver and Adipose Tissue of Mice with High Fat Diet-Induced Obesity and Nonalcoholic Fatty Liver Disease.” *European Journal of Gastroenterology and Hepatology*. https://doi.org/10.1097/MEG.0b013e3282f9b203.

Mouzaki, Marialena, Alice Y. Wang, Robert Bandsma, Elena M. Comelli, Bianca M. Arendt, Ling Zhang, Scott Fung, Sandra E. Fischer, Ian G. McGilvray, and Johane P. Allard. 2016. “Bile Acids and Dysbiosis in Non-Alcoholic Fatty Liver Disease.” *PLoS ONE* 11 (5): 1–13. https://doi.org/10.1371/journal.pone.0151829.

Murata, Masayuki, Johan Peränen, Rupert Schreiner, Felix Wieland, Teymuras V. Kurzchalia, and Kai Simons. 1995. “VIP21/Caveolin Is a Cholesterol-Binding Protein.” *Proceedings of the National Academy of Sciences of the United States of America*. https://doi.org/10.1073/pnas.92.22.10339.

Naim, Adnan, Qiuwei Pan, and Mirza S. Baig. 2017. “Matrix Metalloproteinases (MMPs) in Liver Diseases.” *Journal of Clinical and Experimental Hepatology*. https://doi.org/10.1016/j.jceh.2017.09.004.

Neuschwander-Tetri, Brent A. 2010. “Hepatic Lipotoxicity and the Pathogenesis of Nonalcoholic Steatohepatitis: The Central Role of Nontriglyceride Fatty Acid Metabolites.” *Hepatology*. https://doi.org/10.1002/hep.23719.

Nimer, Nisreen, Ibrahim Choucair, Zeneng Wang, Ina Nemet, Lin Li, Janet Gukasyan, Taylor L. Weeks, et al. 2021. “Bile Acids Profile, Histopathological Indices and Genetic Variants for Non-Alcoholic Fatty Liver Disease Progression.” *Metabolism: Clinical and Experimental*. https://doi.org/10.1016/j.metabol.2020.154457.

Okazaki, Isao, Takuji Noro, Nobuhiro Tsutsui, Eigoro Yamanouchi, Hajime Kuroda, Masayuki Nakano, Hiroaki Yokomori, and Yutaka Inagaki. 2014. “Fibrogenesis and Carcinogenesis in Nonalcoholic Steatohepatitis (NASH): Involvement of Matrix Metalloproteinases (MMPs) and Tissue Inhibitors of Metalloproteinase (TIMPs).” *Cancers*. https://doi.org/10.3390/cancers6031220.

Panarotto, D., P. Rémillard, L. Bouffard, and Pierre Maheux. 2002. “Insulin Resistance Affects the Regulation of Lipoprotein Lipase in the Postprandial Period and in an Adipose Tissue-Specific Manner.” In *European Journal of Clinical Investigation*. https://doi.org/10.1046/j.1365-2362.2002.00945.x.

Pandak, William M., Phillip B. Hylemon, Shunlin Ren, Dalila Marques, Gregorio Gil, Kaye Redford, Darrell Mallonee, and Z. Rano Vlahcevic. 2002. “Regulation of Oxysterol 7α-Hydroxylase (CYP7B1) in Primary Cultures of Rat Hepatocytes.” *Hepatology*. https://doi.org/10.1053/jhep.2002.33200.

Papa, Sergio, Domenico De Rasmo, Zuzana Technikova-Dobrova, Damiano Panelli, Anna Signorile, Salvatore Scacco, Vittoria Petruzzella, et al. 2012. “Respiratory Chain Complex I, a Main Regulatory Target of the CAMP/PKA Pathway Is Defective in Different Human Diseases.” *FEBS Letters*. https://doi.org/10.1016/j.febslet.2011.09.019.

Petersen, Max C., Anila K. Madiraju, Brandon M. Gassaway, Michael Marcel, Ali R. Nasiri, Gina Butrico, Melissa J. Marcucci, et al. 2016. “Insulin Receptor Thr1160 Phosphorylation Mediates Lipid-Induced Hepatic Insulin Resistance.” *Journal of Clinical Investigation*. https://doi.org/10.1172/JCI86013.

Petersen, Max C., and Gerald I. Shulman. 2017. “Roles of Diacylglycerols and Ceramides in Hepatic Insulin Resistance.” *Trends in Pharmacological Sciences* 38 (7): 649–65. https://doi.org/10.1016/j.tips.2017.04.004.

Pradere, Jean Philippe, Johannes Kluwe, Samuele De Minicis, Jing Jing Jiao, Geum Youn Gwak, Dianne H. Dapito, Myoung Kuk Jang, et al. 2013. “Hepatic Macrophages but Not Dendritic Cells Contribute to Liver Fibrosis by Promoting the Survival of Activated Hepatic Stellate Cells in Mice.” *Hepatology*. https://doi.org/10.1002/hep.26429.

Puri, Puneet, Kalyani Daita, Andrew Joyce, Faridoddin Mirshahi, Prasanna K. Santhekadur, Sophie Cazanave, Velimir A. Luketic, et al. 2018. “The Presence and Severity of Nonalcoholic Steatohepatitis Is Associated with Specific Changes in Circulating Bile Acids.” *Hepatology*. https://doi.org/10.1002/hep.29359.

Raabe, Martin, Murielle M. Véniant, Meghan A. Sullivan, Constance H. Zlot, Johan Björkegren, Lars Bo Nielsen, Jinny S. Wong, Robert L. Hamilton, and Stephen G. Young. 1999. “Analysis of the Role of Microsomal Triglyceride Transfer Protein in the Liver of Tissue-Specific Knockout Mice.” *Journal of Clinical Investigation*. https://doi.org/10.1172/JCI6576.

Raselli, Tina, Tom Hearn, Annika Wyss, Kirstin Atrott, Alain Peter, Isabelle Frey-Wagner,

Marianne R. Spalinger, et al. 2019. “Elevated Oxysterol Levels in Human and Mouse Livers Reflect Nonalcoholic Steatohepatitis.” *Journal of Lipid Research* 60 (7): 1270–83. https://doi.org/10.1194/jlr.M093229.

Ratziu, Vlad, Zachary Goodman, and Arun Sanyal. 2015. “Current Efforts and Trends in the Treatment of NASH.” *Journal of Hepatology*. https://doi.org/10.1016/j.jhep.2015.02.041.

Rau, Monika, Anne-Kristin Schilling, Jan Meertens, Ilona Hering, Johannes Weiss, Christian Jurowich, Theodor Kudlich, et al. 2016. “Progression from Nonalcoholic Fatty Liver to Nonalcoholic Steatohepatitis Is Marked by a Higher Frequency of Th17 Cells in the Liver and an Increased Th17/Resting Regulatory T Cell Ratio in Peripheral Blood and in the Liver.” *The Journal of Immunology*. https://doi.org/10.4049/jimmunol.1501175.

Raubenheimer, Peter J., Moffat J. Nyirenda, and Brian R. Walker. 2006. “A Choline-Deficient Diet Exacerbates Fatty Liver but Attenuates Insulin Resistance and Glucose Intolerance in Mice Fed a High-Fat Diet.” *Diabetes*. https://doi.org/10.2337/db06-0097.

Reinmuth, Lisa, Cheng Chih Hsiao, Jörg Hamann, Mette Rosenkilde, and John Mackrill. 2021. “Multiple Targets for Oxysterols in Their Regulation of the Immune System.” *Cells*. https://doi.org/10.3390/cells10082078.

Ren, Shunlin, Dalila Marques, Kaye Redford, Phillip B. Hylemon, Gregorio Gil, Z. Reno Vlahcevic, and William M. Pandak. 2003. “Regulation of Oxysterol 7α-Hydroxylase (CYP7B1) in the Rat.” *Metabolism: Clinical and Experimental*. https://doi.org/10.1053/meta.2003.50106.

Repa, Joyce J., Knut E. Berge, Chris Pomajzl, James A. Richardson, Helen Hobbs, and David J. Mangelsdorf. 2002. “Regulation of ATP-Binding Cassette Sterol Transporters ABCG5 and ABCG8 by the Liver X Receptors α and β.” *Journal of Biological Chemistry*. https://doi.org/10.1074/jbc.M109927200.

Repa, Joyce J., Guosheng Liang, Jiafu Ou, Yuriy Bashmakov, Jean Marc A. Lobaccaro, Iichiro Shimomura, Bei Shan, Michael S. Brown, Joseph L. Goldstein, and David J. Mangelsdorf. 2000. “Regulation of Mouse Sterol Regulatory Element-Binding Protein-1c Gene (SREBP-1c) by Oxysterol Receptors, LXRα and LXRβ.” *Genes and Development*. https://doi.org/10.1101/gad.844900.

Rinella, Mary E., and Richard M. Green. 2004. “The Methionine-Choline Deficient Dietary Model of Steatohepatitis Does Not Exhibit Insulin Resistance.” *Journal of Hepatology*. https://doi.org/10.1016/j.jhep.2003.09.020.

Rudick, Michael, and Richard G.W. Anderson. 2002. “Multiple Functions of Caveolin-1.” *Journal of Biological Chemistry*. https://doi.org/10.1074/jbc.R200020200.

Russell, David W. 2003. “The Enzymes, Regulation, and Genetics of Bile Acid Synthesis.” *Annual Review of Biochemistry* 72 (1): 137–74. https://doi.org/10.1146/annurev.biochem.72.121801.161712.

Sabol, Steven L., H. Bryan Brewer, and Silvia Santamarina-Fojo. 2005. “The Human ABCG1 Gene: Identification of LXR Response Elements That Modulate Expression in Macrophages and Liver.” *Journal of Lipid Research*. https://doi.org/10.1194/jlr.M500080-JLR200.

Sadur, C. N., and R. H. Eckel. 1982. “Insulin Stimulation of Adipose Tissue Lipoprotein Lipase. Use of the Euglycemic Clamp Technique.” *Journal of Clinical Investigation*. https://doi.org/10.1172/JCI110547.

Samuel, Varman T., Zhen Xiang Liu, Amy Wang, Sara A. Beddow, John G. Geisler, Mario Kahn, Xian Man Zhang, Brett P. Monia, Sanjay Bhanot, and Gerald I. Shulman. 2007. “Inhibition of Protein Kinase Cε Prevents Hepatic Insulin Resistance in Nonalcoholic Fatty Liver Disease.” *Journal of Clinical Investigation*. https://doi.org/10.1172/JCI30400.

Schade, David S., Lynda Shey, and R. Philip Eaton. 2020. “Cholesterol Review: A Metabolically Important Molecule.” *Endocrine Practice*. https://doi.org/10.4158/EP-2020-0347.

Schmitt, Johannes, Bo Kong, Bruno Stieger, Oliver Tschopp, Simon M. Schultze, Monika Rau, Achim Weber, Beat Müllhaupt, Grace L. Guo, and Andreas Geier. 2015. “Protective Effects of Farnesoid X Receptor (FXR) on Hepatic Lipid Accumulation Are Mediated by Hepatic FXR and Independent of Intestinal FGF15 Signal.” *Liver International* 35 (4): 1133–44. https://doi.org/10.1111/liv.12456.

Schroepfer, George J., and W. K. Wilson. 2000. “Oxysterols: Modulators of Cholesterol Metabolism and Other Processes.” *Physiological Reviews*. https://doi.org/10.1152/physrev.2000.80.1.361.

Schuppan, Detlef, Rambabu Surabattula, and Xiao Yu Wang. 2018. “Determinants of Fibrosis Progression and Regression in NASH.” *Journal of Hepatology*. https://doi.org/10.1016/j.jhep.2017.11.012.

Schwarz, Margrit, David W. Russell, John M. Dietschy, and Stephen D. Turley. 2001. “Alternate Pathways of Bile Acid Synthesis in the Cholesterol 7α-Hydroxylase Knockout Mouse Are Not Upregulated by Either Cholesterol or Cholestyramine Feeding.” *Journal of Lipid*

Research. https://doi.org/10.1016/s0022-2275(20)32213-6.

Schwinge, Dorothee, Antonella Carambia, Alexander Quaas, Till Krech, Claudia Wegscheid, Gisa Tiegs, Immo Prinz, Ansgar W. Lohse, Johannes Herkel, and Christoph Schramm. 2015. “Testosterone Suppresses Hepatic Inflammation by the Downregulation of IL-17, CXCL-9, and CXCL-10 in a Mouse Model of Experimental Acute Cholangitis.” *The Journal of Immunology* 194 (6): 2522–30. https://doi.org/10.4049/jimmunol.1400076.

Seeley, Randy J., and Ormond A. MacDougald. 2021. “Mice as Experimental Models for Human Physiology: When Several Degrees in Housing Temperature Matter.” *Nature Metabolism*. https://doi.org/10.1038/s42255-021-00372-0.

Setchell, K D, R J Sokol, D W Russell, Oxysterol Gene, Causes Severe, and Neonatal Liver. 1998. “Identification of a New Inborn Error in Bile Acid Synthesis : Mutation of the Oxysterol 7alpha-Hydroxylase Gene Causes Severe Neonatal Liver Disease . Find the Latest Version : Identification of a New Inborn Error in Bile Acid Synthesis : Mutation of The” 102 (9): 1690–1703.

Shapiro, Hagit, Aleksandra A. Kolodziejczyk, Daniel Halstuch, and Eran Elinav. 2018. “Bile Acids in Glucose Metabolism in Health and Disease.” *Journal of Experimental Medicine* 215 (2): 383–96. https://doi.org/10.1084/jem.20171965.

Spann, Nathanael J., and Christopher K. Glass. 2013. “Sterols and Oxysterols in Immune Cell Function.” *Nature Immunology*. https://doi.org/10.1038/ni.2681.

Suga, Takahiro, Hiroaki Yamaguchi, Jiro Ogura, Saori Shoji, Masamitsu Maekawa, and Nariyasu Mano. 2019. “Altered Bile Acid Composition and Disposition in a Mouse Model of Non-Alcoholic Steatohepatitis.” *Toxicology and Applied Pharmacology* 379 (July): 114664. https://doi.org/10.1016/j.taap.2019.114664.

Suppli, Malte P., Kristoffer T.G. Rigbolt, Sanne S. Veidal, Sara Heebøll, Peter Lykke Eriksen, Mia Demant, Jonatan I. Bagger, et al. 2019. “Hepatic Transcriptome Signatures in Patients with Varying Degrees of Nonalcoholic Fatty Liver Disease Compared with Healthy Normal-Weight Individuals.” *American Journal of Physiology - Gastrointestinal and Liver Physiology*. https://doi.org/10.1152/ajpgi.00358.2018.

Sutti, Salvatore, and Emanuele Albano. 2020. “Adaptive Immunity: An Emerging Player in the Progression of NAFLD.” *Nature Reviews Gastroenterology and Hepatology* 17 (2): 81–92. https://doi.org/10.1038/s41575-019-0210-2.

Sutti, Salvatore, Aastha Jindal, Irene Locatelli, Marco Vacchiano, Luca Gigliotti, Cristina

Bozzola, and Emanuele Albano. 2014. “Adaptive Immune Responses Triggered by Oxidative Stress Contribute to Hepatic Inflammation in NASH.” *Hepatology*. https://doi.org/10.1002/hep.26749.

Takahashi, Shogo, Tatsuki Fukami, Yusuke Masuo, Chad N. Brocker, Cen Xie, Kristopher W. Krausz, C. Roland Wolf, Colin J. Henderson, and Frank J. Gonzalez. 2016. “Cyp2c70 Is Responsible for the Species Difference in Bile Acid Metabolism between Mice and Humans.” *Journal of Lipid Research*. https://doi.org/10.1194/jlr.M071183.

Tamasawa, Naoki, Makoto Hayakari, Hiroshi Murakami, Jun Matsui, and Toshihiro Suda. 1997. “Reduction of Oxysterol Levels Up-Regulates HMG-CoA Reductase Activity in Rat Liver.” *Atherosclerosis*. https://doi.org/10.1016/S0021-9150(97)00055-5.

Tanaka, Naoki, Tsutomu Matsubara, Kristopher W. Krausz, Andrew D. Patterson, and Frank J. Gonzalez. 2012. “Disruption of Phospholipid and Bile Acid Homeostasis in Mice with Nonalcoholic Steatohepatitis.” *Hepatology* 56 (1): 118–29. https://doi.org/10.1002/hep.25630.

Tang, Y., Z. Bian, L. Zhao, Y. Liu, S. Liang, Q. Wang, X. Han, et al. 2011. “Interleukin-17 Exacerbates Hepatic Steatosis and Inflammation in Non-Alcoholic Fatty Liver Disease.” *Clinical and Experimental Immunology*. https://doi.org/10.1111/j.1365-2249.2011.04471.x.

Teodoro, J. S., P. Zouhar, P. Flachs, K. Bardova, P. Janovska, A. P. Gomes, F. V. Duarte, et al. 2014. “Enhancement of Brown Fat Thermogenesis Using Chenodeoxycholic Acid in Mice.” *International Journal of Obesity*. https://doi.org/10.1038/ijo.2013.230.

Thiele, Nina D., Jan W. Wirth, David Steins, Anja C. Koop, Harald Ittrich, Ansgar W. Lohse, and Johannes Kluwe. 2017. “TIMP-1 Is Upregulated, but Not Essential in Hepatic Fibrogenesis and Carcinogenesis in Mice.” *Scientific Reports*. https://doi.org/10.1038/s41598-017-00671-1.

Thomas, Charles, Roberto Pellicciari, Mark Pruzanski, Johan Auwerx, and Kristina Schoonjans. 2008. “Targeting Bile-Acid Signalling for Metabolic Diseases.” *Nature Reviews Drug Discovery* 7 (8): 678–93. https://doi.org/10.1038/nrd2619.

Tian, Xiao Yu, Kirthana Ganeshan, Cynthia Hong, Khoa D. Nguyen, Yifu Qiu, Jason Kim, Rajendra K. Tangirala, Peter Tonotonoz, and Ajay Chawla. 2016. “Thermoneutral Housing Accelerates Metabolic Inflammation to Potentiate Atherosclerosis but Not Insulin Resistance.” *Cell Metabolism*. https://doi.org/10.1016/j.cmet.2015.10.003.

Tilg, Herbert. 2010. “The Role of Cytokines in Non-Alcoholic Fatty Liver Disease.” *Digestive*

Diseases. https://doi.org/10.1159/000282083.

Töröcsik, Dániel, Attila Szanto, and László Nagy. 2009. “Oxysterol Signaling Links Cholesterol Metabolism and Inflammation via the Liver X Receptor in Macrophages.” *Molecular Aspects of Medicine*. https://doi.org/10.1016/j.mam.2009.02.002.

Trefts, Elijah, Maureen Gannon, and David H. Wasserman. 2017. “The Liver.” *Current Biology*. https://doi.org/10.1016/j.cub.2017.09.019.

Trigatti, Bernardo L., Richard G.W. Anderson, and Gerhard E. Gerber. 1999. “Identification of Caveolin-1 as a Fatty Acid Binding Protein.” *Biochemical and Biophysical Research Communications*. https://doi.org/10.1006/bbrc.1998.0123.

Ueki, Isao, Akihiko Kimura, Atsushi Nishiyori, Huey Ling Chen, Hajime Takei, Hiroshi Nittono, and Takao Kurosawa. 2008. “Neonatal Cholestatic Liver Disease in an Asian Patient with a Homozygous Mutation in the Oxysterol 7α-Hydroxylase Gene.” *Journal of Pediatric Gastroenterology and Nutrition*. https://doi.org/10.1097/MPG.0b013e31815a9911.

Vandel, Jimmy, Julie Dubois-Chevalier, Céline Gheeraert, Bruno Derudas, Violetta Raverdy, Dorothée Thuillier, Luc Gaal, et al. 2021. “Hepatic Molecular Signatures Highlight the Sexual Dimorphism of Nonalcoholic Steatohepatitis (NASH).” *Hepatology*. https://doi.org/10.1002/hep.31312.

Velazquez-Villegas, Laura A., Alessia Perino, Vera Lemos, Marika Zietak, Mitsunori Nomura, Thijs Willem Hendrik Pols, and Kristina Schoonjans. 2018. “TGR5 Signalling Promotes Mitochondrial Fission and Beige Remodelling of White Adipose Tissue.” *Nature Communications*. https://doi.org/10.1038/s41467-017-02068-0.

Vikram, Ajit, and Gopabandhu Jena. 2010. “S961, an Insulin Receptor Antagonist Causes Hyperinsulinemia, Insulin-Resistance and Depletion of Energy Stores in Rats.” *Biochemical and Biophysical Research Communications*. https://doi.org/10.1016/j.bbrc.2010.06.070.

Vvedenskaya, Olga, Tim Daniel Rose, Oskar Knittelfelder, Alessandra Palladini, Judith Andrea Heidrun Wodke, Kai Schuhmann, Jacobo Miranda Ackerman, et al. 2021. “Nonalcoholic Fatty Liver Disease Stratification by Liver Lipidomics.” *Journal of Lipid Research*. https://doi.org/10.1016/j.jlr.2021.100104.

Wada, Taira, Soon Kang Hong, Martin Angers, Haibiao Gong, Shikha Bhatia, Shaheen Khadem, Songrong Ren, et al. 2008. “Identification of Oxysterol 7α-Hydroxylase (Cyp7b1) as a Novel Retinoid-Related Orphan Receptor α (RORα) (NR1F1) Target Gene and a Functional Cross-Talk between RORα and Liver X Receptor (NR1H3).” *Molecular*

Pharmacology. https://doi.org/10.1124/mol.107.040741.

Wang, David Q.H., Susumu Tazuma, David E. Cohen, and Martin C. Carey. 2003. “Feeding Natural Hydrophilic Bile Acids Inhibits Intestinal Cholesterol Absorption: Studies in the Gallstone-Susceptible Mouse.” *American Journal of Physiology - Gastrointestinal and Liver Physiology*. https://doi.org/10.1152/ajpgi.00156.2003.

Wang, Yan Dong, Wei Dong Chen, Donna Yu, Barry M. Forman, and Wendong Huang. 2011. “The G-Protein-Coupled Bile Acid Receptor, Gpbar1 (TGR5), Negatively Regulates Hepatic Inflammatory Response through Antagonizing Nuclear Factor Kappa Light-Chain Enhancer of Activated B Cells (NF-KB) in Mice.” *Hepatology* 54 (4): 1421–32. https://doi.org/10.1002/hep.24525.

Wang, Yongjun, Naresh Kumar, Philippe Nuhant, Michael D. Cameron, Monica A. Istrate, William R. Roush, Patrick R. Griffin, and Thomas P. Burris. 2010. “Identification of SR1078, a Synthetic Agonist for the Orphan Nuclear Receptors RORα and RORγ.” *ACS Chemical Biology*. https://doi.org/10.1021/cb100223d.

Watanabe, Mitsuhiro, Sander M. Houten, Chikage Mataki, Marcelo A. Christoffolete, Brian W. Kim, Hiroyuki Sato, Nadia Messaddeq, et al. 2006. “Bile Acids Induce Energy Expenditure by Promoting Intracellular Thyroid Hormone Activation.” *Nature*. https://doi.org/10.1038/nature04330.

Wei, Meilin, Fengjie Huang, Ling Zhao, Yunjing Zhang, Wei Yang, Shouli Wang, Mengci Li, et al. 2020. “A Dysregulated Bile Acid-Gut Microbiota Axis Contributes to Obesity Susceptibility.” *EBioMedicine*. https://doi.org/10.1016/j.ebiom.2020.102766.

Willinger, T. 2019. “Oxysterols in Intestinal Immunity and Inflammation.” *Journal of Internal Medicine*. https://doi.org/10.1111/joim.12855.

Wolf, Monika Julia, Arlind Adili, Kira Piotrowitz, Zeinab Abdullah, Yannick Boege, Kerstin Stemmer, Marc Ringelhan, et al. 2014a. “Metabolic Activation of Intrahepatic CD8+ T Cells and NKT Cells Causes Nonalcoholic Steatohepatitis and Liver Cancer via Cross-Talk with Hepatocytes.” *Cancer Cell*. https://doi.org/10.1016/j.ccell.2014.09.003.

———. 2014b. “Metabolic Activation of Intrahepatic CD8+T Cells and NKT Cells Causes Nonalcoholic Steatohepatitis and Liver Cancer via Cross-Talk with Hepatocytes.” *Cancer Cell* 26 (4): 549–64. https://doi.org/10.1016/j.ccell.2014.09.003.

Worthmann, Anna, Clara John, Malte C. Rühlemann, Miriam Baguhl, Femke Anouska Heinsen, Nicola Schaltenberg, Markus Heine, et al. 2017. “Cold-Induced Conversion of Cholesterol

to Bile Acids in Mice Shapes the Gut Microbiome and Promotes Adaptive Thermogenesis." *Nature Medicine* 23 (7): 839–49. https://doi.org/10.1038/nm.4357.

Yamaguchi, Kanji, Liu Yang, Shannon McCall, Jiawen Huang, Xian Yu Xing, Sanjay K. Pandey, Sanjay Bhanot, Brett P. Monia, Yin Xiong Li, and Anna Mae Diehl. 2007. "Inhibiting Triglyceride Synthesis Improves Hepatic Steatosis but Exacerbates Liver Damage and Fibrosis in Obese Mice with Nonalcoholic Steatohepatitis." *Hepatology*. https://doi.org/10.1002/hep.21655.

Yamashita, Hiromi, Makoto Takenoshita, Masaharu Sakurai, Richard K. Bruick, William J. Henzel, Wendy Shillinglaw, David Arnot, and Kosaku Uyeda. 2001. "A Glucose-Responsive Transcription Factor That Regulates Carbohydrate Metabolism in the Liver." *Proceedings of the National Academy of Sciences of the United States of America*. https://doi.org/10.1073/pnas.161284298.

Yang, Zhao Xia, Wei Shen, and Hang Sun. 2010. "Effects of Nuclear Receptor FXR on the Regulation of Liver Lipid Metabolism in Patients with Non-Alcoholic Fatty Liver Disease." *Hepatology International*. https://doi.org/10.1007/s12072-010-9202-6.

Yao, Z., and D. E. Vance. 1988. "The Active Synthesis of Phosphatidylcholine Is Required for Very Low Density Lipoprotein Secretion from Rat Hepatocytes." *Journal of Biological Chemistry*. https://doi.org/10.1016/s0021-9258(18)69166-5.

Yki-Järvinen, Hannele. 2014. "Non-Alcoholic Fatty Liver Disease as a Cause and a Consequence of Metabolic Syndrome." *The Lancet Diabetes and Endocrinology* 2 (11): 901–10. https://doi.org/10.1016/S2213-8587(14)70032-4.

Yu, Liqing, Guoqing Cao, Joyce Repa, and Herbert Stangl. 2004. "Sterol Regulation of Scavenger Receptor Class B Type I in Macrophages." *Journal of Lipid Research*. https://doi.org/10.1194/jlr.M300461-JLR200.

Zhang, Ming, and John Y.L. Chiang. 2001. "Transcriptional Regulation of the Human Sterol 12α-Hydroxylase Gene (CYP8B1): Roles of Hepatocyte Nuclear Factor 4α in Mediating Bile Acid Repression." *Journal of Biological Chemistry*. https://doi.org/10.1074/jbc.M105117200.

Zhang, Xiang, Jiayun Shen, Kwan Man, Eagle S.H. Chu, Tung On Yau, Joanne C.Y. Sung, Minnie Y.Y. Go, et al. 2014. "CXCL10 Plays a Key Role as an Inflammatory Mediator and a Non-Invasive Biomarker of Non-Alcoholic Steatohepatitis." *Journal of Hepatology*. https://doi.org/10.1016/j.jhep.2014.07.006.

Part I: Attachments

Table 7 List of hazardous substances according to GHS

Chemical	Manufacturer	Purity	GHS Symbol	Hazard Statement H	Precaution Statement P
[4-^{14}C]-Cholesterol	Perkin Elmer, Waltham, USA	-	-	-	-
[9,10-^{3}H(N)]-Triolein	Perkin Elmer, Waltham, USA	-	-	-	-
22(S)-hydroxycholesterol	Avanti Polaroids, Alabaster, USA	≥ 99%	-	-	-
24(S)-hydroxycholesterol	Avanti Polaroids, Alabaster, USA	≥ 99%	-	-	-
25(S)-hydroxycholesterol	Avanti Polaroids, Alabaster, USA	≥ 99%	-	-	-
27-hydroxycholesterol	Avanti Polaroids, Alabaster, USA	≥ 99%	-	-	-
40% Acrylamide/Bis Solution 37.5:1	Bio-Rad Laboratories, CA, USA	99.9 %	GHS07, GHS08	H302, H315, H317, H319, H332, H340, H350, H361f, H372, H412	P260, P264, P312, P501
7α-hydroxycholesterol	Avanti Polaroids, Alabaster, USA	≥ 99%	-	-	-
7β-hydroxycholesterol	Avanti Polaroids, Alabaster, USA	≥ 99%	-	-	-
Acetonitrile	Merck, Darmstadt, Germany	≥ 99.9 %	GHS02, GHS07	H225, H302 + H312 + H332, H319	P210, P240, P302 + P352, P305 + P351 + P338, P403 + P233
Agarose	Biozym, Hessisch Oldendorf	-	-	-	-
Atorvastatin	Hexal, Holzkirchen, Germany	40mg tablets	-	-	-
Boric acid	Sigma-Aldrich, Taufkirchen, Germany	≥ 99.5%	GHS08	H360	P201, P202, P280, P308+P313, P405, P501

BSA	Sigma-Aldrich, Taufkirchen, Germany	≥ 98%	-	-	-
Butylated hydroxytoluene, BHT	Sigma-Aldrich, Taufkirchen, Germany	≥ 99.0%	GHS09	H410	P273, P391, P501
Chenodeoxycholic Acid	Sigma-Aldrich, Taufkirchen, Germany	≥ 99%	-	-	-
Cholic acid	Steraloids Inc, Newport, UK	≥ 99%	-	-	-
$CuSO_4$ X 5 H_2O	Sigma-Aldrich, Taufkirchen, Germany	≥ 98%	GHS05, GHS07, GHS09	H302, H318, H410	P264, P270, P273, P280, P301+P312, P305+P351+P338
d4 Chenodeoxycholic acid	Cayman chemicals, Michigan, USA	≥ 95%	GHS07	H315, H319	-
d4 cholic acid	Steraloids Inc, Newport, UK	≥ 99%	-	-	-
d4 Deoxycholic acid	Cayman chemicals, Michigan, USA	≥ 99%	GHS07	H302, H302, H302, H335	-
d4 Lithocholic acid	Cayman chemicals, Michigan, USA	≥ 99%	-	-	-
Deoxycholic Acid	Sigma-Aldrich, Taufkirchen, Germany	≥ 98%	-	-	-
Dimethyl sulfoxide	Carl Roth, Karlsruhe, Germany	≥ 99.5 %	GHS07	H227, H315, H319	P264, P280, P305+P351+P338, P332+P313, P337+P313, P362
EDTA	Sigma-Aldrich, Taufkirchen, Germany	≥ 98.5%	GHS08	H319	P305 + P351 + P338
Ethanol	Merck, Darmstadt, Germany	≥ 99.9%	GHS02, GHS07	H225, H319	P210, P233, P240, P241, P242, P305 + P351 + P338, P403 + P233
Ezetrol	MSD, New Jersey, USA	10mg tablets	GHS07, GHS08	H332, H302, H312, H315, H319, H335	
Formic acid	Sigma-Aldrich, Taufkirchen, Germany	≥ 98 %	GHS02, GHS05, GHS06	H226, H302, H314, H331	P210, P280, P301+P312, P303+P361+P353, P304+P340+P310
Girard′s Reagent P	TCI Europe,	>95.0%	GHS07	H315, H319	P264, P280,

	Zwijndrecht Belgium				P302 + P352, P337 + P313, P362 + P364, P332 + P313
Glycochenodeoxycholic acid nur sod salt	Steraloids Inc, Newport, UK	≥ 99%	-	-	-
Hydrochloric acid 25%	Merck, Darmstadt, Germany	25%	GHS05, GHS07	H290, H314, H335	P280, P301 + P330 + P331, P305 + P351 + P338, P308 + P310
Ionomycin	Sigma-Aldrich, Taufkirchen, Germany	≥ 98%	-	-	-
KCl	Sigma-Aldrich, Taufkirchen, Germany	≥ 99%	-	-	-
Ketamine	Albrecht, Aulendorf, Germany	10 mg/ml	GHS07	H301, H315, H319, H335	P261-P306-P351-P338
Lithocholic acid	Steraloids Inc, Newport, UK	≥ 99%	-	-	-
Methanol, Rotisolv, Ultra LC-MS-Grade	Merck, Darmstadt, Germany	≥ 99.97 %	GHS02, GHS06, GHS08		
N,N,N',N'-Tetramethyl-ethylenediamine (TEMED)	SERVA, Heidelberg, Germany	≥ 99 %	GHS02, GHS05, GHS07	H302, H332, H225, H302+H332, H314	P243, P280, P301+P330+P331, P303+P361+P353, P304+P340, P305+P351+P338
Na_2CO_3	Sigma-Aldrich, Taufkirchen, Germany	≥ 99.0%	GHS07	H319	P264, P280, P305+P351+P338, P337+P313
NaCl	Sigma-Aldrich, Taufkirchen, Germany	≥ 99,5 %	-	-	-
NAOH	Sigma-Aldrich, Taufkirchen, Germany	≥ 97 %	GHS05	H290, H314	P234, P260, P280, P301 + P330 + P331, P303 + P361 + P353, P305 + P351 + P338
NH_4Ac	Sigma-Aldrich, Taufkirchen, Germany	≥ 99%	-	-	-
PMA	Sigma-Aldrich, Taufkirchen, Germany	≥ 99%	GHS05, GHS06, GHS08,	H300 + H310 + H330, H315, H318, H351	P201, P208, P280, P302 + P352 + P310, P304 + P340 + P310, P305 + P351 + P338
Potassium sodium tartrate tetrahydrate	Merck, Darmstadt, Germany	≥ 99.0%	-	-	-

Rompun	Bayer, Leverkusen, Germany	0.2%	GHS06	H301	P301 + P310
SDS ultra-pure	Carl Roth, Karlsruhe, Germany	≥ 99%	GHS02, GHS05, GHS07	H228, H302+H332, H315, H318, H335, H412	P210, P261, P280, P302+P352, P305+P351+P338, P312
Skim Milk powder	Sigma-Aldrich, Taufkirchen, Germany	-	-	-	-
Sodium azide	Fulka	≥ 99.0%	GHS06, GHS08, GHS09	H300 + H310 + H330, H373, H410	P262, P273, P280, P302 + P352 + P310, P304 + P340 + P310, P314
SR1078	TOCRIS, Bristol, UK	≥ 98%	-	-	-
SR3335	Cayman chemicals, Michigan, USA	≥ 95%	-	-	-
Taurochenodeoxycholic acid, sodium salt	Steraloids Inc, Newport, UK	≥ 99%	-	-	-
Taurocholic acid	Steraloids Inc, Newport, UK	≥ 99%	-	-	-
Taurohyodeoxycholic acid	Steraloids Inc, Newport, UK	≥ 99%	-	-	-
Taurolithocholic acid	Steraloids Inc, Newport, UK	≥ 99%	-	-	-
Tauroursodeoxycholic acid sodium salt	Steraloids Inc, Newport, UK	≥ 99%	-	-	-
Tauro-α-Muricholic acid sodium salt	Steraloids Inc, Newport, UK	≥ 99%	-	-	-
Tauro-β-Muricholic acid sodium salt hydroscopic	Steraloids Inc, Newport, UK	≥ 99%	-	-	-
Tauro-ω-Muricholic acid sodium salt	Steraloids Inc, Newport, UK	≥ 99%	-	-	-
Trizma-Base	Sigma-Aldrich, Taufkirchen, Germany	≥ 99.8%	-	-	-
Tween 20	Sigma-Aldrich, Taufkirchen, Germany	≥ 40%	-	-	-
Tyloxapol (Triton WR1339)	Sigma-Aldrich, Taufkirchen, Germany	≥ 98%	GHS07	H315, H319, H335	P261 P264, P271, P280, P302 + P352, P304 + P340 + P312, P305 + P351 + P338, P332 + P313, P337 + P313, P362, P403 + P233, P405, P501

Ursodeoxycholic Acid	Sigma-Aldrich, Taufkirchen, Germany	≥ 99%	-	-	-
Water, LC-MS Ultra CHROMASOLV, tested for UHPLC-MS	Sigma-Aldrich, Taufkirchen	≥ 99.9 %	-	-	-
α-Muricholic acid	Steraloids Inc, Newport, UK	≥ 99%	-	-	-
β-Muricholic acid	Steraloids Inc, Newport, UK	≥ 99%	-	-	-
ω-Muricholic acid	Steraloids Inc, Newport, UK	≥ 99%	-	-	-

Table 8 Kits

Product/Kit	**Manufacturer**
ALT Activity Assay	Sigma-Aldrich, Taufkirchen, Germany
Amplex® Red Cholesterol Assay Kit	Thermo Fisher Scientific, Waltham, USA
Cholesterol determination Kit (Cholesterol CHOD-PAP)	Roche Diagonstics®, Mannheim, Germany
Eukitt® Quick-hardening mounting medium	Sigma-Aldrich, Taufkirchen, Germany
High Capacity cDNA Reverse Transcription Kit	Applied Biosystems Inc., USA
Internal Standard Kit for Lipidyzer™ Platform	SCIEX, Framingham, USA
NEFA-HR(2) Assay	FUJIFILM Wako, Neuss, Germany
NucleoSpin RNA II	Macherey & Nagel, Düren, Germany
Rat Insulin ELISA Kit	Crystal Chem, Zaandam, Netherlands
SuperSignal™ West Femto Maximum Sensitivity Substrate kit	Thermo Fisher Scientifi, Waltham, USA
SYBR™ Green PCR Master Mix	Applied Biosystems Inc., USA
TaqMan™ Universal Master Mix II	Applied Biosystems Inc., USA
Triglycerol determination Kit (Triglycerides GPO-PAP)	Roche Diagonstics®, Mannheim, Germany
Universal PCR MasterMix	Applied Biosystems Inc., USA

Table 9 Buffers and solutions

Buffer/Solution	**Manufacturer/Composition**
1.5M Tris-HCl	• 181.7 g Tris-Base • Adjust pH 8.8 with HCl 25% in final 1 L with H_2O dest.
1M Tris-HCl	• 121.1 g Tris-Base • Adjust pH 6.8 with HCl 25% in final 1 L with H_2O dest.
Anesthesia	ketamine (100 mg/ml)/rompun (2 %)/NaCl (0.9 %); 2.3/1.0/6.7, v/v/v; 15 µL/g bodyweight
Blocking buffer milk 5%	• 2.5 g Milk Skim Powder

	in final 50 mL with TBST
Blotting buffer	• 56.2 g Glycine • 12.1 g Tris-base • 1 L Methanol in final 5 L with H_2O dest.
BSA 5 % with NaAzid 0.02%	• 2.5 g BSA • 50 µL Sodium azide 20% in final 50 mL with TBST
cOmplete™, Mini, EDTA-free Protease Inhibitor Cocktail	Roche Diagonstics®, Mannheim, Germany
EDTA solution 0.5M	Sigma-Aldrich, Taufkirchen, Germany
Eluent A	• 20 mM NH_4Ac • 1 mL formic acid in final 1 L with H_2O dest.
Eluent B	• 20 mM NH_4Ac • 1 mL formic acid in final 1 L with Methanol/Acetonitrile (1/3, v/v)
Eukitt® Quick-hardening mounting medium	Sigma-Aldrich, Taufkirchen, Germany
Folin-Ciocalteu's phenol reagent	Merck, Darmstadt, Germany
Formaldehyde solution 3.7%	• 100 mL Formaldehyde solution 37% in final 1 L with PBS
Formaldehyde solution 37%	Sigma-Aldrich, Taufkirchen, Germany
FPLC buffer	• 100 mM Tris pH 8.0 • 1.5 M NaCl • 100 mM EDTA in final 1 L with H_2O dest.
GeneRuler™ DNA Ladder Mix	Thermo Fisher Scientific, Waltham, USA
Hematoxylin Solution, Mayer's	Sigma-Aldrich, Taufkirchen, Germany
Lowry Solution A	• 20 g Na_2CO_3 • 0,2 g Potassium sodium tartrate in final 1 L with 0,1 M NaOH
Lowry Solution B	• 5 g $CuSO_4$ x 5 H2O • 50 g SDS in final 1 L with H_2O dest.
Methanol-BHT	• 500 mL methnaol • 0,5 g BHT

MTBE	
NaCl 5M	• 14.61 g NaCl in final 50 mL with H_2O dest.
NaCl, 0,9 w/v %	Braun, Melsungen, Germany
NaOH 0.1M	• 3.99 g NaOH in final 1 L with H_2O dest.
NuPAGE™ LDS Sample Buffer (4X)	Thermo Fisher Scientific, Waltham, USA
NuPAGE™ Sample Reducing Agent (10X)	Thermo Fisher Scientific, Waltham, USA
PageRuler™ Prestained Protein Ladder	Thermo Fisher Scientific, Waltham, USA
PBS (10X)	• 100 g NaCl • 10 g KCl • 10 g KH_2PO_4 x $2H_2O$ in final 5 L with H_2O dest., pH 6.9
peqGOLD TriFast™	Peqlab, Erlangen, Germany
Phosphatase Inhibitor Cocktail	Biotool (bimake.com), Texas, USA
Pierce™ Bovine Serum Albumin Standard	Thermo Fisher Scientific, Waltham, USA
Ponceau S solution	Sigma-Aldrich, Taufkirchen, Germany
Precipath®	Roche Diagonstics, Mannheim
Proteinase K, recombinant	Thermo Fisher Scientific, Waltham, USA
RIPA buffer	• 50 mM Tris-HCl pH 7.4 • 5 mM EDTA • 150 mM sodium chloride • 1 mM sodium pyrophosphate • 1 mM sodium fluoride • 1 mM sodium orthovanadate • 1 % NP-40
ROTI®Block	Carl Roth, Karlsruhe, Germany
ROTI®-Block	Carl Roth, Karlsruhe, Germany
ROTI®-GelStain	Carl Roth, Karlsruhe, Germany
Running buffer (10X)	• 54 g Tris-Base • 144 g Glycine • 10 g SDS in final 1 L with H_2O dest.
Scintillation Fluid Aquasafe 500+	Zinsser Analytic, Frankfurt, Germany
SDS 10 %	• 10 g SDS in final 100 mL with H_2O dest.

Sodium azide 20% (w/v)	• 10 g Sodium Azide in final 50 mL with H_2O dest.
Solvable	Perkin Elmer, Waltham, USA
STE buffer (1X)	• 2,92 g NaCl • 1.21 g Tris-Base • 5 g SDS • 3.72 g EDTA • Adjust pH 7,4 in final 1 L with H_2O dest.
TBE-Puffer (5X)	• 54 g Tris-Base • 27.5 g Boric acid • 3.7 g EDTA in final 1 L with H_2O dest.
TBS - Tween 0.1%	• 100 mL TBS 10X • 1 mL TWEEN® 20 in final 1 L with H_2O dest.
TBS buffer (10X)	• 0.2M Tris-Base • 1.37M NaCl in final 1 L with H_2O dest., pH7.4
TRIzol™ Reagent	Life technologies, Ontario, Canada
OptiPrep™ Density Gradient Medium	Sigma-Aldrich, Taufkirchen, Germany
Pacific Orange™ Succinimidyl Ester	Thermo Fisher Scientific, Waltham, USA
GolgiPlug™	BD Biosciences, USA

Part J: Register of figures

Part K: Register of tables

Acknowledgments

First and foremost, I would like to express my special thanks to **Prof. Dr. Jörg Heeren**, who trusted me and generously opened the doors of his lab to pursue firstly my internship as an exchange master student and subsequently my doctoral research. Definitely I couldn't have asked for a better mentor or boss (and when I say that, I truly believe it!). By being so supportive, understanding and open-hearted, you have inspired everyone and established the greatest lab environment, so that I could keep up working with great pleasure regardless the difficulties, the late hours, the weekends or the unsuccessful experiments. I am really grateful for all the efforts that you did all these years to support and teach me, and I will for sure carry everything that I learned in my future career with a big smile. I would also like to express a big thank you to **Prof. Dr. Markus Fischer**, who admitted my doctoral studies under his co-supervision and supported me throughout their duration as well to **Prof. Dr. Markus Perbandt** that evaluated my thesis.

I would like to thank each and every member of the IBMZ (old and new) for their constant help and above all for the amazing common experiences that we had in and out of the lab! Definitely, the entire Heeren group, by being so warm-hearted, friendly, fun… is the best I could ask for!

Special thanks go to **Anna Worthmann** and **Clara John** who trusted me from the very beginning of my internship to carry out important experiments and later on for supervising the first steps of my own doctoral projects. Thank you for your kindness and support, I really enjoyed working with you and very looking forward to continuing so in the future! **Christian Schlein**, I really appreciate your willingness to show me Hamburg when I first came in the city, needless to refer to the loads of help with housing and everything around it. On top, I am definitely looking forward to our future collaboration.

Of course, I have to thank **Dorothee Schwinge**, who helped me with crucial experiments and analyses during my thesis. I always felt welcomed in your lab and despite the load of work that we carried out, we collaborated nicely and most importantly we had fun! **Prof. Johannes Herkel** and **Antonella Carambia** I would like to thank you

for acting as my supervising committee in the graduate school, for our yearly talks and fruitful discussions as well as the continuous support throughout my studies. **Tarek Moustafa**, despite that we collaborated in projects not related with my doctoral thesis, I want to thank you for the research input, the ideas and for always being available to discuss. **Ludger Scheja**, thank you for the input during our meetings and for the great help during manuscript preparations.

For the numerous experiences and endless hours spent in and out of the lab, I would like to thank **Julia Rohde** (το μπουμπούκι μου)! Your company meant a lot to me throughout these years and you know best why! **Tian Tian**, **Manju Kumari**, **Paul Pertzborn**, **Rieke Haumann**, **Hassib Siffeti**, **Carlotta Corban** and **Esther Verkade** I am really glad for sharing so many nice moments with you. Our discussions, activities and fun stories at individual but also collective level are the things that I will always cherish. So, thank you for all the unforgettable days. **Markus Heine**, **Nicola Schaltenberg**, **Alexander Fischer**, **Mira Pauly, Janina Behrens**, **Michelle Yvonne Jäckstein**, **Anastasia Kuhl, Simon Meyer**, **Sebastian Graute, Ellen Thiemann, Nadia Kokaly, Kim Hurkmans** thank you very much for all the help all these years. Despite collaborating in different - sometimes longer, sometimes shorter - time periods, yet we all made the (countless) animal experiments feasible, much more bearable and fun! **Manka Fuh** and **Niklas Röder** thank you very much for your will and contribution with data analysis whenever I asked for, that was really valuable. **Birgit Henkel**, **Sandra Ehret**, **Evi Azizi**, **Walter Tauscher**, **Meike Kröger**, **Laura Ehlen**, **Friederike Behler-Janbeck** thank you for the nice daily collaboration, the relaxed environment in the lab and your help whenever I needed it. From bench sharing, to lunches in the kitchen as well as kicker sessions, I enjoyed spending time with you all! **Emely Borngräber** and **Finnja Sass**, needless to say that your assistance was more than important and much appreciated. The “factory mode” was always fun with you. **Svenja Moser, Christine Runge**, **Laura Mitsching**, **Miriam Pesold** and **Isabel Schultz** thank you so much for everything from day one and throughout my journey, your willingness for solving even the tiniest administration-related headache was honestly of great help for me!

I would like to refer to my friends worldwide for their constant support and love (they all know who they are and I thank them from the bottom of my heart). Ευχαριστώ

πολύ όλους τους συγγενείς και τους φίλους μου στην Ελλάδα και το εξωτερικό, που έστω και με τη σκέψη τους ήταν – και συνεχίζουν να είναι – δίπλα μου όλα αυτά τα χρόνια (ξέρουν όλοι ποιοι είναι και τους ευχαριστώ από τα βάθη της καρδιάς μου).

Πιο πολύ από όλους, θα ήθελα όμως να ευχαριστήσω την οικογένειά μου, τη μητέρα μου **Κατερίνα**, τον πατέρα μου **Γρηγόρη** και τον αδερφό μου **Μάνο**, για όλες τις ανιδιοτελείς θυσίες και την έμπρακτη αγάπη τους όλα αυτά τα χρόνια, που με βοήθησαν να φτάσω σήμερα εδώ. Σας εχαριστώ μαμά, μπαμπά και «μικρέ». Η καθημερινή μας εποικοινωνία και εννοείται με τη Μάιρα, αλλά και οι στιγμές που ξαναβρισκόμασταν μέσα στο χρόνο όλοι μαζί, μου έδιναν σίγουρα δύναμη και χαμόγελο να συνεχίσω παρ' όλη την απόσταση και τις καταστάσεις. Όσο δύσκολο και αν φάνταζε στην αρχή, στη μέση αλλά και στο τελείωμά του το διδακτορικό, το κατάφερα και σας το αφιερώνω. Και αν ένας άνθρωπος δεν χρειάζεται τις ιδιαίτερες ευχαριστίες μου, πολύ απλά επειδή ζήσαμε τα πάντα μαζί, είναι ο **Νίκος**. Πάντα ειλικρινής, υποστηρικτικός, ενθαρρυντικός και παρών όλα αυτά τα χρόνια, ανεξαρτήτως απόστασης ή δυσκολιών, φώτιζες περίεργα μονοπάτια και πλούτιζες την καθημερινότητά μου, θυμίζοντάς μου να κοιτάω πάντα ψηλά και σε ό,τι έχει πραγματικά σημασία. Το καταφέραμε μαζί.

Journal permissions

For the composition of the current thesis, texts, parts and figures where reused, adapted or changed from my following first-author publications:

1) Evangelakos, I., Heeren, J., Verkade, E. et al. Role of bile acids in inflammatory liver diseases. Semin Immunopathol 43, 577–590 (2021)
https://doi.org/10.1007/s00281-021-00869-6
This Article is licensed under the Creative Commons Attribution 4.0 International License. The Creative Commons license can be found under the following link:
http://creativecommons.org/licenses/by/4.0/

2) Evangelakos I, Schwinge D, Worthmann A, John C, Roeder N, Pertzborn P, Behrens J, Schramm C, Scheja L, Heeren J. Oxysterol 7-α Hydroxylase (CYP7B1) Attenuates Metabolic-Associated Fatty Liver Disease in Mice at Thermoneutrality. *Cells*. 2021 Oct;10(10):2656
https://doi.org/10.3390/cells10102656
This is an open access article distributed under the Creative Commons Attribution License which permits unrestricted use, distribution, and reproduction in any medium, provided the original work is properly cited. The Creative Commons license can be found under the following link:
https://creativecommons.org/licenses/by/4.0/

Additionally, parts of the current thesis, texts and figures are included in the currently submitted manuscript:

3) Evangelakos I, Kuhl A, Baguhl M, Schlein C, John C, Rohde JK, Heine M, Heeren J, Worthmann A. Cold-induced lipoprotein clearance in *Cyp7b1* deficient mice. Front Cell Dev Biol (in revision)

Declaration on Oath

“I hereby declare on oath that this doctoral dissertation is written independently and solely by my own based on the original work of my PhD and has not been used other than the acknowledged resources and aids. The submitted written version corresponds to the version on the electronic storage medium. I declare that the present dissertation was prepared maintaining the Rules of Good Scientific Practice of the German Research Foundation and it has never been submitted in the present form or similar to any other.”

02/03/2022 , Evangelakos Ioannis

Date, Signature